

This material is for your own internal use only.  
Any form of duplication or publication is not permitted.  
LightTrans expressly reserves the right to penalize any violation

**VirtualLab Fusion Applications, Technology & Workflows**

# **Anisotropic Media & Crystals in VirtualLab Fusion**

LightTrans International GmbH

Presenter: Olga Baladron-Zorita, Senior Optical Engineer

# Links of Interest

- LightTrans website: [www.LightTrans.com](http://www.LightTrans.com)
- Our past webinars: [www.LightTrans.com/products-services/learning/webinars](http://www.LightTrans.com/products-services/learning/webinars)
- Find a VirtualLab Fusion distributor in your region: [www.LightTrans.com/company/distributors](http://www.LightTrans.com/company/distributors)
- You have further questions? Drop us a line at [info@LightTrans.com](mailto:info@LightTrans.com), for technical questions [support@lighttrans.com](mailto:support@lighttrans.com)
- Subscribe to our newsletter: [www.LightTrans.com/newsletter](http://www.LightTrans.com/newsletter)
- Connect with us on the following social networks:
  - LinkedIn ([www.linkedin.com/company/lighttrans](http://www.linkedin.com/company/lighttrans))
  - Twitter ([www.twitter.com/LightTrans](http://www.twitter.com/LightTrans))
  - YouTube ([www.youtube.com/LightTransInternational](http://www.youtube.com/LightTransInternational))
- Check out our downloads page to see VirtualLab in action across a broad range of fields of application: [www.LightTrans.com/resources/downloads](http://www.LightTrans.com/resources/downloads)
- Want to give VirtualLab Fusion a test drive? Request a trial version: [www.LightTrans.com/resources/trial-software](http://www.LightTrans.com/resources/trial-software)
- Interested in purchasing VirtualLab Fusion? Check out our products, licence model and learn more about additional evaluation possibilities: [www.LightTrans.com/products-services/virtuallab-fusion/editions-toolboxes](http://www.LightTrans.com/products-services/virtuallab-fusion/editions-toolboxes)
- Latest release (VirtualLab Fusion 2021.1): [www.lighttrans.com/products-services/virtuallab-fusion/virtuallab-fusion-release-20211.html](http://www.lighttrans.com/products-services/virtuallab-fusion/virtuallab-fusion-release-20211.html)

# Quick Index:

---

- **Introduction to the teams**
- **PART 1:** Light as an electromagnetic field
- **PART 2:** The electromagnetic field solvers
- **PART 3:** The Fourier transform
- **PART 4:** Optically Anisotropic Media in VirtualLab Fusion
- **EXAMPLE 1:** Birefringence Effect of Anisotropic Calcite Crystal
- **EXAMPLE 2:** Polarization Conversion in Uniaxial Crystals
- **EXAMPLE 3:** Simulation of Multilayer Birefringent Reflective Polarizer with VirtualLab Fusion
- **EXAMPLE 4:** Simulation and Analysis of Anisotropic Coating on Plane and Curved Surface
- **EXAMPLE 5:** Conical Refraction in Biaxial Crystals



## **Introduction to the Teams**

# Who We Are



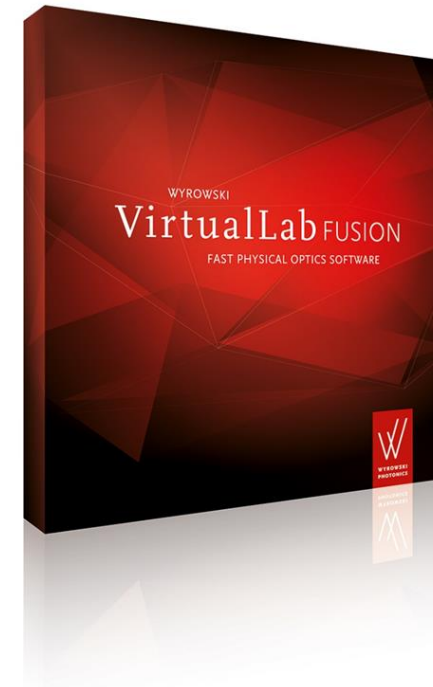
Founded 1999



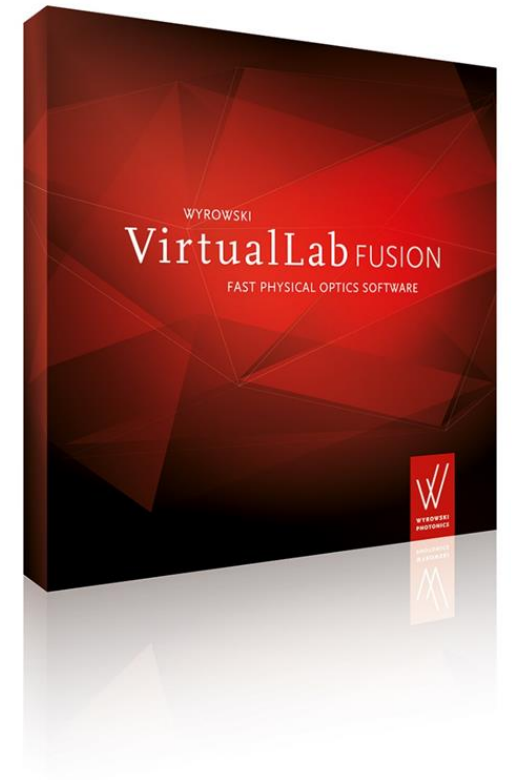
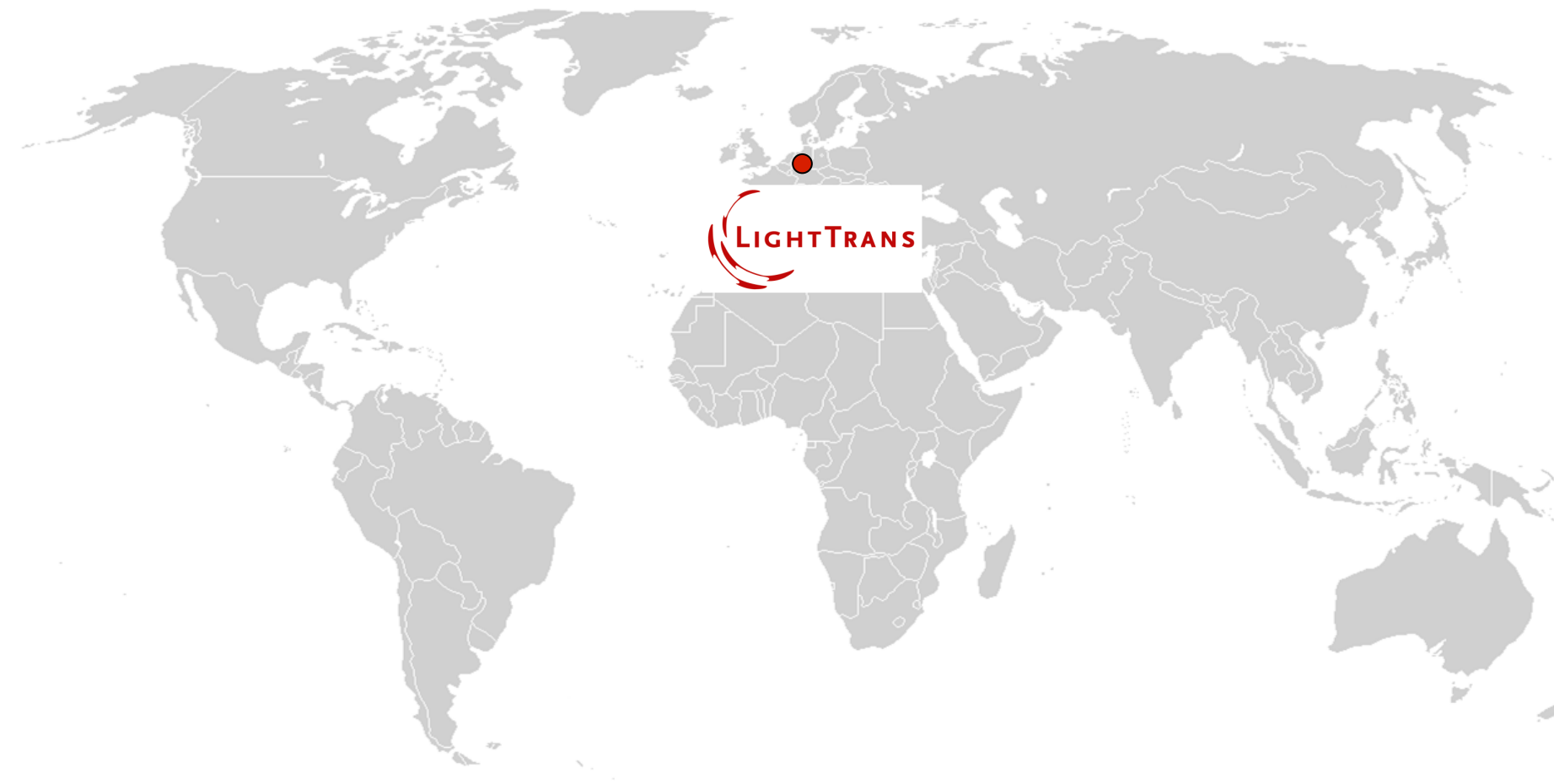
Founded 2014

General Distributor of the  
Fast Physical Optics Software  
**VirtualLab Fusion**

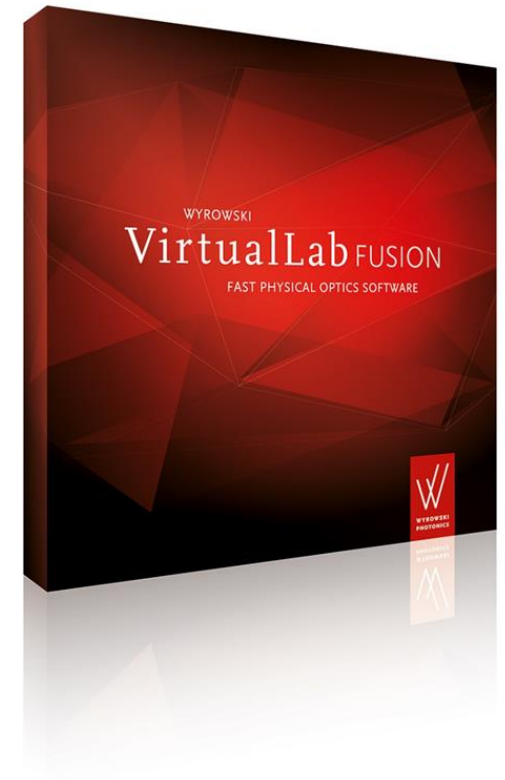
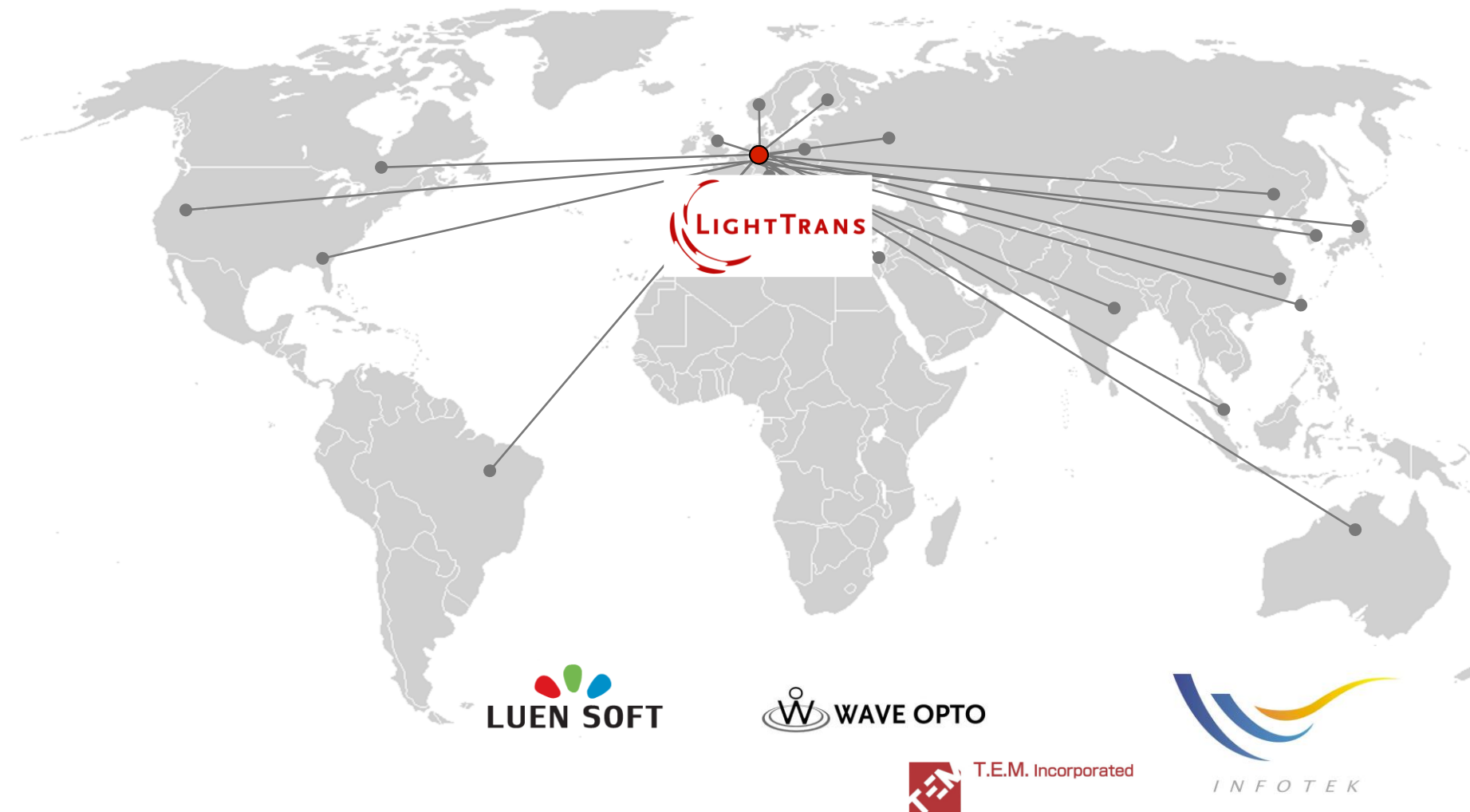
Developer of the  
Fast Physical Optics Software  
**VirtualLab Fusion**



# Fast Physical Optics Modeling and Design Software



# Fast Physical Optics Modeling and Design Software



Part 1

# Light as an Electromagnetic Field



# The Objective Behind VirtualLab Fusion

---

To perform physical optics simulations of optical systems

# The Objective Behind VirtualLab Fusion

---

To perform **physical optics simulations** of optical systems

# The Objective Behind VirtualLab Fusion

---

To perform **physical optics simulations** of optical systems

Finding the expression of the **six-dimensional vector field that solves Maxwell's equations** under the conditions imposed by the system in question



# The Objective Behind VirtualLab Fusion

---

To perform **physical optics simulations** of optical systems

Finding the expression of the **electromagnetic field** for the system in question

# The Objective Behind VirtualLab Fusion

To perform **physical optics simulations** of optical systems

Finding the expression of the **electromagnetic field** for the system in question

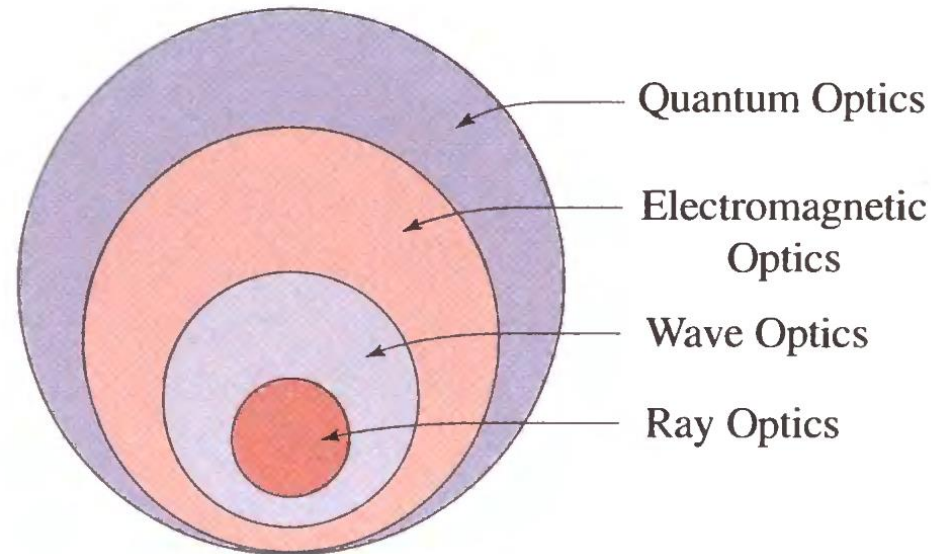
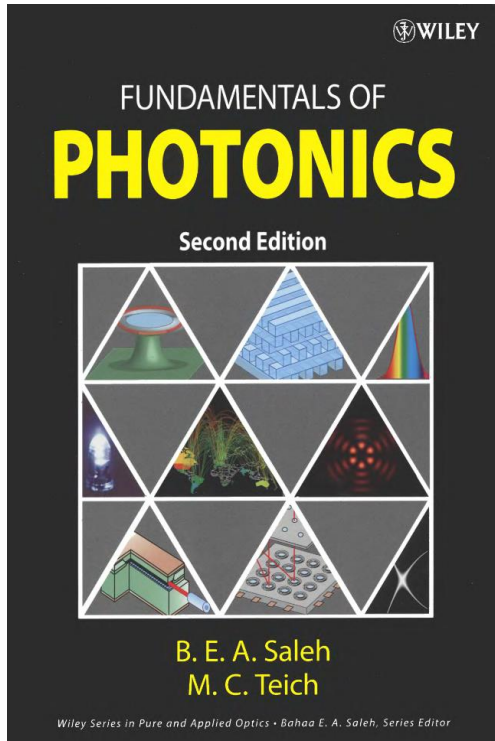
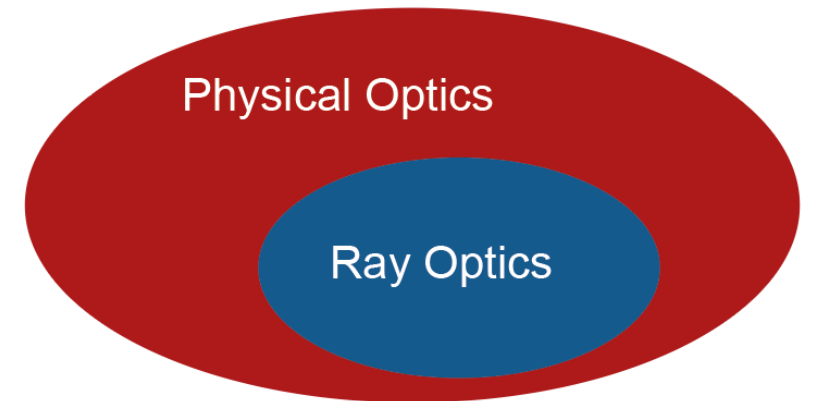
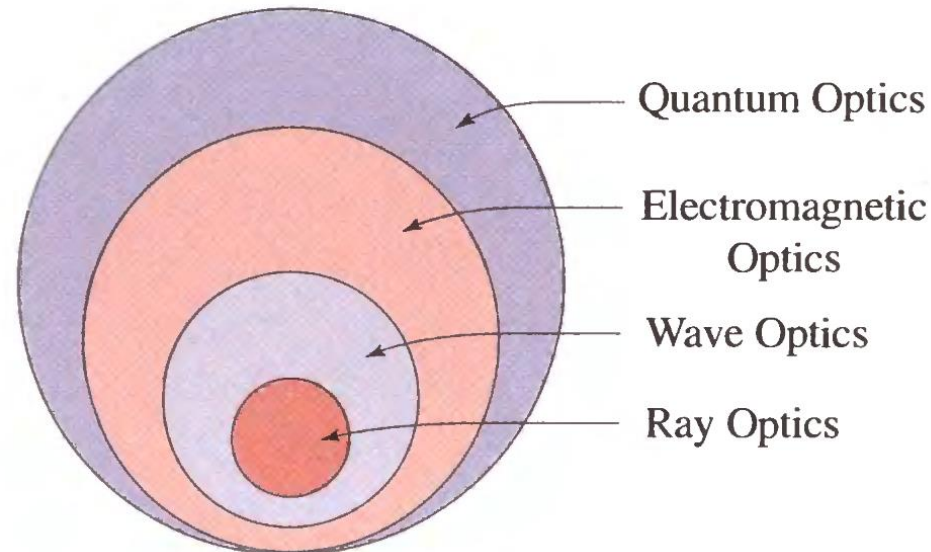
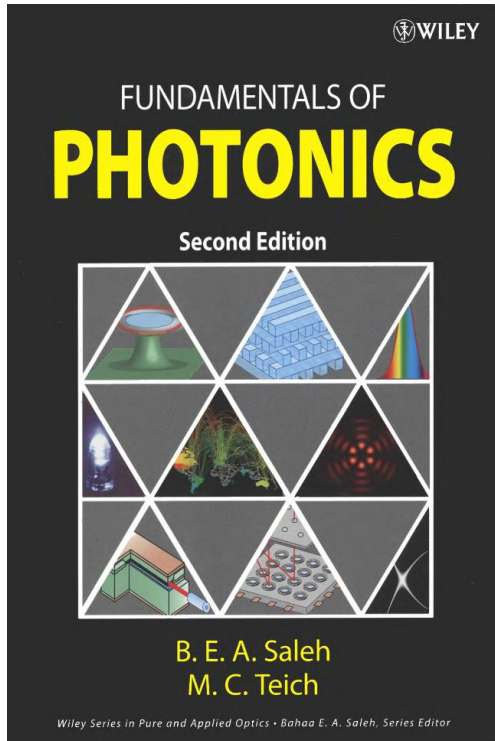


Image reference: "Fundamentals of Photonics", B. E. A. Saleh and M. C. Teich, 2nd Edition, Wiley

# The Objective Behind VirtualLab Fusion

To perform **physical optics simulations** of optical systems

Finding the expression of the **electromagnetic field** for the system in question



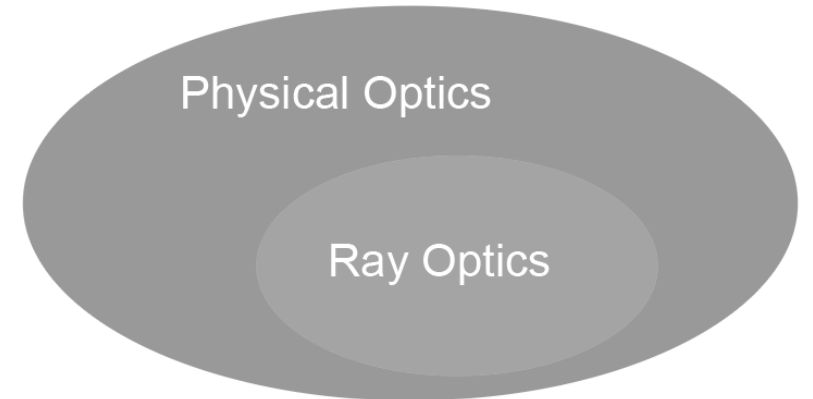
... in VirtualLab Fusion

Image reference: "Fundamentals of Photonics", B. E. A. Saleh and M. C. Teich, 2nd Edition, Wiley

# The Objective Behind VirtualLab Fusion

To perform **physical optics simulations** of optical systems

Finding the expression of the **electromagnetic field** for the system in question



Quantum Optics

**Important:**

no distinction between physical optics and electromagnetic optics.  
We never use the scalar approximation!

... in VirtualLab Fusion

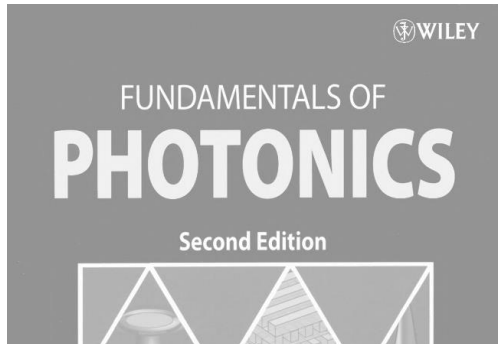


Image reference: "Fundamentals of Photonics", B. E. A. Saleh and M. C. Teich, 2nd Edition, Wiley

Part 2

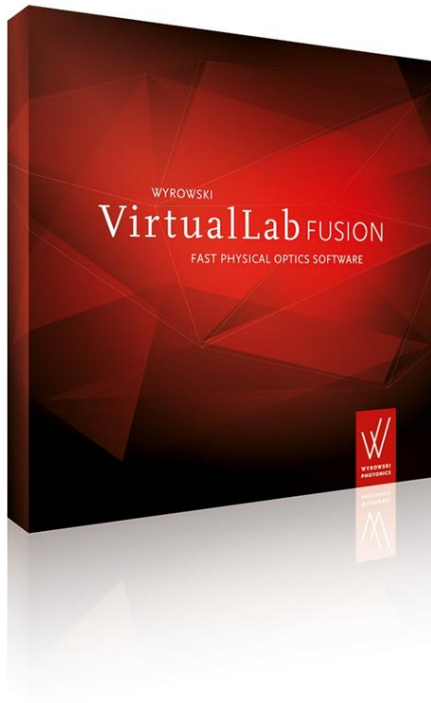
# The Electromagnetic Field Solvers



# One Platform, Many Solvers

Fast physical optics simulations...

... made possible by **connecting field solvers!**



VirtualLab Fusion acts a software platform to connect electromagnetic field solvers in a **seamless, fully non-sequential manner**



**solving Maxwell's equations for the whole system!**

# Electromagnetic Field Solvers

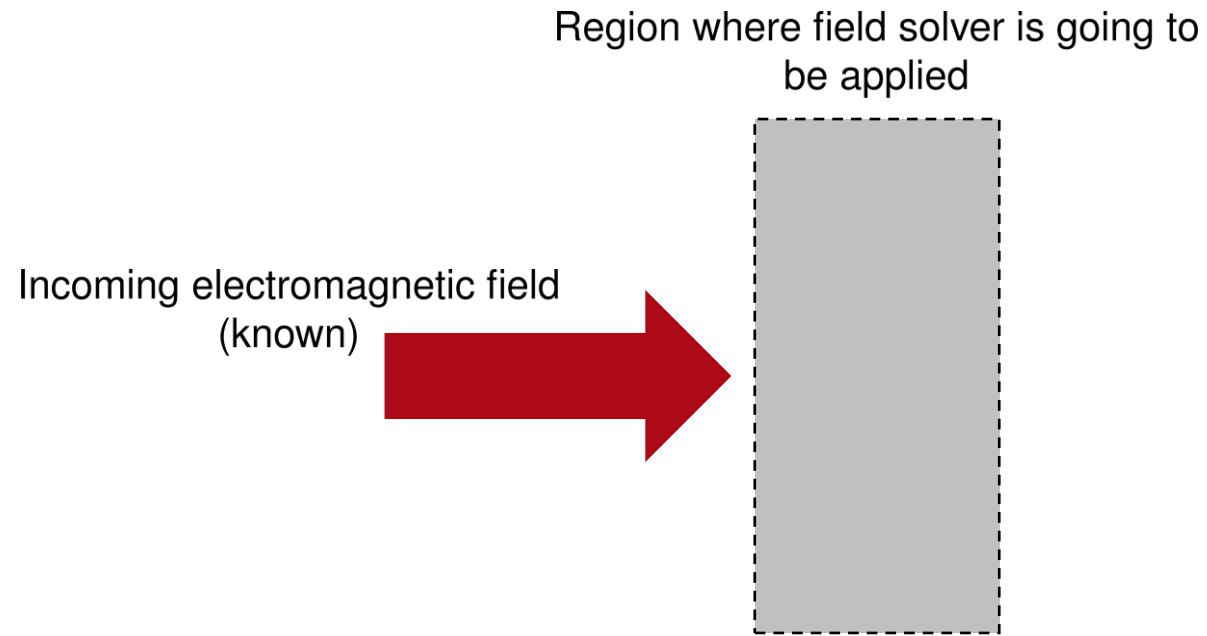
---

Region where field solver is going to  
be applied



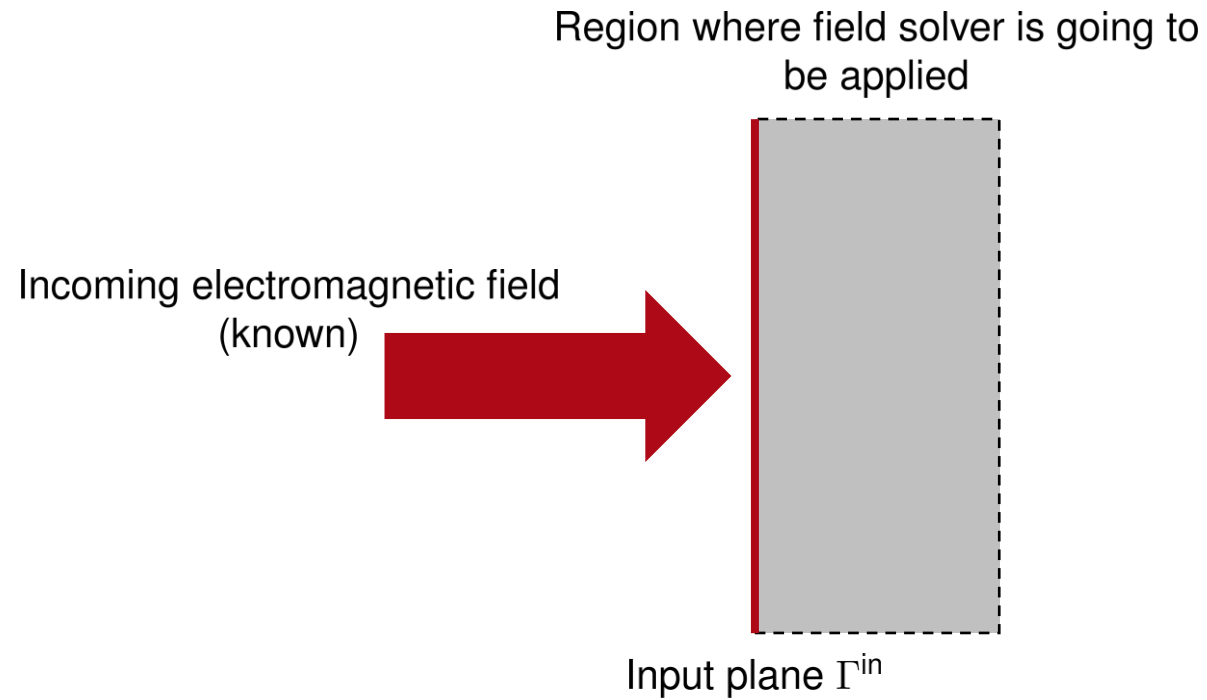
# Electromagnetic Field Solvers

---

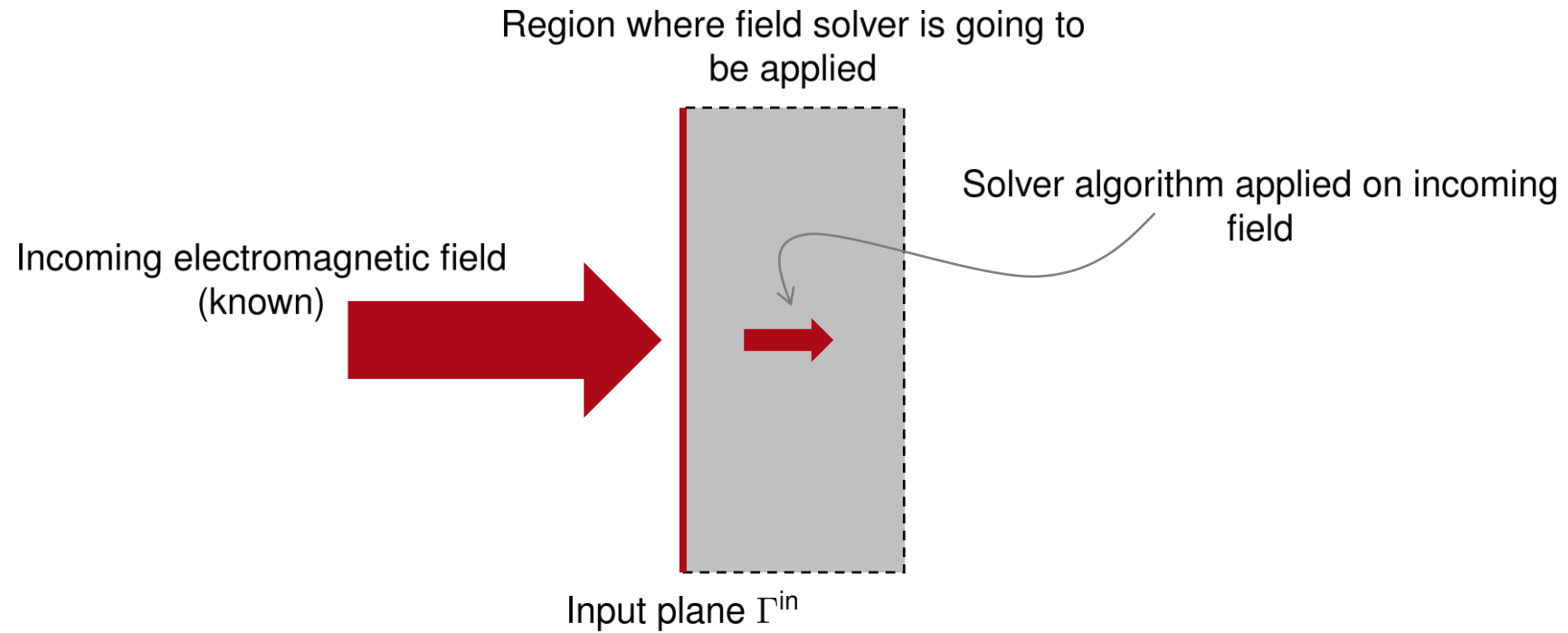




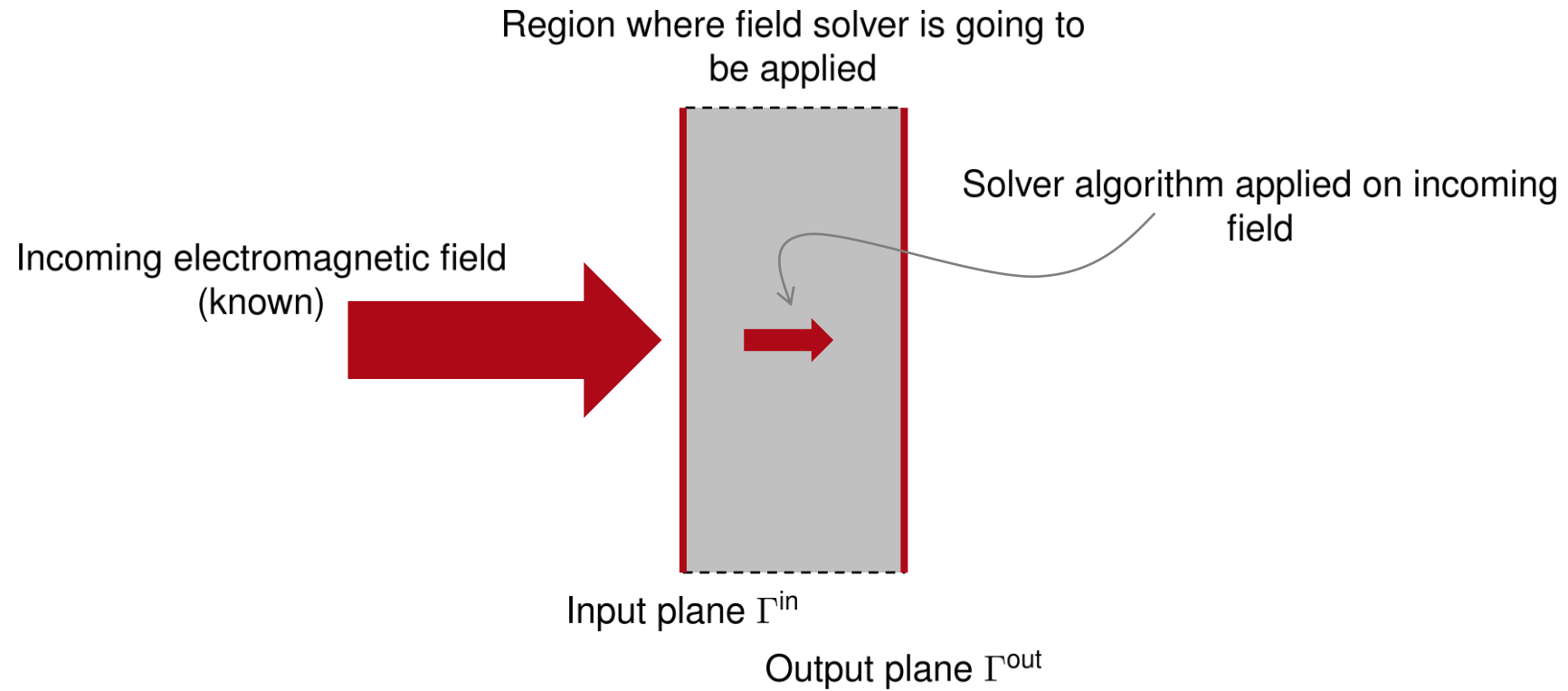
# Electromagnetic Field Solvers



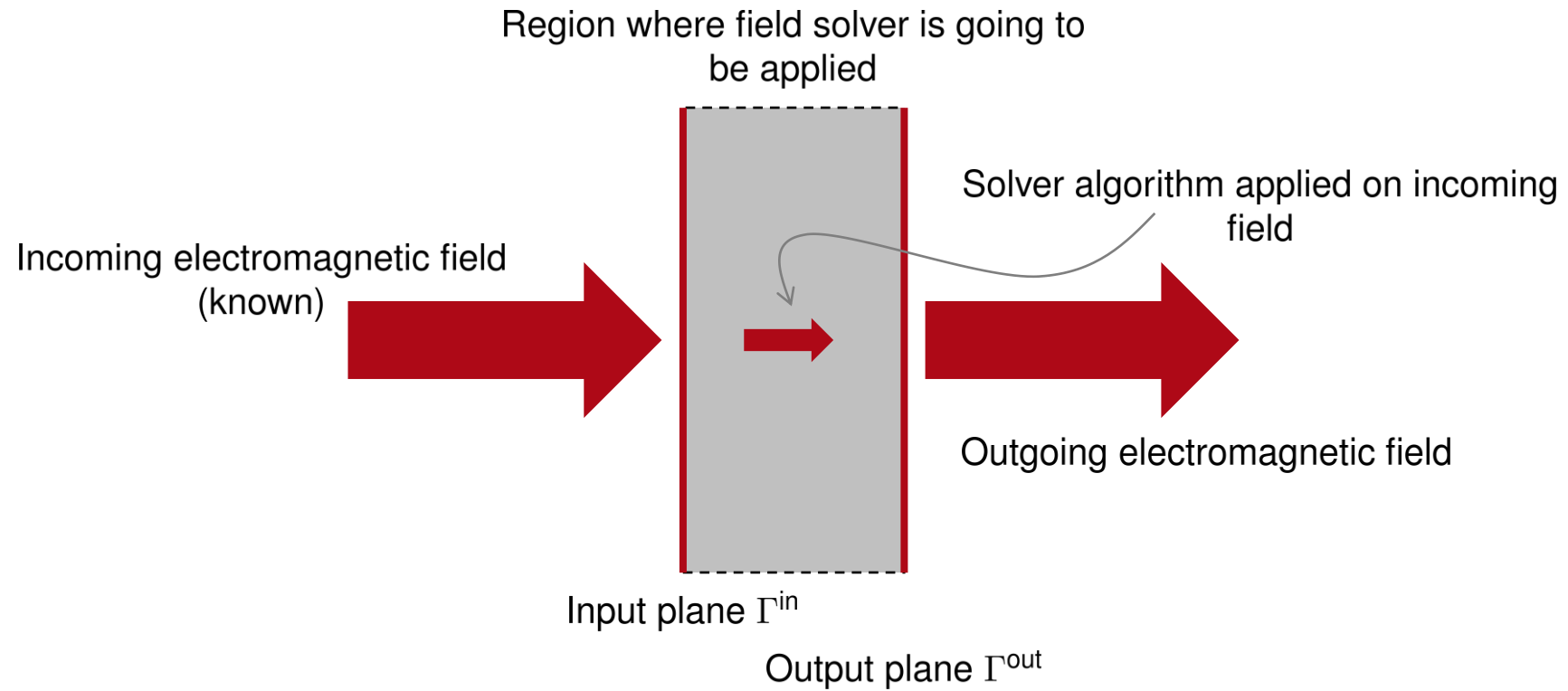
# Electromagnetic Field Solvers



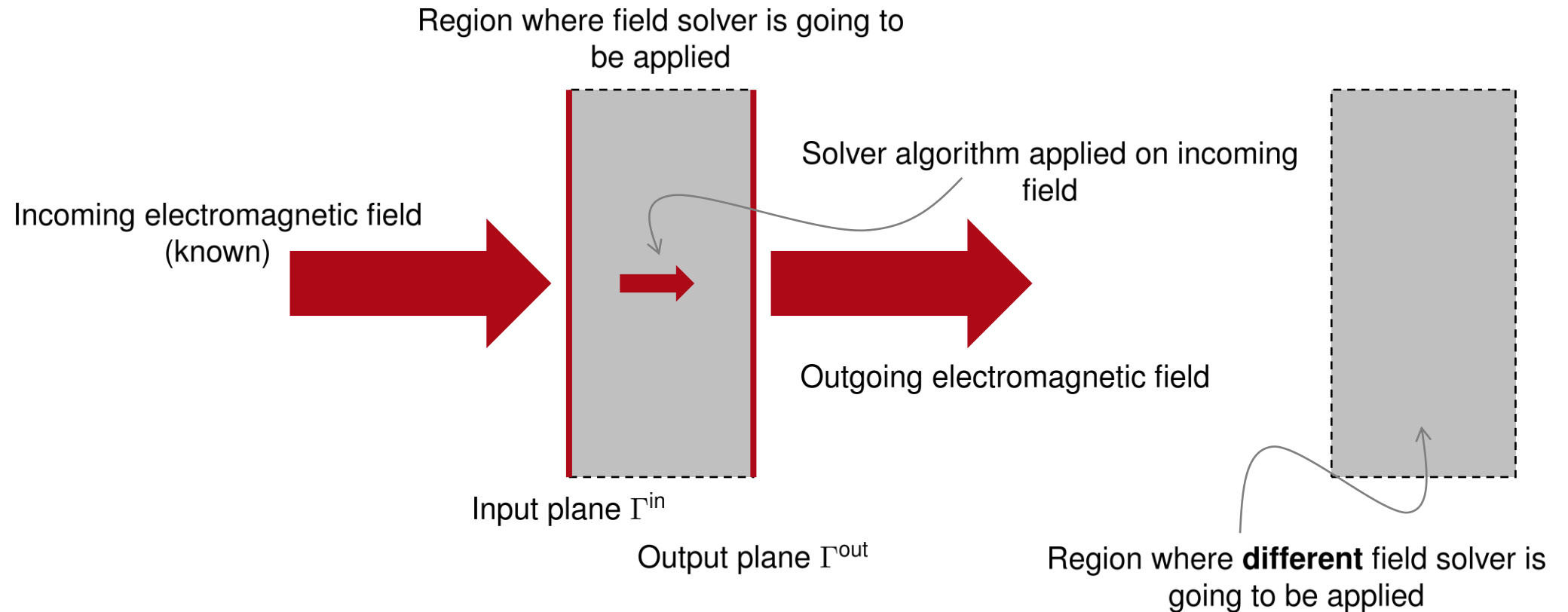
# Electromagnetic Field Solvers



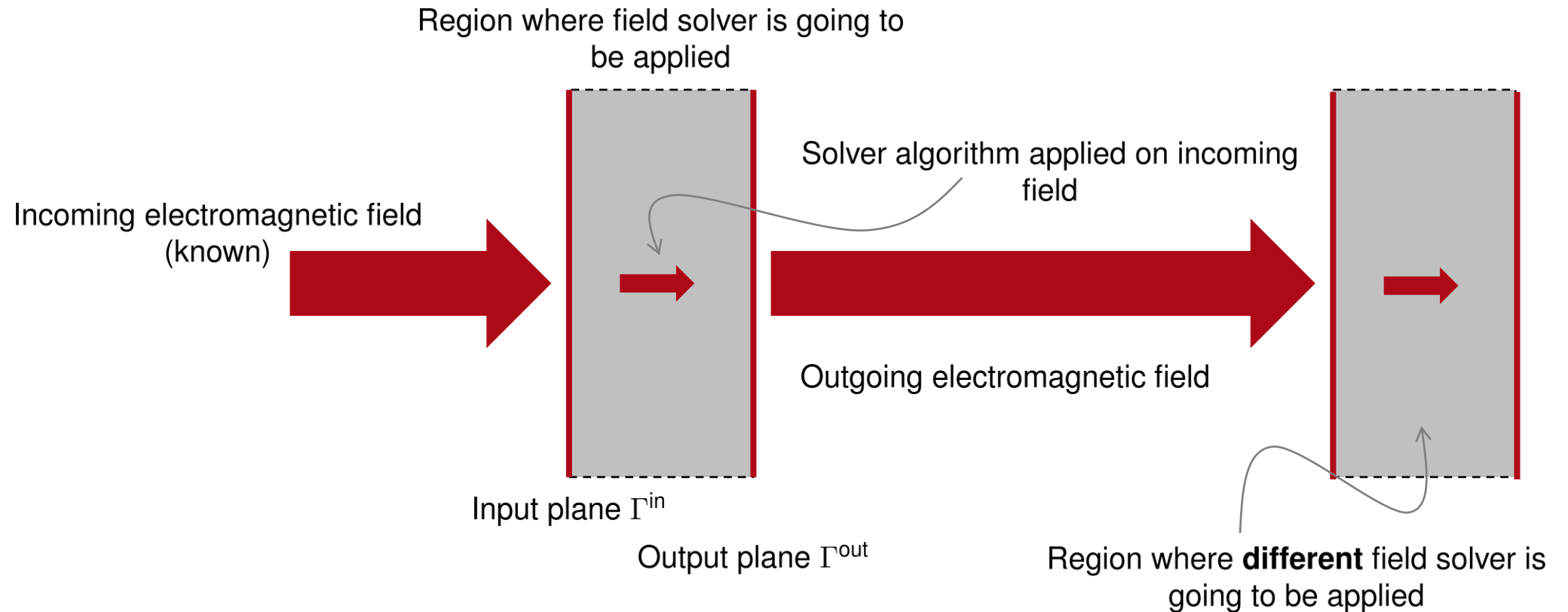
# Electromagnetic Field Solvers



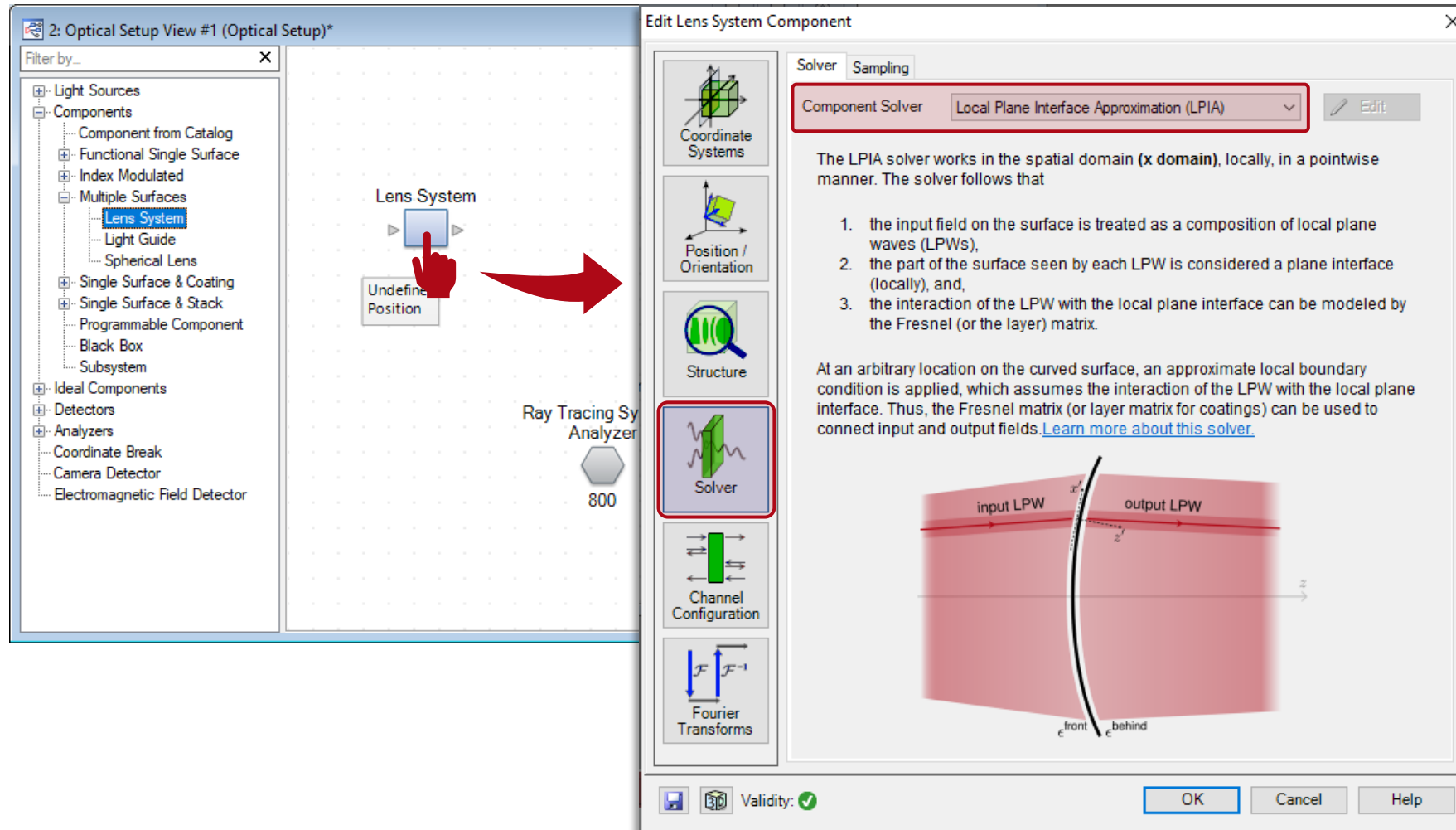
# Electromagnetic Field Solvers



# Electromagnetic Field Solvers

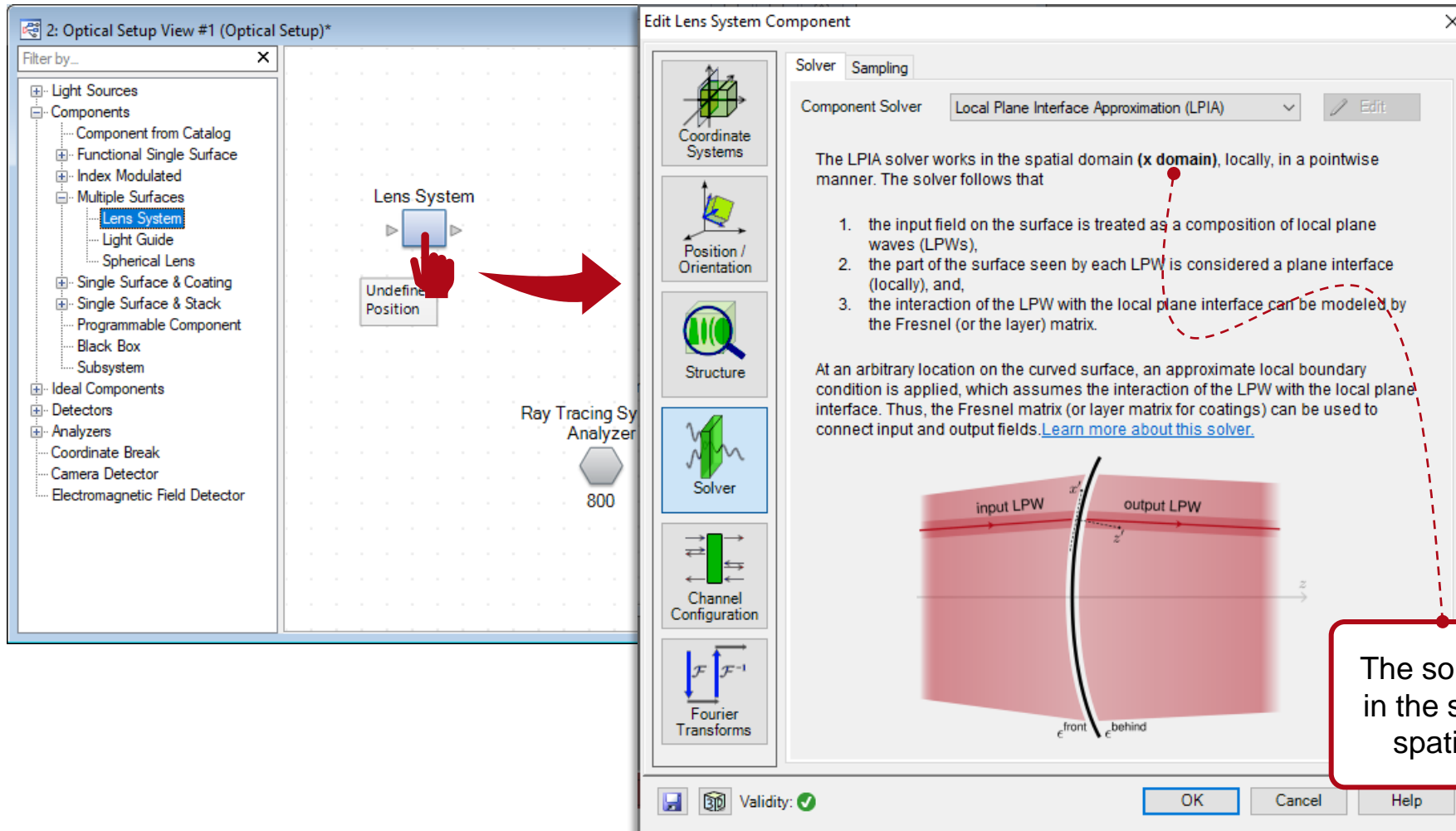


# Components & Solvers



In VirtualLab Fusion, including a certain type of component in your system means, in practice, selecting an **electromagnetic field solver** to model that part of the system

# Components & Solvers

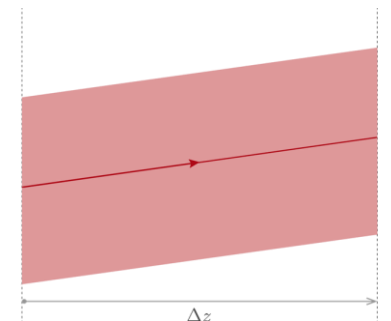
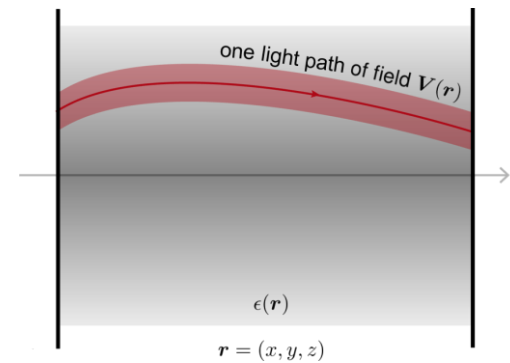
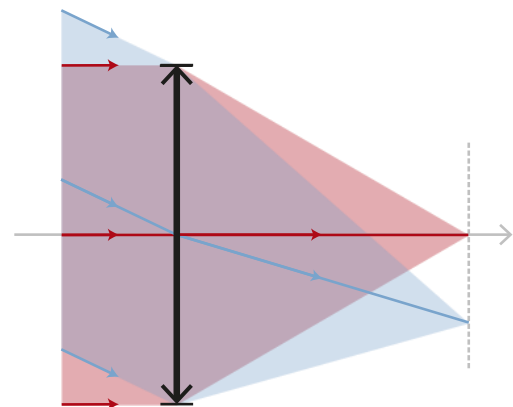
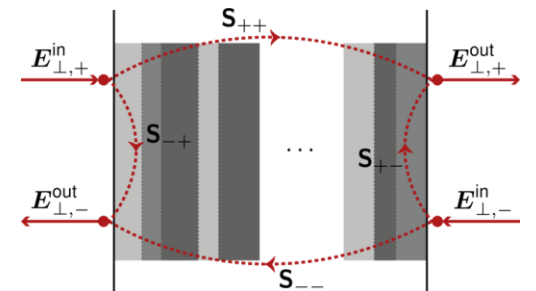
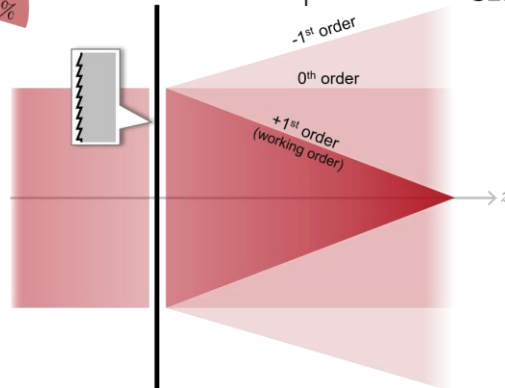
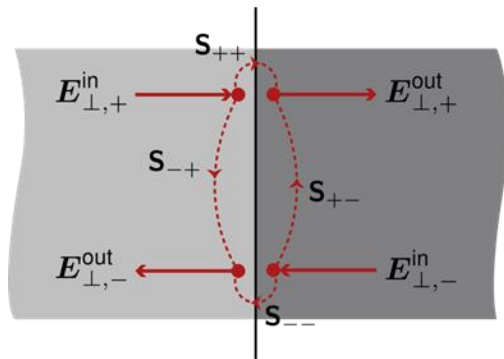
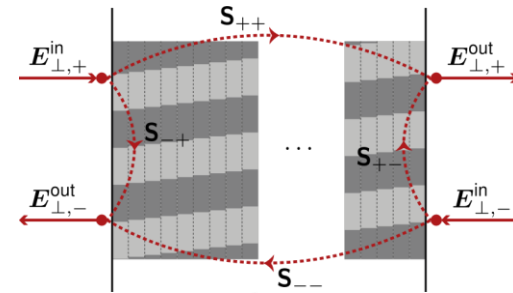
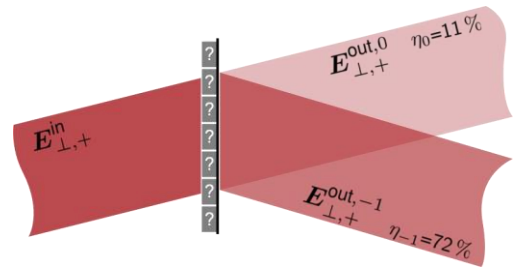
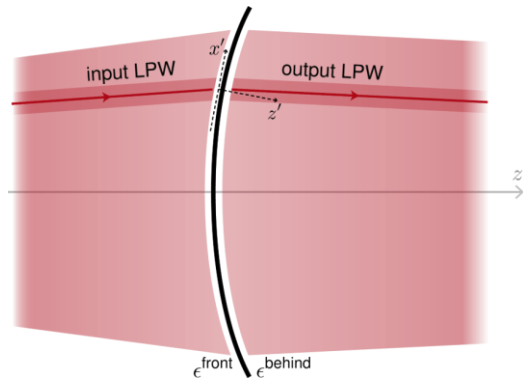


In VirtualLab Fusion, including a certain type of component in your system means, in practice, selecting an **electromagnetic field solver** to model that part of the system

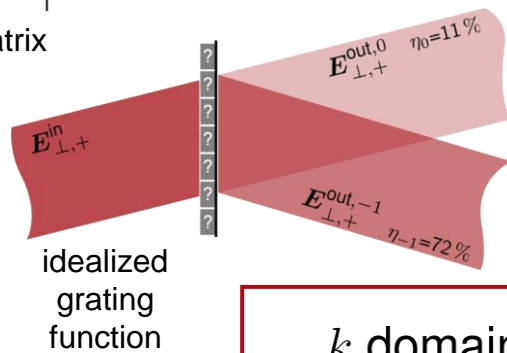
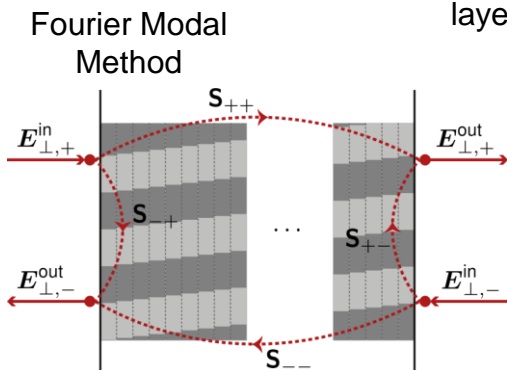
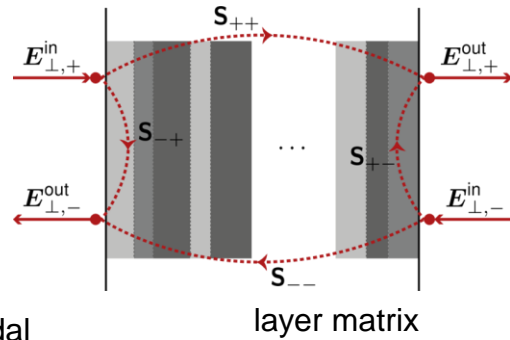
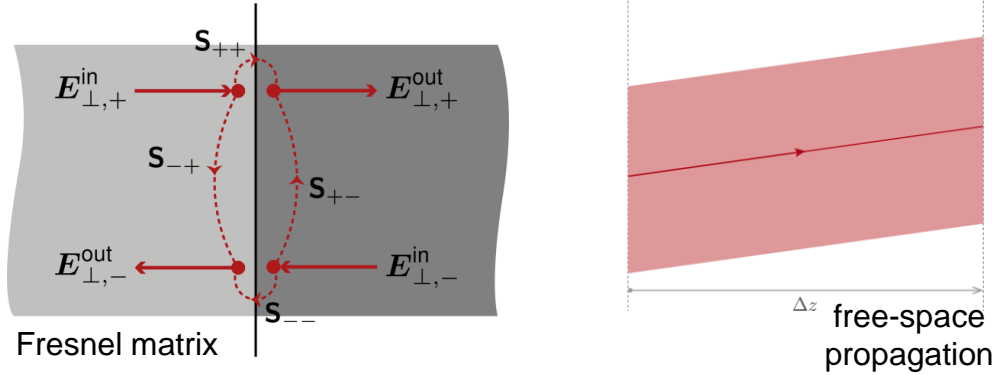
The solvers may be implemented in the space ( $x$ ) domain, or in the spatial-frequency ( $k$ ) domain



# Why Different Domains?

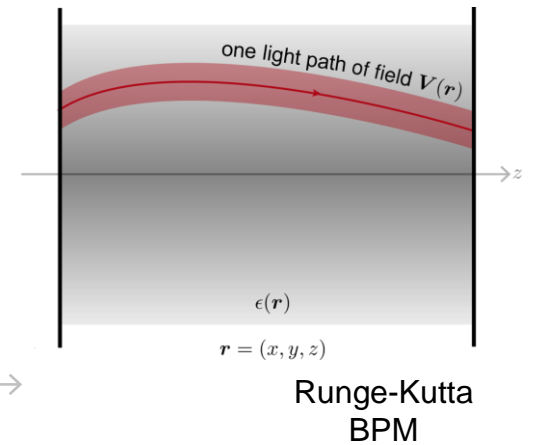
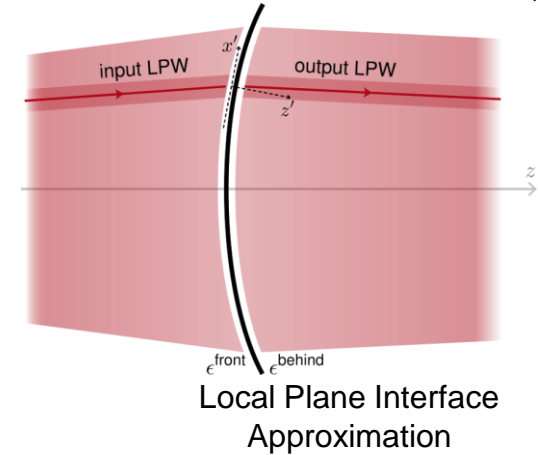
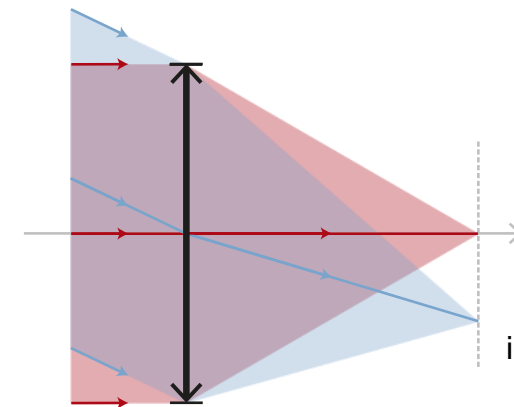
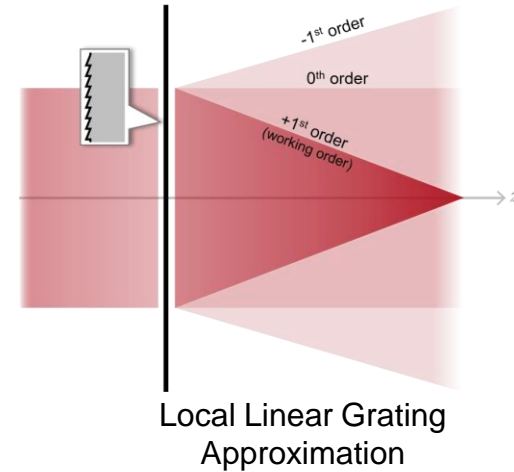


# Why Different Domains?

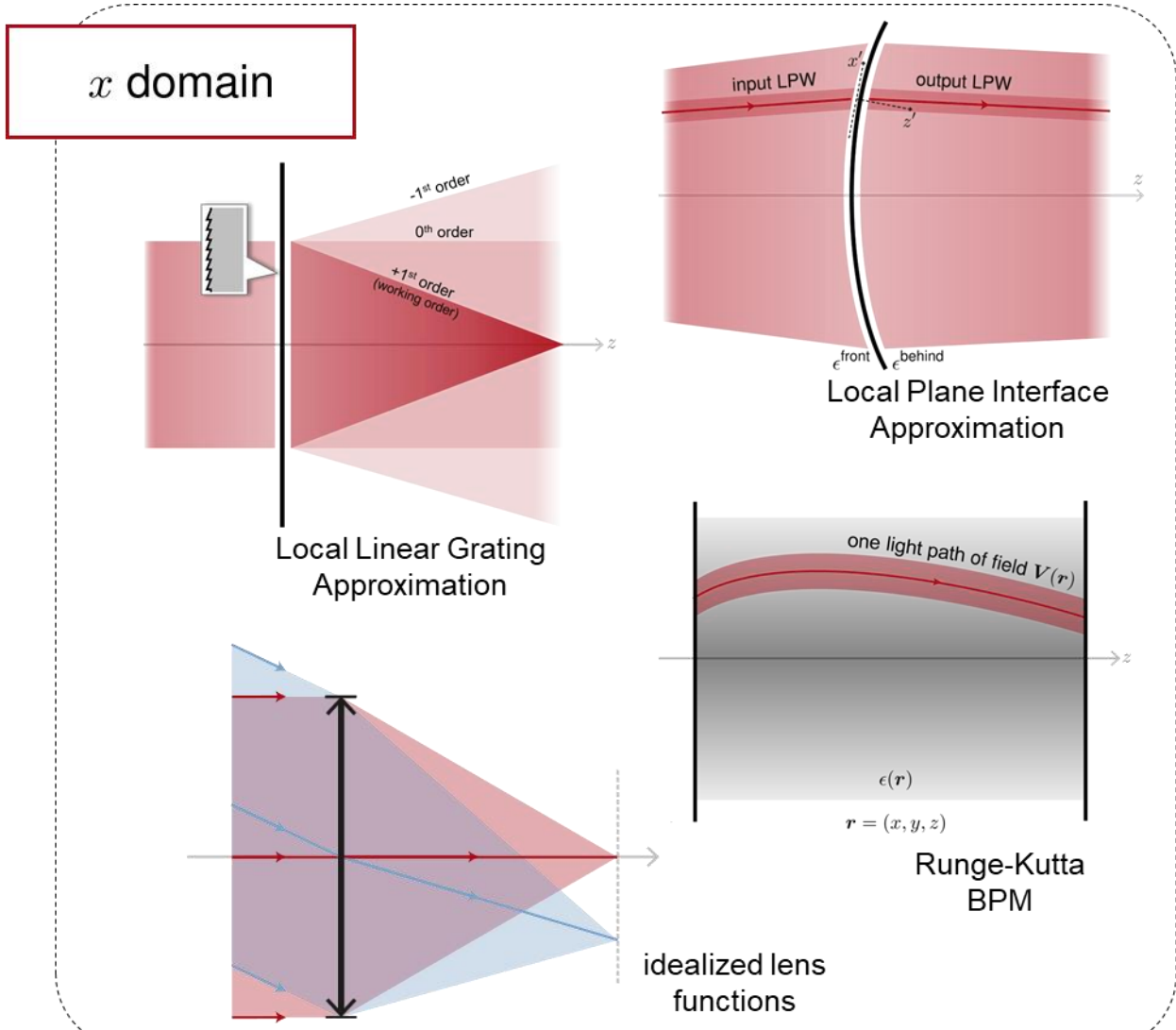
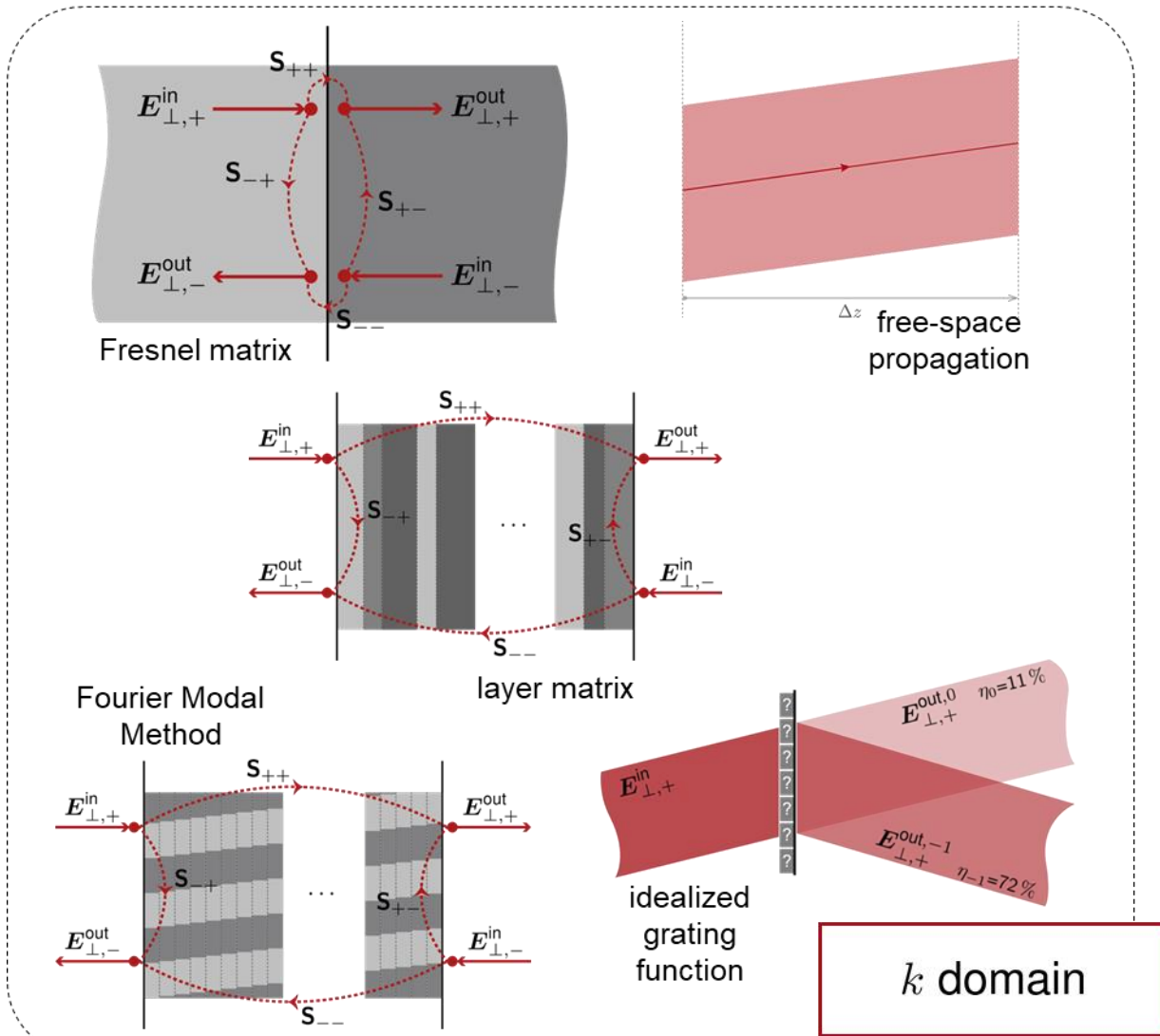


**$k$  domain**

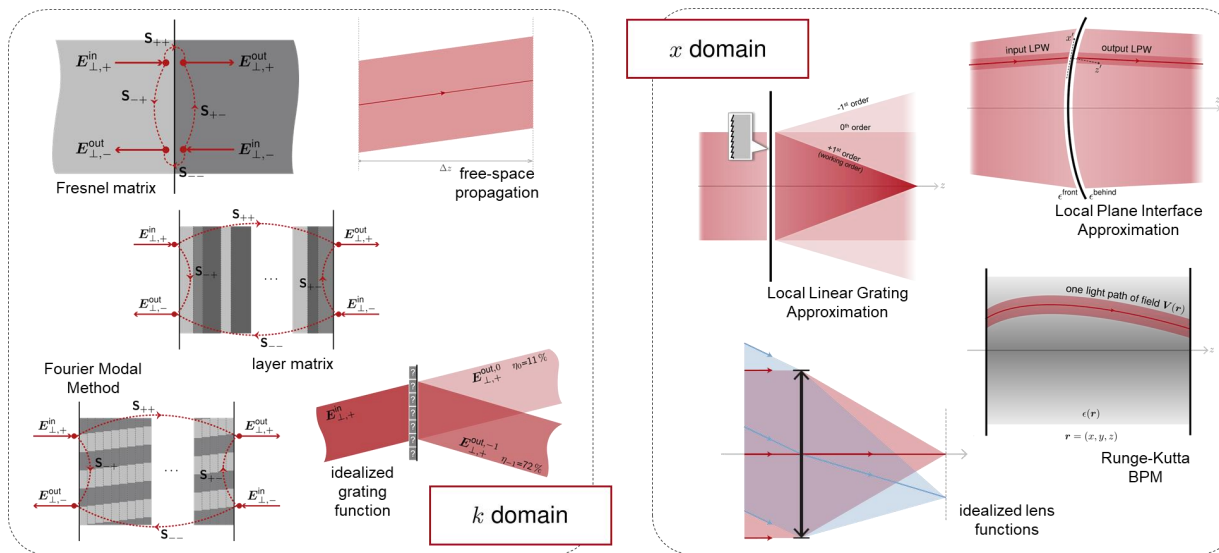
**$x$  domain**



# Why Different Domains?

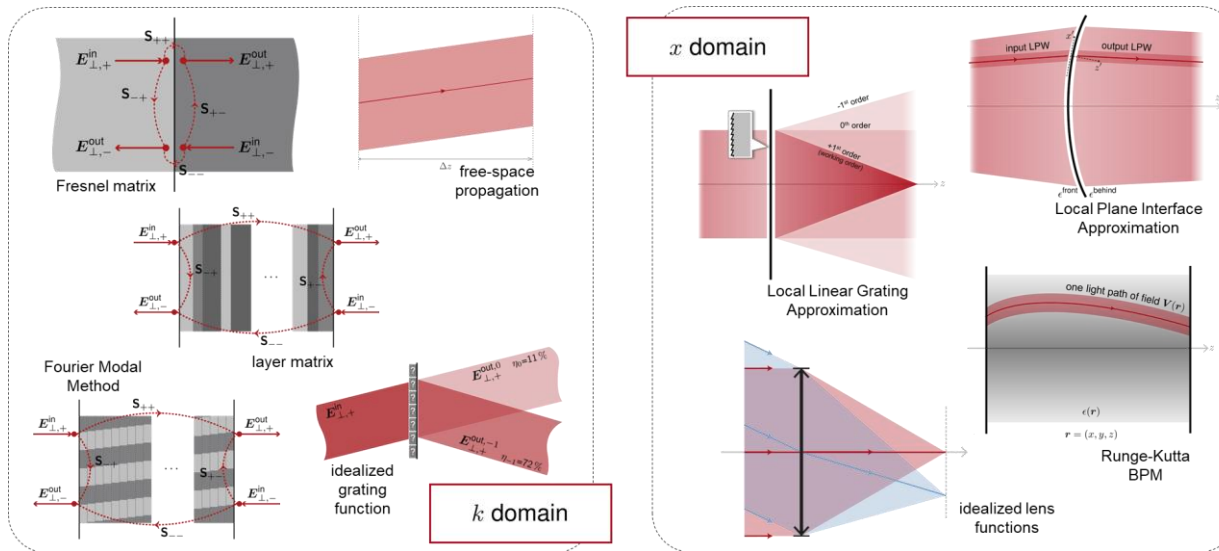


# Why Different Domains?



# Why Different Domains?

Although, in general, electromagnetic field solvers have an **integral** behaviour, with the resulting high numerical complexity, the characteristics of some of the most common optical components mean they can be modeled with **pointwise** operators in one of the Fourier domains – when this happens, it entails a **massive computational advantage**!



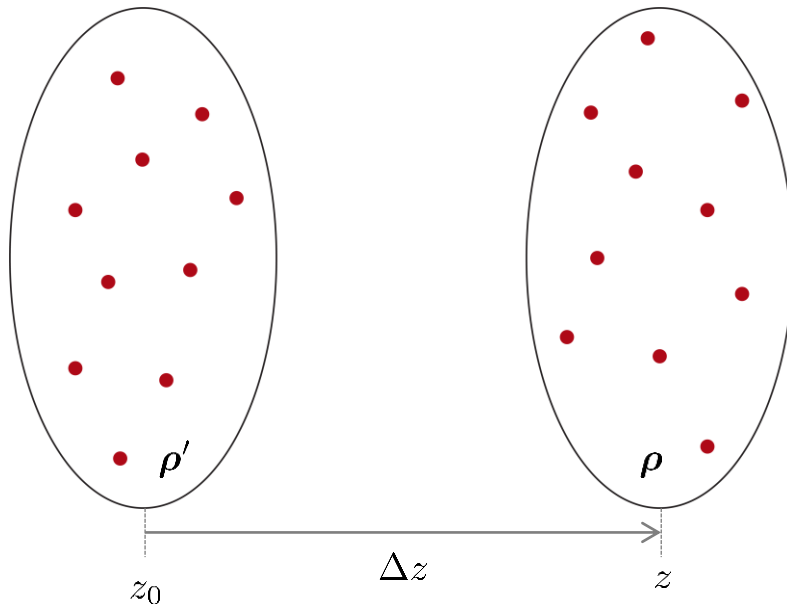
# Example: Free-Space Propagation

## Space domain

Rayleigh-Sommerfeld integral:

$$V_{\ell}^{\text{out}}(\boldsymbol{\rho}, z) \propto \iint_{-\infty}^{+\infty} V_{\ell}^{\text{in}}(\boldsymbol{\rho}', z_0) \frac{e^{ik_0 n R}}{R} \left( ik_0 n - \frac{1}{R} \right) \frac{\Delta z}{R} d^2 \rho'$$

with  $R = \sqrt{(x - x')^2 + (y - y')^2 + (\Delta z)^2}$



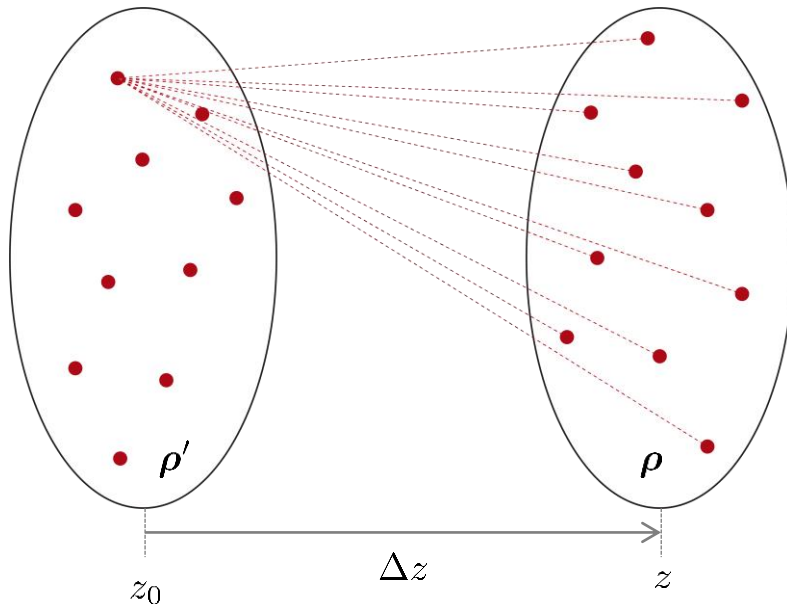
# Example: Free-Space Propagation

## Space domain

Rayleigh-Sommerfeld integral:

$$V_{\ell}^{\text{out}}(\boldsymbol{\rho}, z) \propto \iint_{-\infty}^{+\infty} V_{\ell}^{\text{in}}(\boldsymbol{\rho}', z_0) \frac{e^{ik_0 n R}}{R} \left( ik_0 n - \frac{1}{R} \right) \frac{\Delta z}{R} d^2 \rho'$$

with  $R = \sqrt{(x - x')^2 + (y - y')^2 + (\Delta z)^2}$



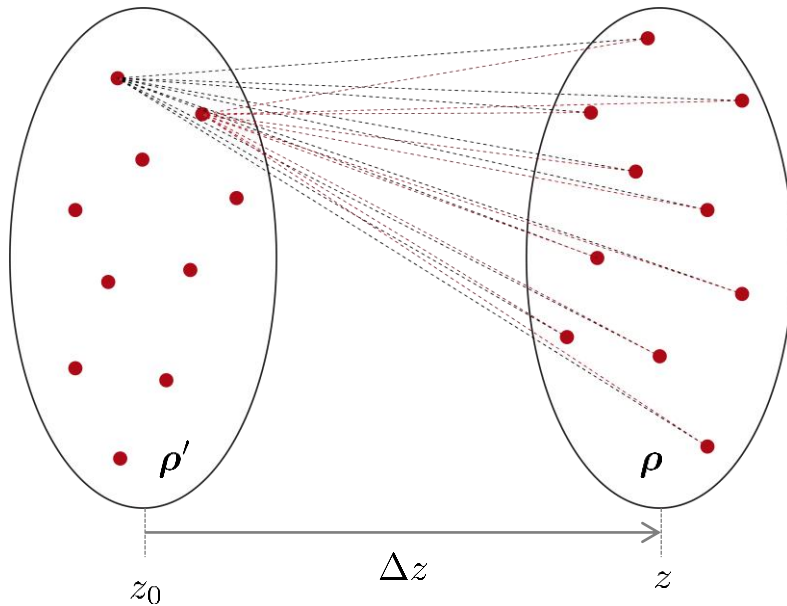
# Example: Free-Space Propagation

## Space domain

Rayleigh-Sommerfeld integral:

$$V_{\ell}^{\text{out}}(\boldsymbol{\rho}, z) \propto \iint_{-\infty}^{+\infty} V_{\ell}^{\text{in}}(\boldsymbol{\rho}', z_0) \frac{e^{ik_0 n R}}{R} \left( ik_0 n - \frac{1}{R} \right) \frac{\Delta z}{R} d^2 \rho'$$

with  $R = \sqrt{(x - x')^2 + (y - y')^2 + (\Delta z)^2}$





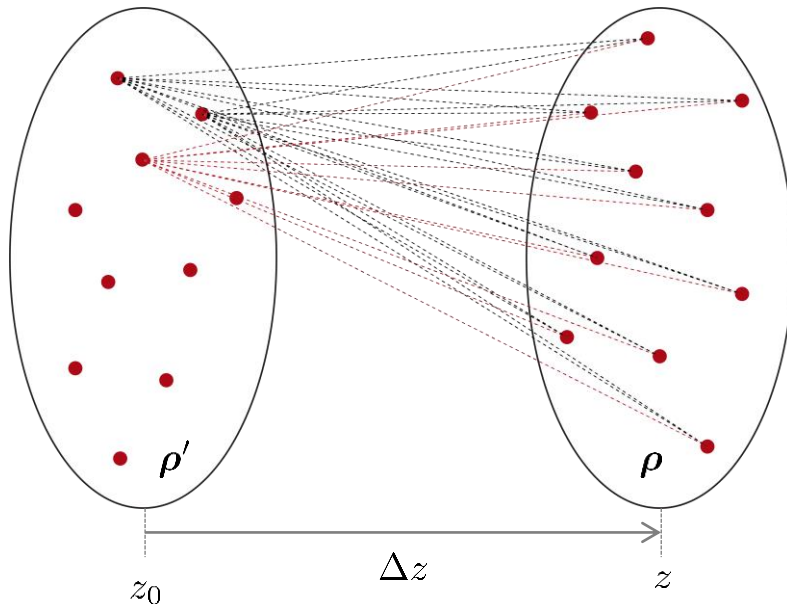
# Example: Free-Space Propagation

## Space domain

Rayleigh-Sommerfeld integral:

$$V_{\ell}^{\text{out}}(\boldsymbol{\rho}, z) \propto \iint_{-\infty}^{+\infty} V_{\ell}^{\text{in}}(\boldsymbol{\rho}', z_0) \frac{e^{ik_0 n R}}{R} \left( ik_0 n - \frac{1}{R} \right) \frac{\Delta z}{R} d^2 \rho'$$

with  $R = \sqrt{(x - x')^2 + (y - y')^2 + (\Delta z)^2}$



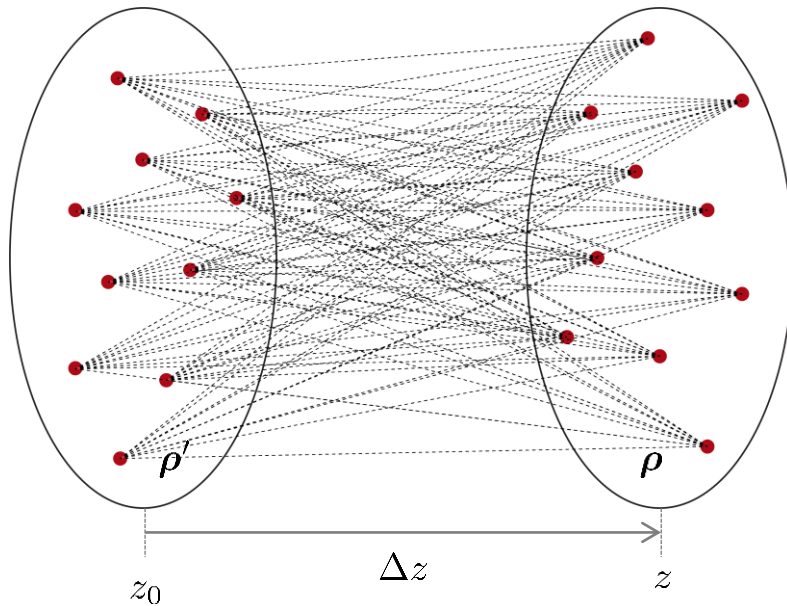
# Example: Free-Space Propagation

## Space domain

Rayleigh-Sommerfeld integral:

$$V_{\ell}^{\text{out}}(\boldsymbol{\rho}, z) \propto \iint_{-\infty}^{+\infty} V_{\ell}^{\text{in}}(\boldsymbol{\rho}', z_0) \frac{e^{ik_0 n R}}{R} \left( ik_0 n - \frac{1}{R} \right) \frac{\Delta z}{R} d^2 \rho'$$

with  $R = \sqrt{(x - x')^2 + (y - y')^2 + (\Delta z)^2}$



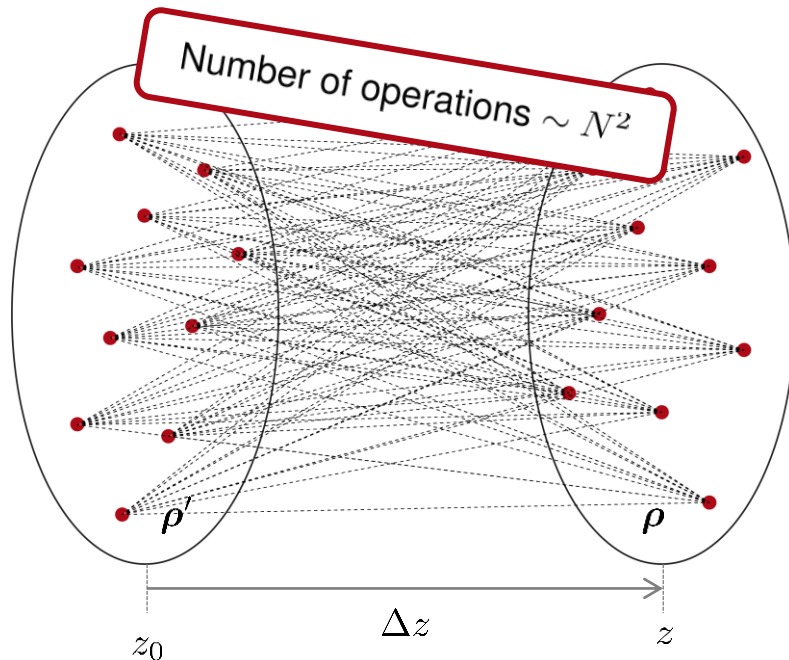
# Example: Free-Space Propagation

## Space domain

Rayleigh-Sommerfeld integral:

$$V_{\ell}^{\text{out}}(\boldsymbol{\rho}, z) \propto \iint_{-\infty}^{+\infty} V_{\ell}^{\text{in}}(\boldsymbol{\rho}', z_0) \frac{e^{ik_0 n R}}{R} \left( ik_0 n - \frac{1}{R} \right) \frac{\Delta z}{R} d^2 \rho'$$

with  $R = \sqrt{(x - x')^2 + (y - y')^2 + (\Delta z)^2}$



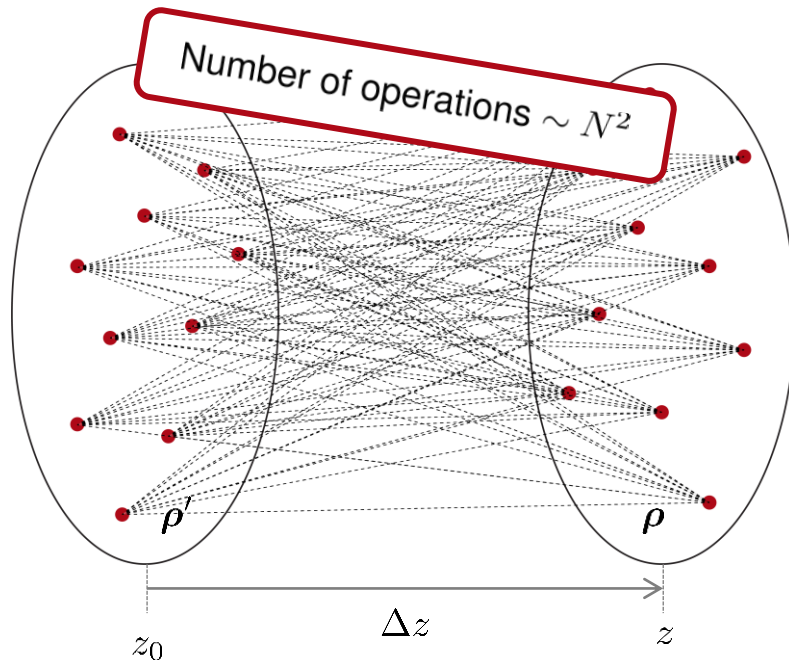
# Example: Free-Space Propagation

## Space domain

Rayleigh-Sommerfeld integral:

$$V_{\ell}^{\text{out}}(\boldsymbol{\rho}, z) \propto \iint_{-\infty}^{+\infty} V_{\ell}^{\text{in}}(\boldsymbol{\rho}', z_0) \frac{e^{ik_0 n R}}{R} \left( ik_0 n - \frac{1}{R} \right) \frac{\Delta z}{R} d^2 \rho'$$

with  $R = \sqrt{(x - x')^2 + (y - y')^2 + (\Delta z)^2}$



## Spatial-frequency domain

Plane-wave propagation operator:

$$\tilde{V}_{\ell}^{\text{out}}(\boldsymbol{\kappa}, z) = \tilde{V}_{\ell}^{\text{in}}(\boldsymbol{\kappa}, z_0) \times e^{ik_z(\boldsymbol{\kappa})\Delta z}$$

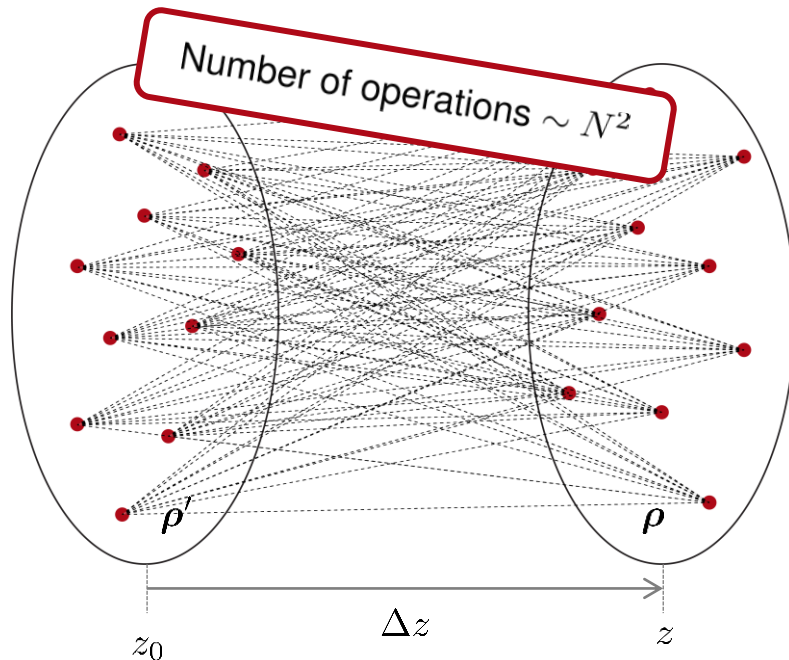
# Example: Free-Space Propagation

## Space domain

Rayleigh-Sommerfeld integral:

$$V_{\ell}^{\text{out}}(\boldsymbol{\rho}, z) \propto \iint_{-\infty}^{+\infty} V_{\ell}^{\text{in}}(\boldsymbol{\rho}', z_0) \frac{e^{ik_0 n R}}{R} \left( ik_0 n - \frac{1}{R} \right) \frac{\Delta z}{R} d^2 \rho'$$

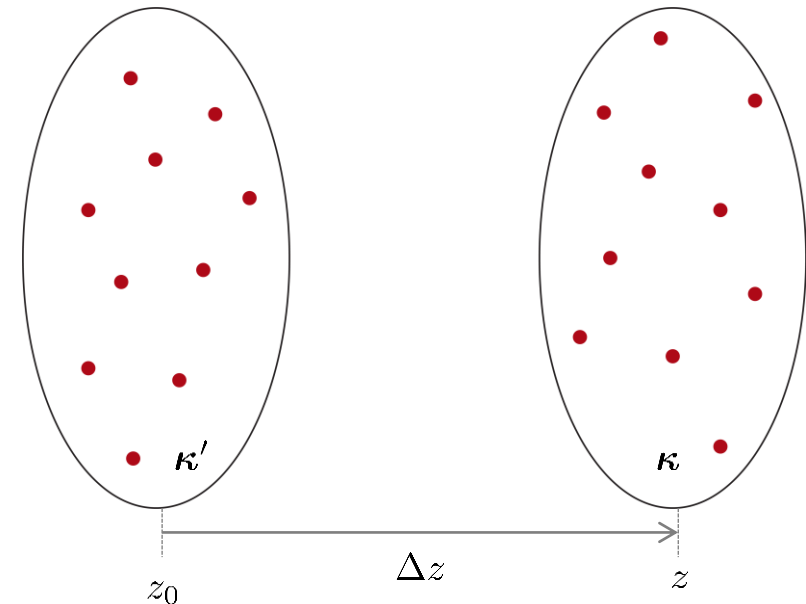
with  $R = \sqrt{(x - x')^2 + (y - y')^2 + (\Delta z)^2}$



## Spatial-frequency domain

Plane-wave propagation operator:

$$\tilde{V}_{\ell}^{\text{out}}(\boldsymbol{\kappa}, z) = \tilde{V}_{\ell}^{\text{in}}(\boldsymbol{\kappa}, z_0) \times e^{ik_z(\boldsymbol{\kappa})\Delta z}$$



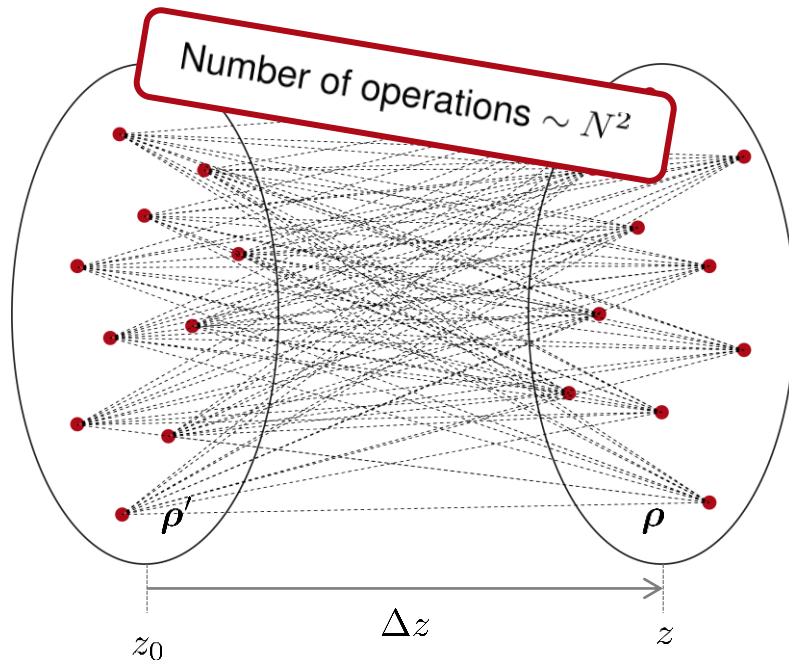
# Example: Free-Space Propagation

## Space domain

Rayleigh-Sommerfeld integral:

$$V_{\ell}^{\text{out}}(\boldsymbol{\rho}, z) \propto \iint_{-\infty}^{+\infty} V_{\ell}^{\text{in}}(\boldsymbol{\rho}', z_0) \frac{e^{ik_0 n R}}{R} \left( ik_0 n - \frac{1}{R} \right) \frac{\Delta z}{R} d^2 \rho'$$

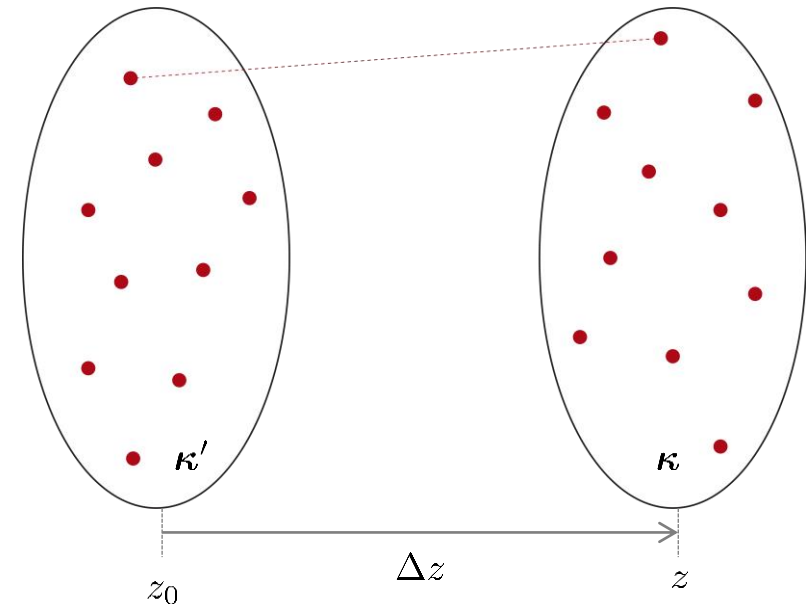
with  $R = \sqrt{(x - x')^2 + (y - y')^2 + (\Delta z)^2}$



## Spatial-frequency domain

Plane-wave propagation operator:

$$\tilde{V}_{\ell}^{\text{out}}(\boldsymbol{\kappa}, z) = \tilde{V}_{\ell}^{\text{in}}(\boldsymbol{\kappa}, z_0) \times e^{ik_z(\boldsymbol{\kappa})\Delta z}$$



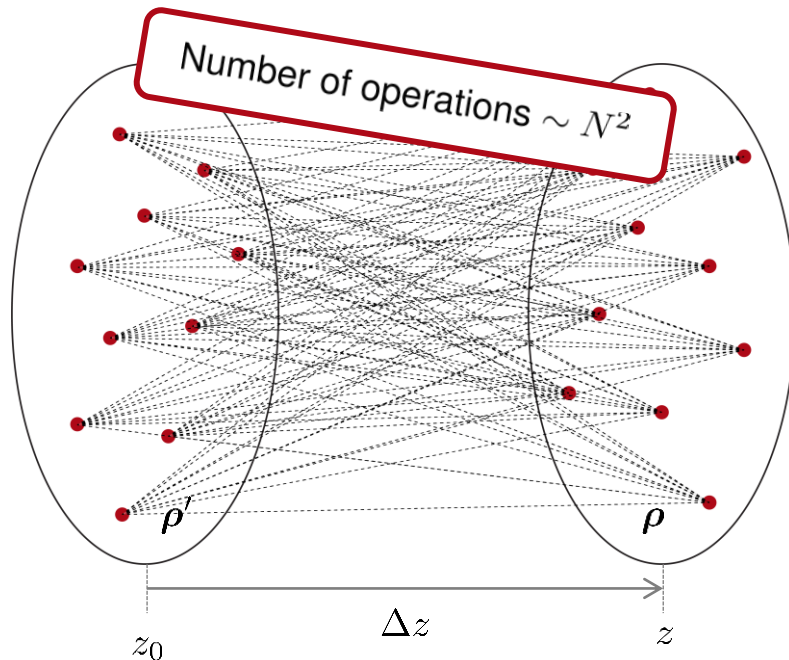
# Example: Free-Space Propagation

## Space domain

Rayleigh-Sommerfeld integral:

$$V_{\ell}^{\text{out}}(\boldsymbol{\rho}, z) \propto \iint_{-\infty}^{+\infty} V_{\ell}^{\text{in}}(\boldsymbol{\rho}', z_0) \frac{e^{ik_0 n R}}{R} \left( ik_0 n - \frac{1}{R} \right) \frac{\Delta z}{R} d^2 \rho'$$

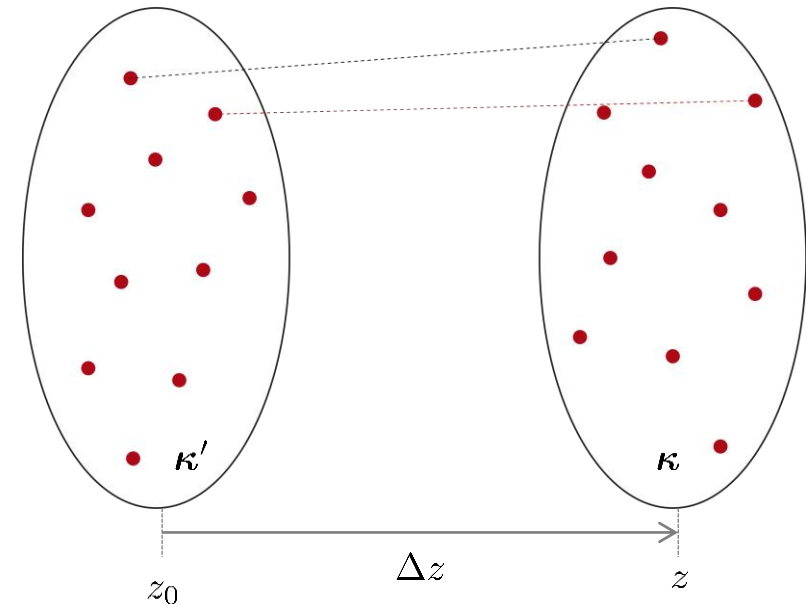
with  $R = \sqrt{(x - x')^2 + (y - y')^2 + (\Delta z)^2}$



## Spatial-frequency domain

Plane-wave propagation operator:

$$\tilde{V}_{\ell}^{\text{out}}(\boldsymbol{\kappa}, z) = \tilde{V}_{\ell}^{\text{in}}(\boldsymbol{\kappa}, z_0) \times e^{ik_z(\boldsymbol{\kappa})\Delta z}$$





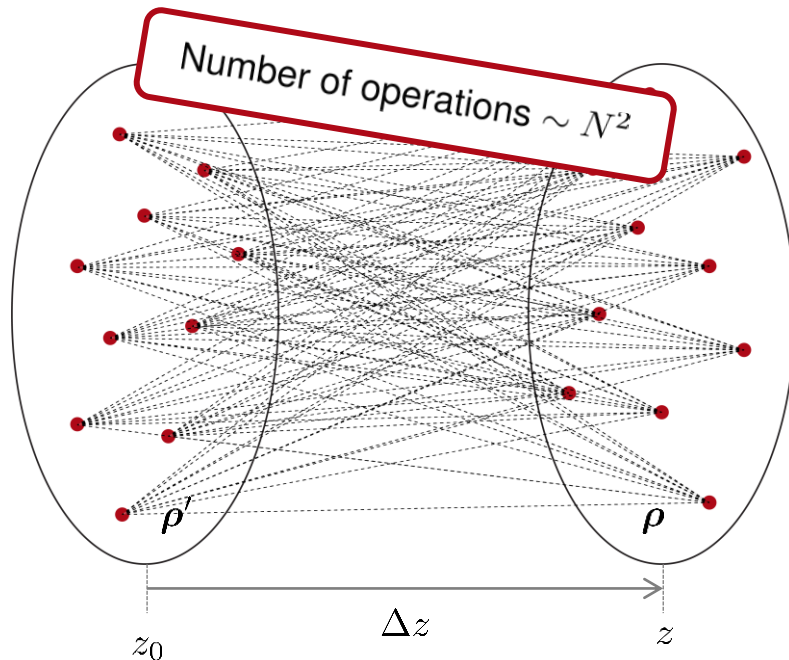
# Example: Free-Space Propagation

## Space domain

Rayleigh-Sommerfeld integral:

$$V_{\ell}^{\text{out}}(\boldsymbol{\rho}, z) \propto \iint_{-\infty}^{+\infty} V_{\ell}^{\text{in}}(\boldsymbol{\rho}', z_0) \frac{e^{ik_0 n R}}{R} \left( ik_0 n - \frac{1}{R} \right) \frac{\Delta z}{R} d^2 \rho'$$

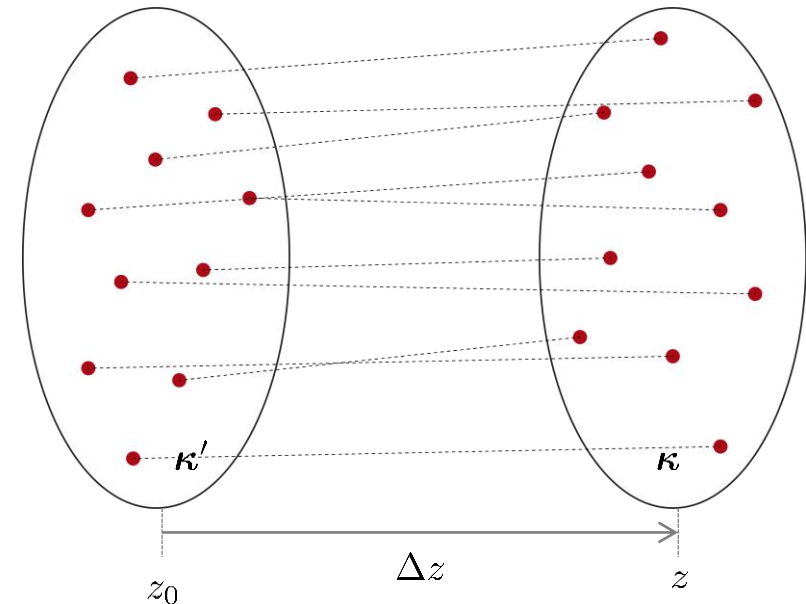
with  $R = \sqrt{(x - x')^2 + (y - y')^2 + (\Delta z)^2}$



## Spatial-frequency domain

Plane-wave propagation operator:

$$\tilde{V}_{\ell}^{\text{out}}(\boldsymbol{\kappa}, z) = \tilde{V}_{\ell}^{\text{in}}(\boldsymbol{\kappa}, z_0) \times e^{ik_z(\boldsymbol{\kappa})\Delta z}$$





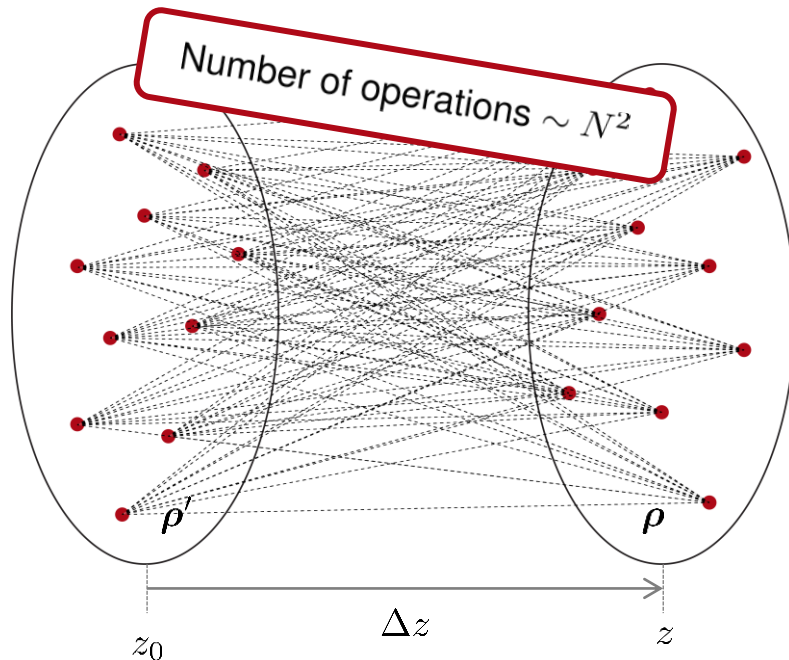
# Example: Free-Space Propagation

## Space domain

Rayleigh-Sommerfeld integral:

$$V_{\ell}^{\text{out}}(\boldsymbol{\rho}, z) \propto \iint_{-\infty}^{+\infty} V_{\ell}^{\text{in}}(\boldsymbol{\rho}', z_0) \frac{e^{ik_0 n R}}{R} \left( ik_0 n - \frac{1}{R} \right) \frac{\Delta z}{R} d^2 \rho'$$

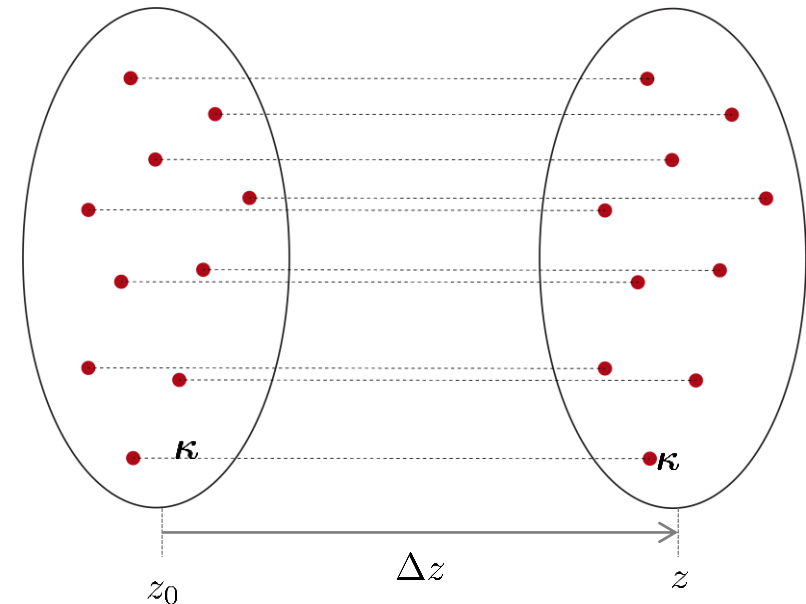
with  $R = \sqrt{(x - x')^2 + (y - y')^2 + (\Delta z)^2}$



## Spatial-frequency domain

Plane-wave propagation operator:

$$\tilde{V}_{\ell}^{\text{out}}(\boldsymbol{\kappa}, z) = \tilde{V}_{\ell}^{\text{in}}(\boldsymbol{\kappa}, z_0) \times e^{ik_z(\boldsymbol{\kappa})\Delta z}$$



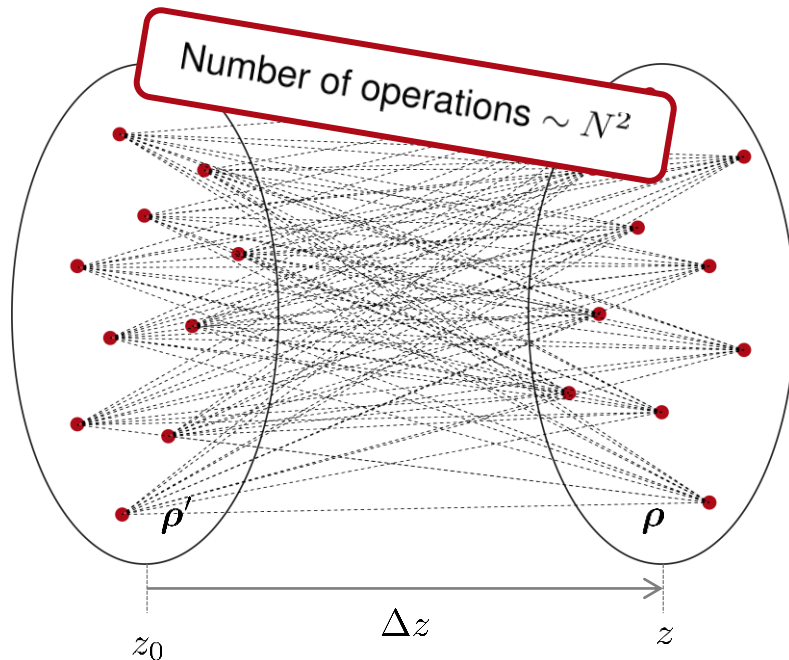
# Example: Free-Space Propagation

## Space domain

Rayleigh-Sommerfeld integral:

$$V_{\ell}^{\text{out}}(\boldsymbol{\rho}, z) \propto \iint_{-\infty}^{+\infty} V_{\ell}^{\text{in}}(\boldsymbol{\rho}', z_0) \frac{e^{ik_0 n R}}{R} \left( ik_0 n - \frac{1}{R} \right) \frac{\Delta z}{R} d^2 \rho'$$

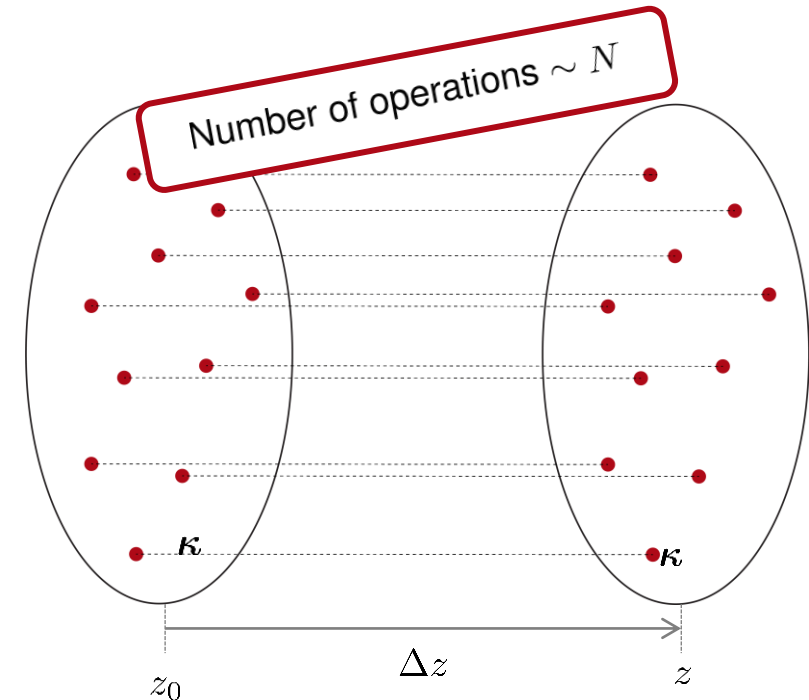
with  $R = \sqrt{(x - x')^2 + (y - y')^2 + (\Delta z)^2}$



## Spatial-frequency domain

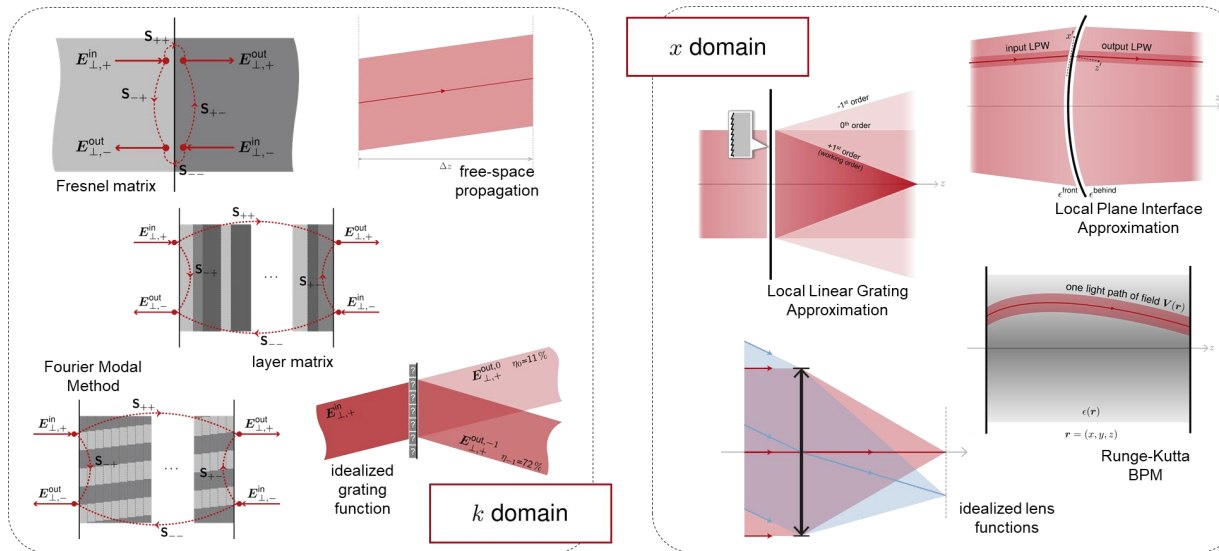
Plane-wave propagation operator:

$$\tilde{V}_{\ell}^{\text{out}}(\boldsymbol{\kappa}, z) = \tilde{V}_{\ell}^{\text{in}}(\boldsymbol{\kappa}, z_0) \times e^{ik_z(\boldsymbol{\kappa})\Delta z}$$



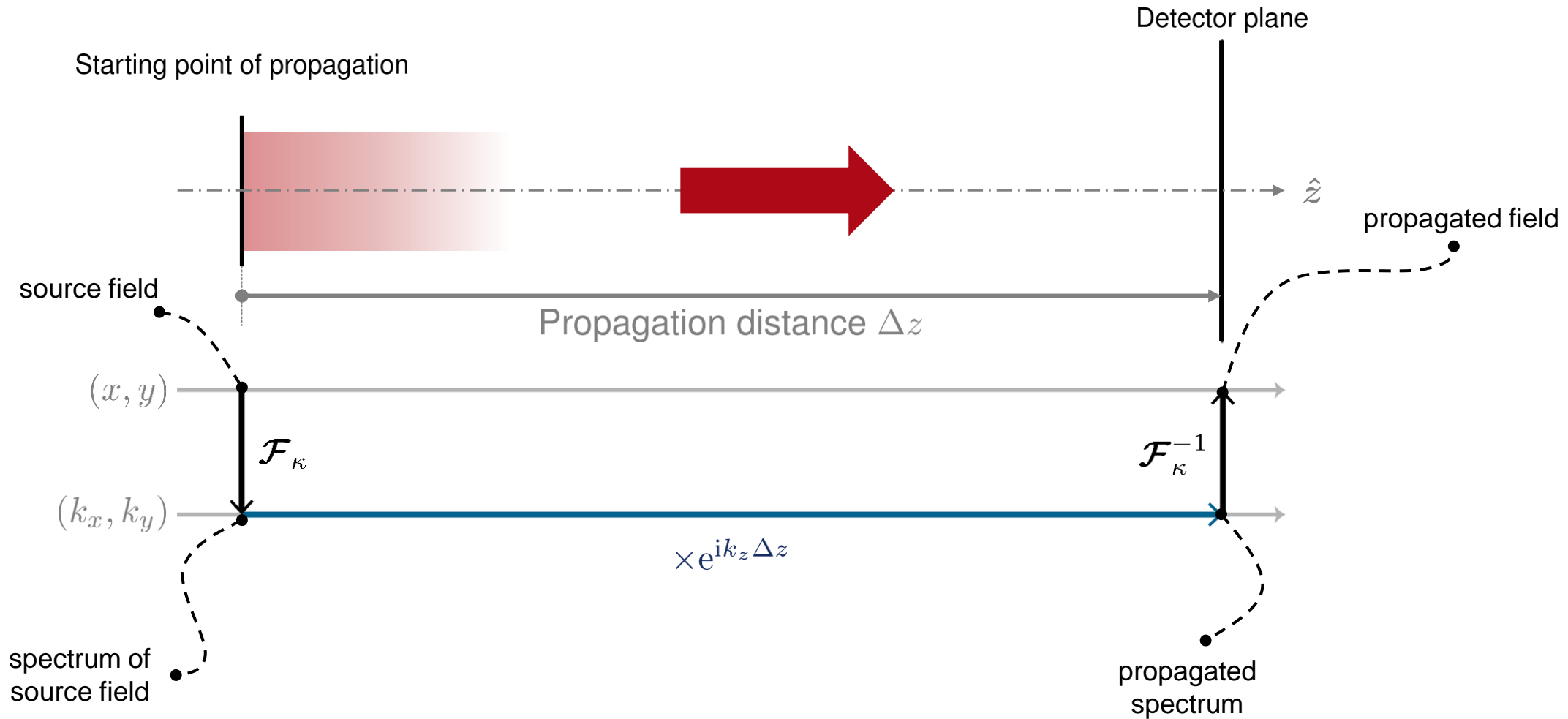
# Why Different Fourier Domains?

Although, in general, electromagnetic field solvers have an **integral** behaviour, with the resulting high numerical complexity, the characteristics of some of the most common optical components mean they can be modeled with **pointwise** operators in one of the Fourier domains – when this happens, it entails a **massive computational advantage**!

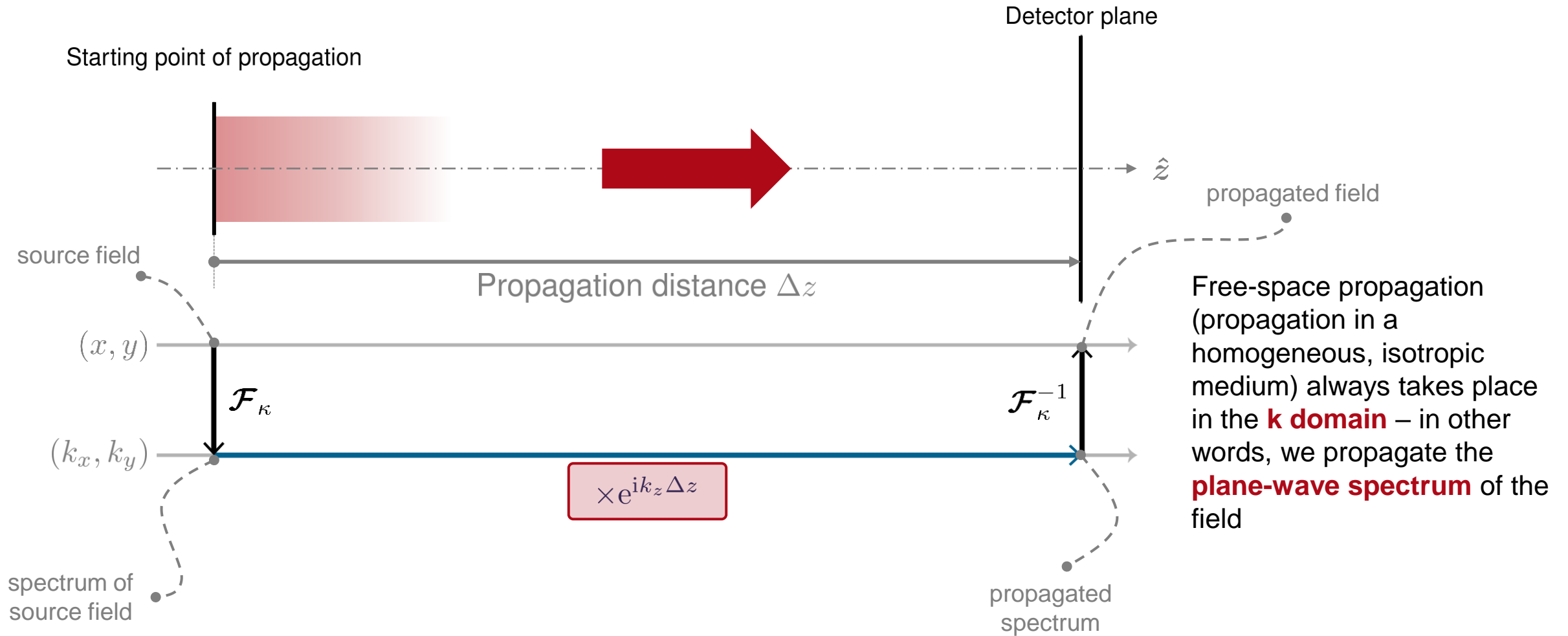


**Conclusion:** Whenever this mathematical property presents itself, we implement the solver in the domain where it exhibits **pointwise behaviour**!

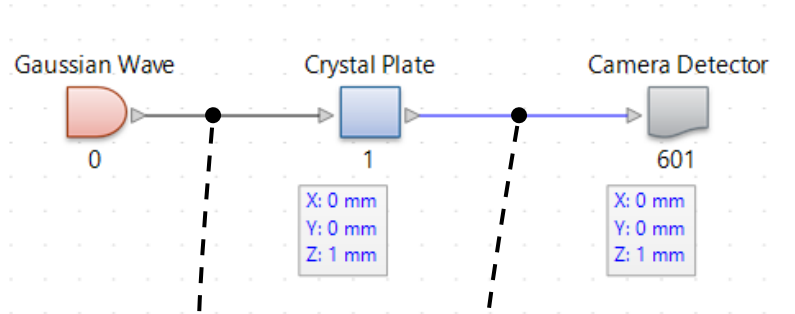
# Free-Space Propagation



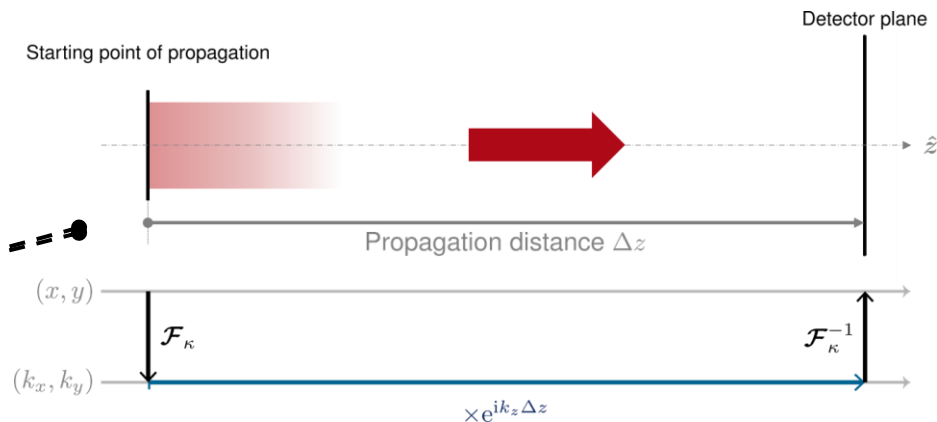
# Free-Space Propagation



# Propagation Through a System with a Crystal Plate

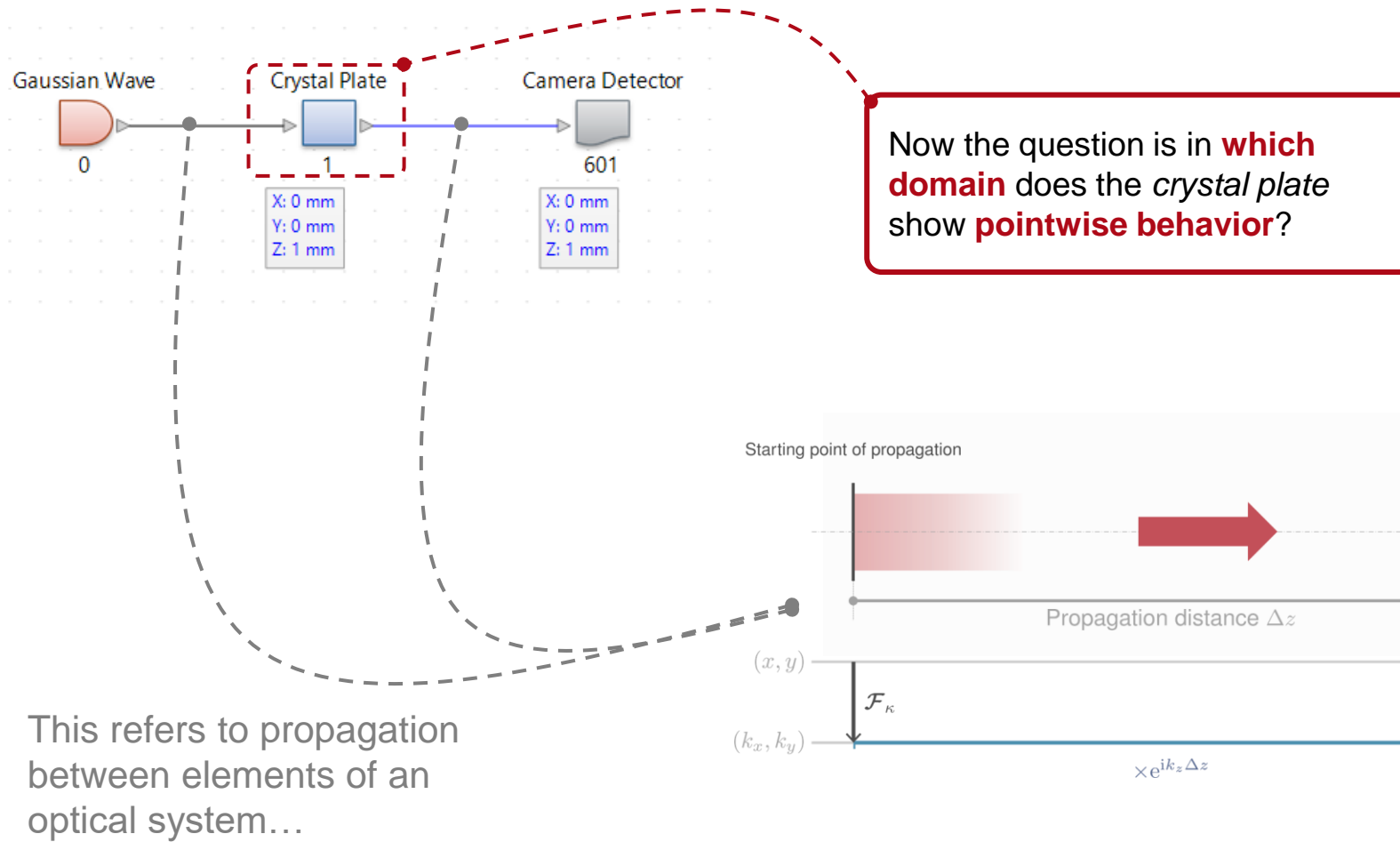


This refers to propagation between elements of an optical system...



Free-space propagation (propagation in a homogeneous, isotropic medium) always takes place in the **k domain** – in other words, we propagate the **plane-wave spectrum** of the field

# Propagation Through a System with a Crystal Plate



Free-space propagation (propagation in a homogeneous, isotropic medium) always takes place in the **k domain** – in other words, we propagate the **plane-wave spectrum** of the field

# Field Solver for an Anisotropic Media

4: Optical Setup View #3 (Optical Setup)\*

Filter by...

- Light Sources
- Components
  - Component from Catalog
    - Index Modulated & Crystals
      - Crystal Plate**
      - Fiber Element
      - GRIN Lens
      - Inhomogeneous Medium
    - Multiple Surfaces
      - Single Surface & Coating
      - Single Surface & Function
      - Single Surface & Stack
    - Programmable Component
    - Subsystem
  - Ideal Components
  - Detectors
  - Analyzers
    - Coordinate Break
    - Camera Detector
    - Electromagnetic Field Detector

Gaussian Wave 0

Crystal Plate

X: 0 mm  
Y: 0 mm  
Z: 1 mm

Ray Tracing Sy Analyzer 800

Edit Crystal Plate Component

Solver Sampling

Component Solver Layer Matrix [S-Matrix] Edit

The layer matrix solver works in the spatial frequency domain (**k domain**). It consists of

1. an eigenmode solver for the homogeneous and isotropic media on both sides of the crystal as well as for the anisotropic crystal itself and
2. an S-matrix for matching the boundary conditions at all surfaces.

The eigenmode solver computes the field solution in the k domain for the homogeneous and isotropic or anisotropic medium in the crystal and its adjacent media. The S-matrix algorithm calculates the response of the whole system by matching the boundary conditions in a recursive manner. [Learn more about this solver.](#)

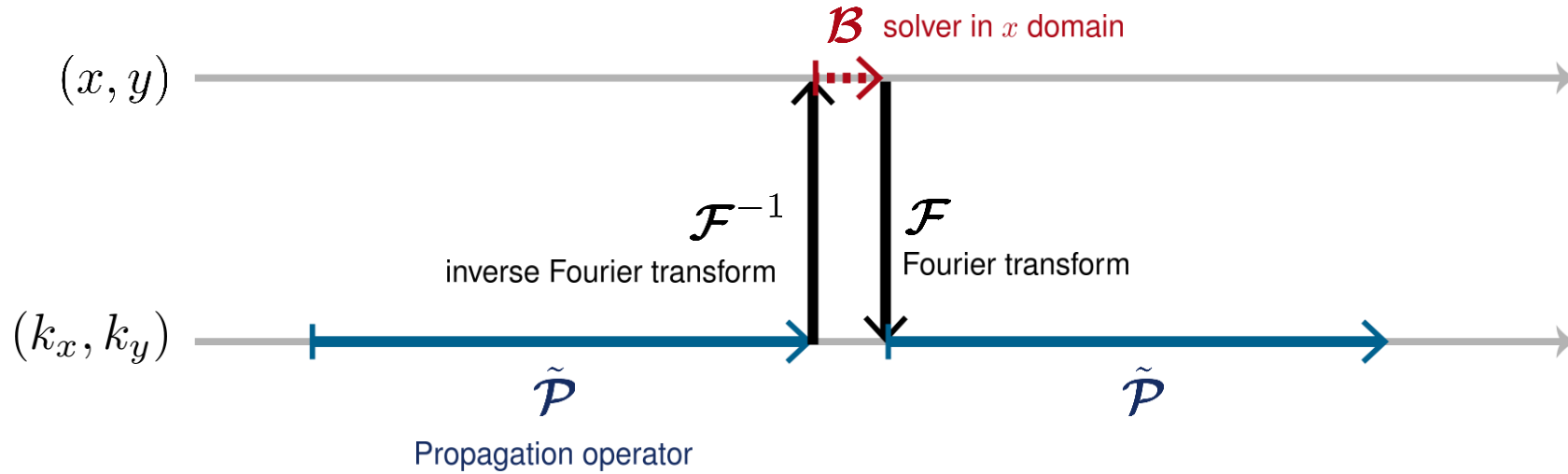
$E_{\perp,+}^{in}$   $S_{++}$   $E_{\perp,+}^{out}$   $S_{-+}$   $S_{+-}$   $E_{\perp,-}^{out}$   $S_{--}$   $E_{\perp,-}^{in}$

This solver is implemented in the spatial-frequency (k) domain

Validity: OK Cancel Help

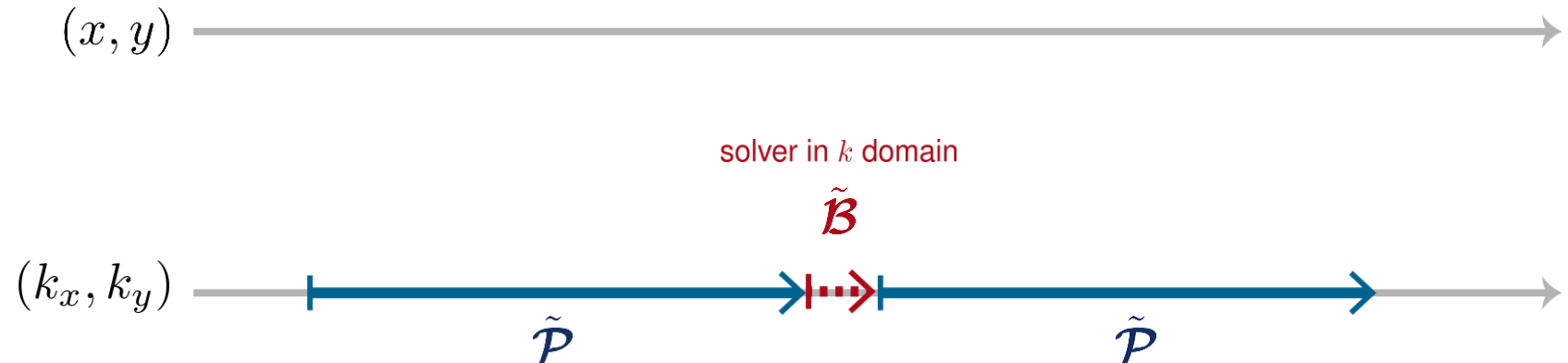


# Domain of Application of the Solvers

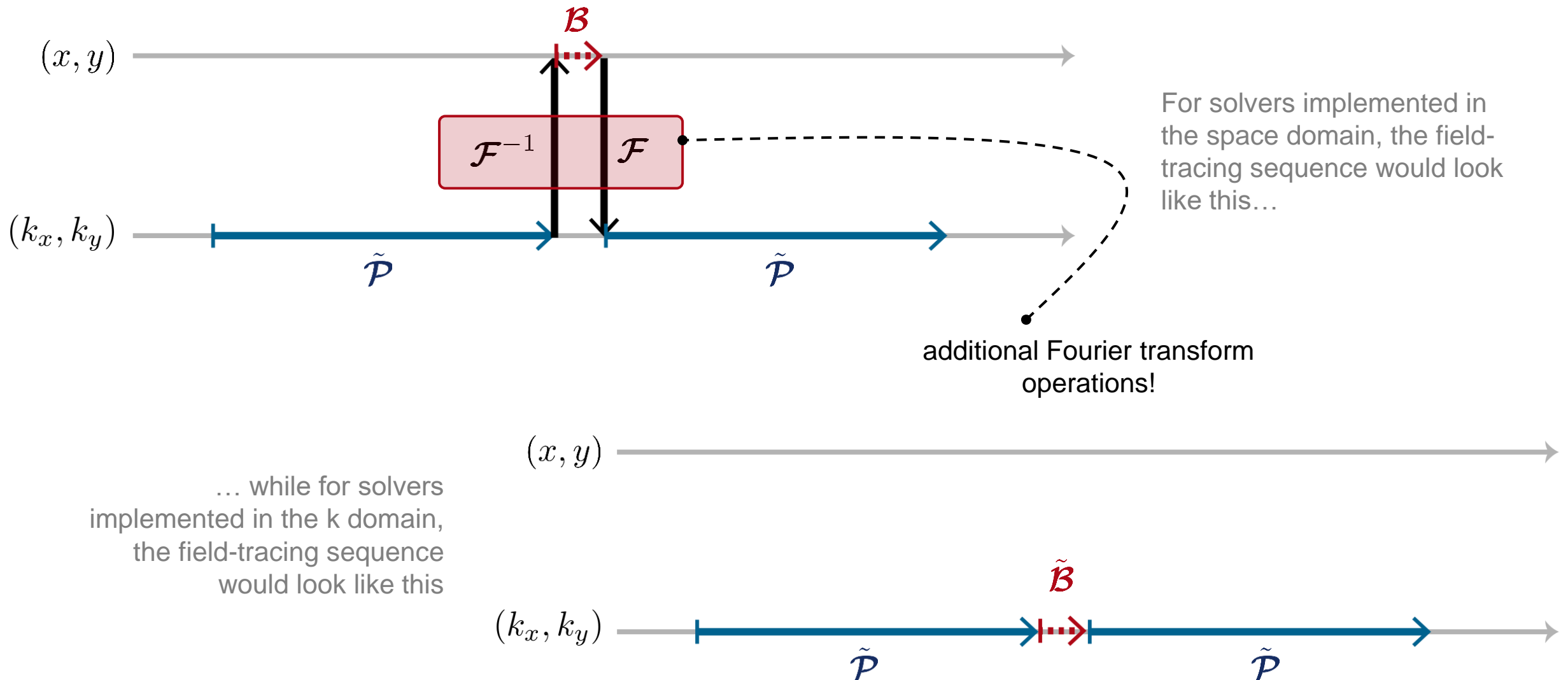


For solvers implemented in the space domain, the field-tracing sequence would look like this...

... while for solvers implemented in the  $k$  domain, the field-tracing sequence would look like this



# Domain of Application of the Solvers



# Layer Matrix [S-Matrix] Solver Characteristics

The layer matrix solver consists of:

1. An eigenmode solver for the homogeneous and **isotropic media** before and after the crystal surfaces
2. An eigenmode solver for the homogenous and **anisotropic media** in the crystal itself
3. An S-matrix for matching the **boundary conditions** at all the surfaces of the crystal

## Eigenmode Solver:

- Computes the field solution in each layer.
- Works in spatial-frequency (k) domain.
- Assumes constant **permittivity** in each layer.
- The layers must have constant thickness in x-,y- plane (infinite in x & y).

## S-Matrix:

- Calculates the response of the whole layered system using the boundary condition.
- Works in spatial-frequency (k) domain.
- Exhibits unconditional numerical stability  
➔ potential numerical gain.

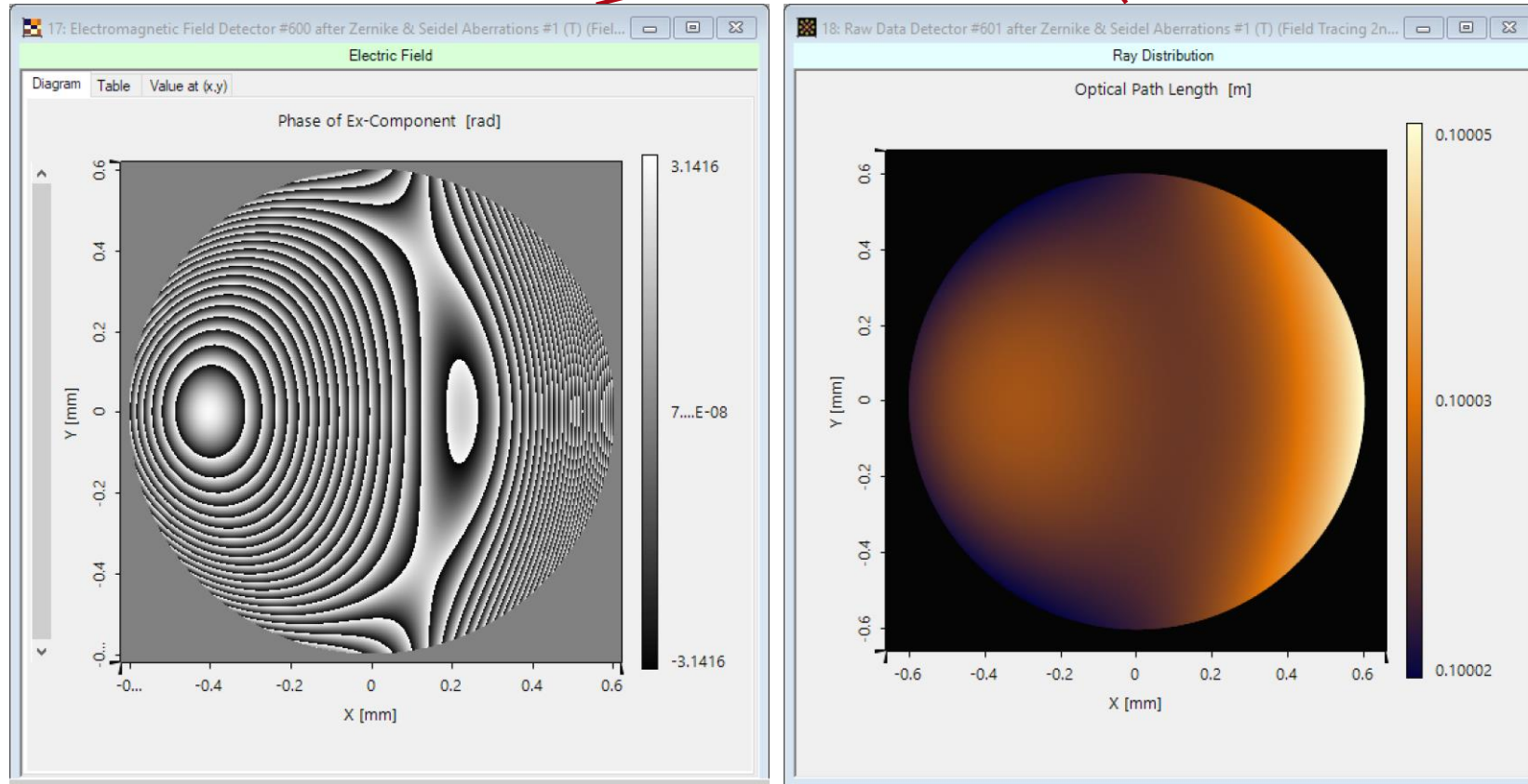
Part 3

# The Fourier Transform



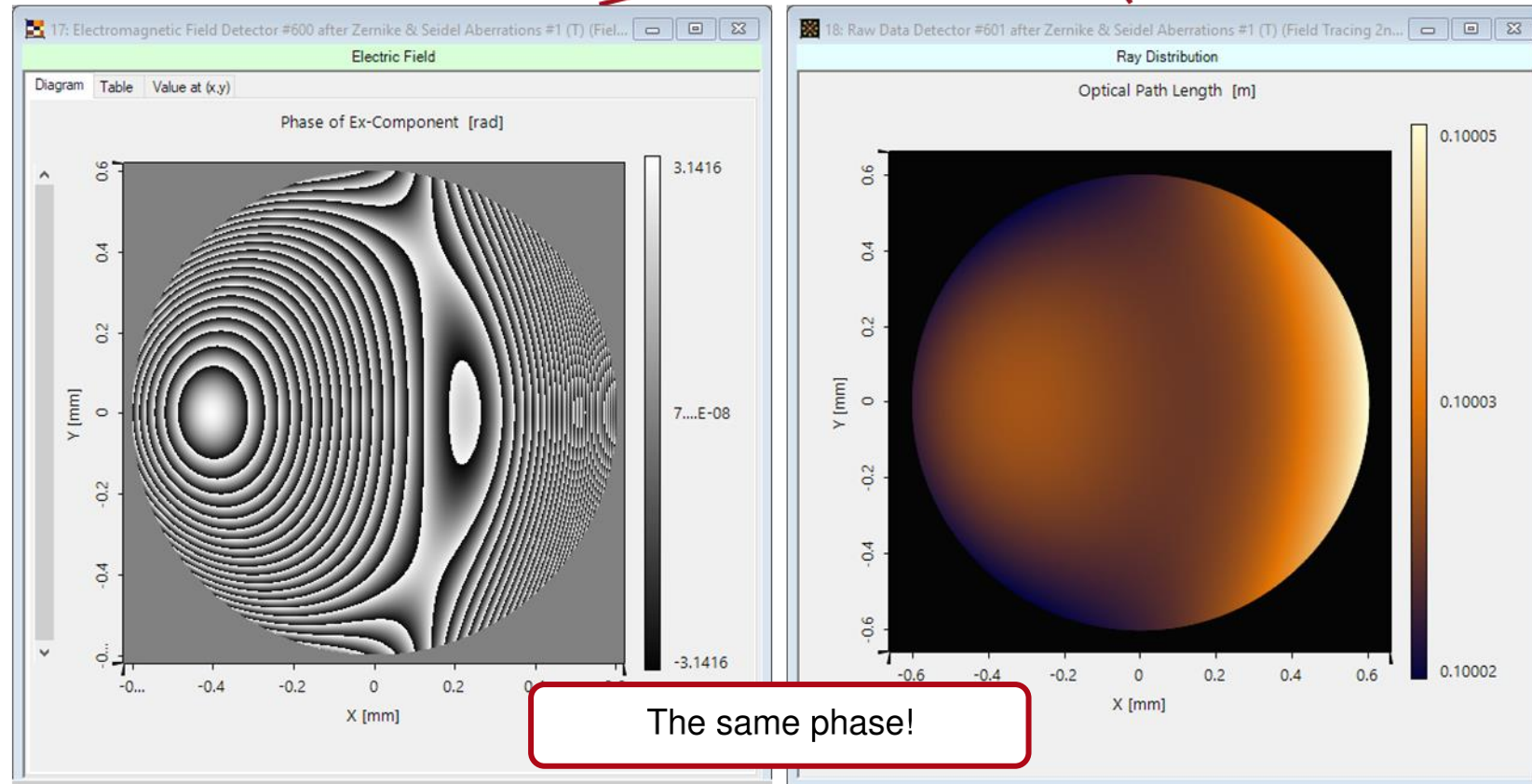
# Fourier-Transforming an Arbitrary Field

$$V_\ell(\rho, z, \omega) = |V_\ell(\rho, z, \omega)| \exp(i\phi_\ell(\rho, z, \omega)) \exp(i\psi(\rho, z, \omega))$$



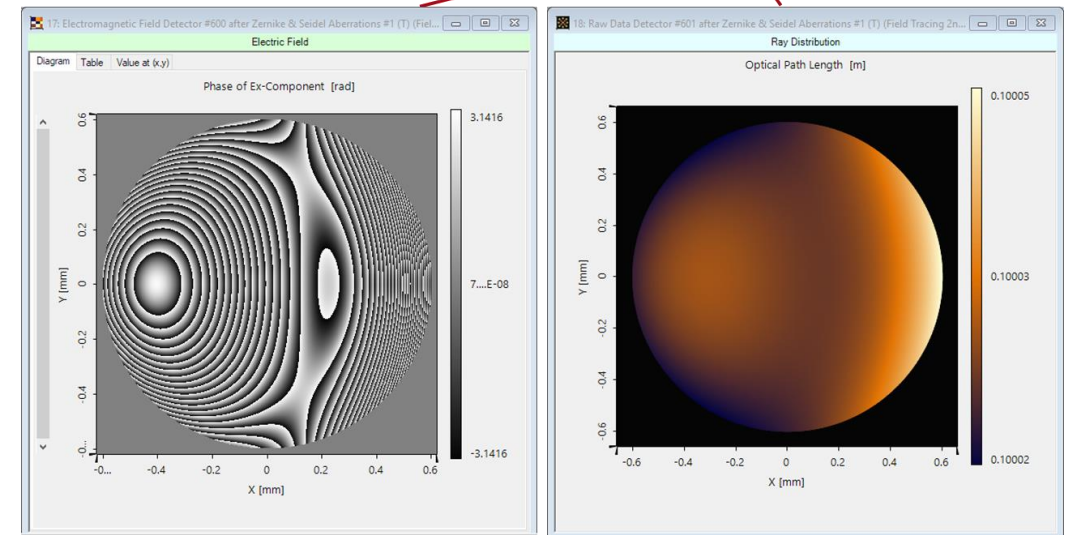
# Fourier-Transforming an Arbitrary Field

$$V_\ell(\rho, z, \omega) = |V_\ell(\rho, z, \omega)| \exp(i\varphi_\ell(\rho, z, \omega)) \exp(i\psi(\rho, z, \omega))$$



# Fourier-Transforming an Arbitrary Field

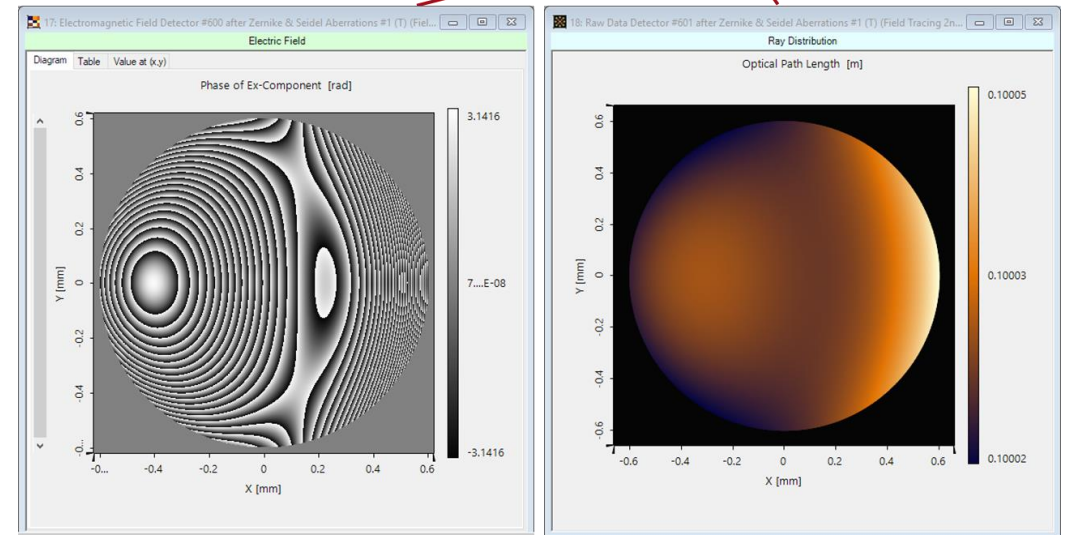
$$V_{\ell}(\rho, z, \omega) = |V_{\ell}(\rho, z, \omega)| \exp(i\varphi_{\ell}(\rho, z, \omega)) \exp(i\psi(\rho, z, \omega))$$



# Fourier-Transforming an Arbitrary Field

- Direct discretization of Fourier integral  $\rightarrow$  DFT (Discrete Fourier Transform): numerical complexity  $\sim N^2$

$$V_\ell(\boldsymbol{\rho}, z, \omega) = |V_\ell(\boldsymbol{\rho}, z, \omega)| \exp(i\varphi_\ell(\boldsymbol{\rho}, z, \omega)) \exp(i\psi(\boldsymbol{\rho}, z, \omega))$$

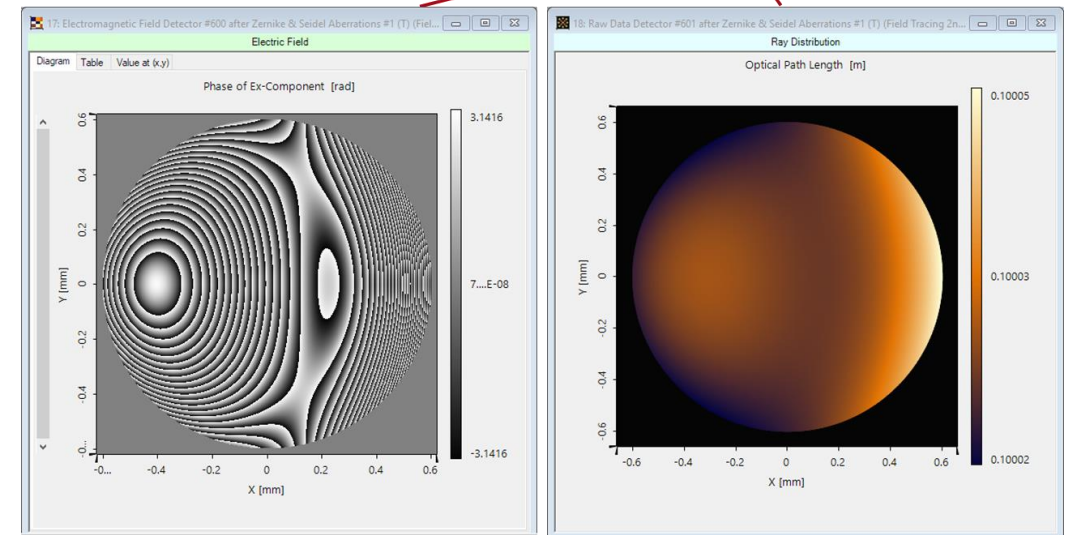




# Fourier-Transforming an Arbitrary Field

- Direct discretization of Fourier integral  $\rightarrow$  DFT (Discrete Fourier Transform): numerical complexity  $\sim N^2$
- Numerical trick in Fast Fourier Transform (FFT) brings down computational effort to  $\sim N \log N \rightarrow \sim N$

$$V_\ell(\boldsymbol{\rho}, z, \omega) = |V_\ell(\boldsymbol{\rho}, z, \omega)| \exp(i\varphi_\ell(\boldsymbol{\rho}, z, \omega)) \exp(i\psi(\boldsymbol{\rho}, z, \omega))$$

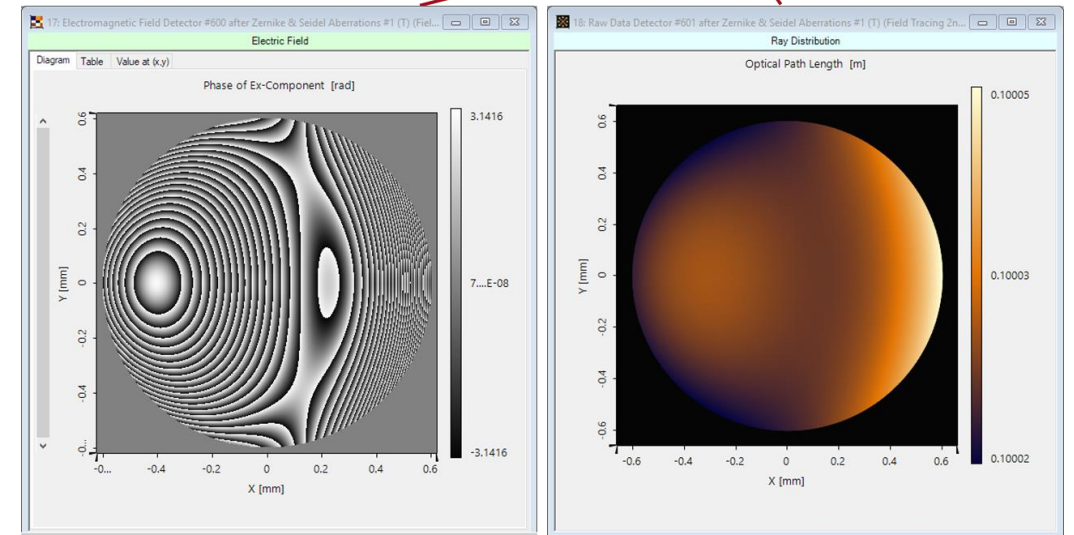


# Fourier-Transforming an Arbitrary Field

- Direct discretization of Fourier integral  $\rightarrow$  DFT (Discrete Fourier Transform): numerical complexity  $\sim N^2$
- Numerical trick in Fast Fourier Transform (FFT) brings down computational effort to  $\sim N \log N \rightarrow \sim N$

This already means **pointwise** operation, right?  
Job done! ✓

$$V_\ell(\boldsymbol{\rho}, z, \omega) = |V_\ell(\boldsymbol{\rho}, z, \omega)| \exp(i\varphi_\ell(\boldsymbol{\rho}, z, \omega)) \exp(i\psi(\boldsymbol{\rho}, z, \omega))$$

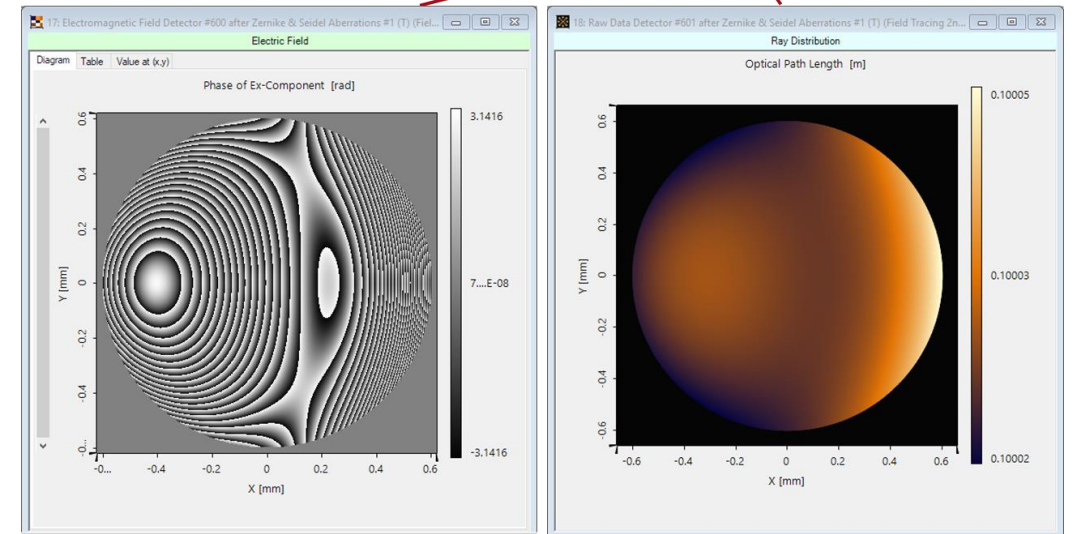


# Fourier-Transforming an Arbitrary Field

- Direct discretization of Fourier integral  $\rightarrow$  DFT (Discrete Fourier Transform): numerical complexity  $\sim N^2$
- Numerical trick in Fast Fourier Transform (FFT) brings down computational effort to  $\sim N \log N \rightarrow \sim N$

This already means **pointwise** operation, right?  
Job done! ✗

$$V_\ell(\boldsymbol{\rho}, z, \omega) = |V_\ell(\boldsymbol{\rho}, z, \omega)| \exp(i\varphi_\ell(\boldsymbol{\rho}, z, \omega)) \exp(i\psi(\boldsymbol{\rho}, z, \omega))$$



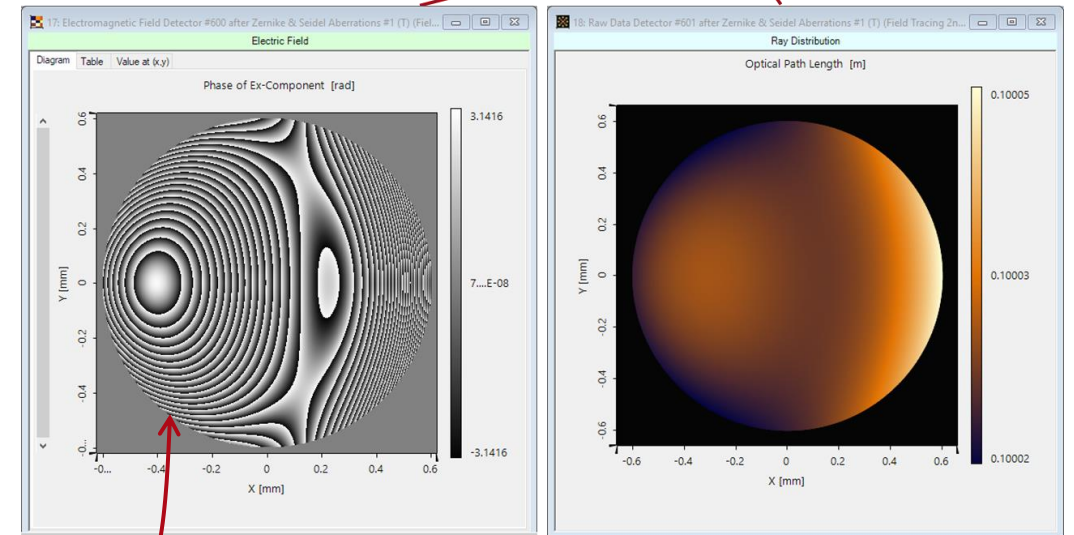
# Fourier-Transforming an Arbitrary Field

- Direct discretization of Fourier integral  $\rightarrow$  DFT (Discrete Fourier Transform): numerical complexity  $\sim N^2$
- Numerical trick in Fast Fourier Transform (FFT) brings down computational effort to  $\sim N \log N \rightarrow \sim N$

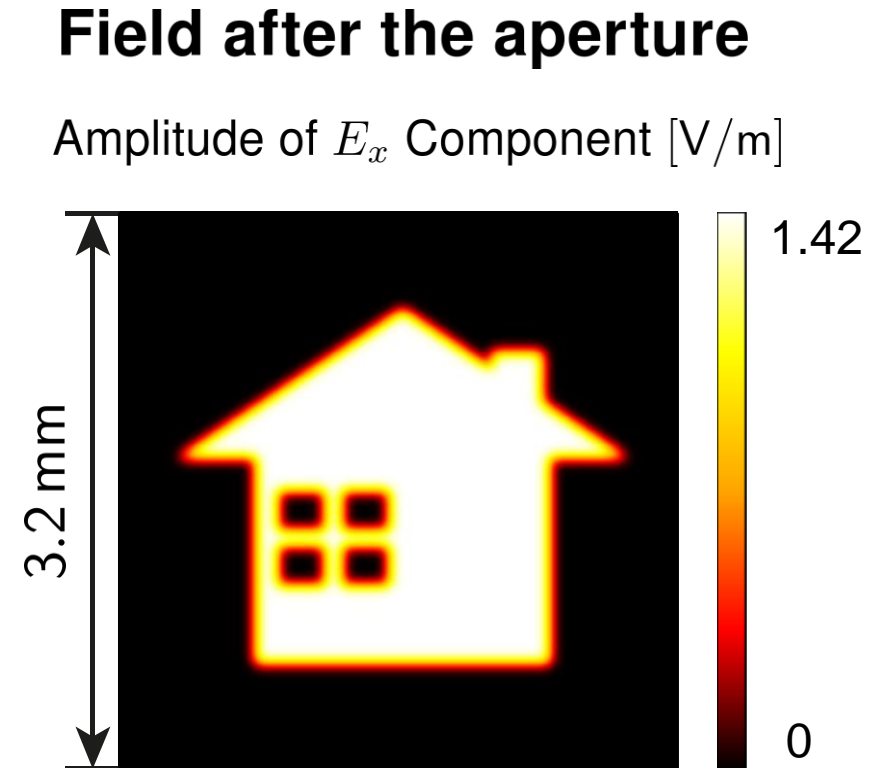
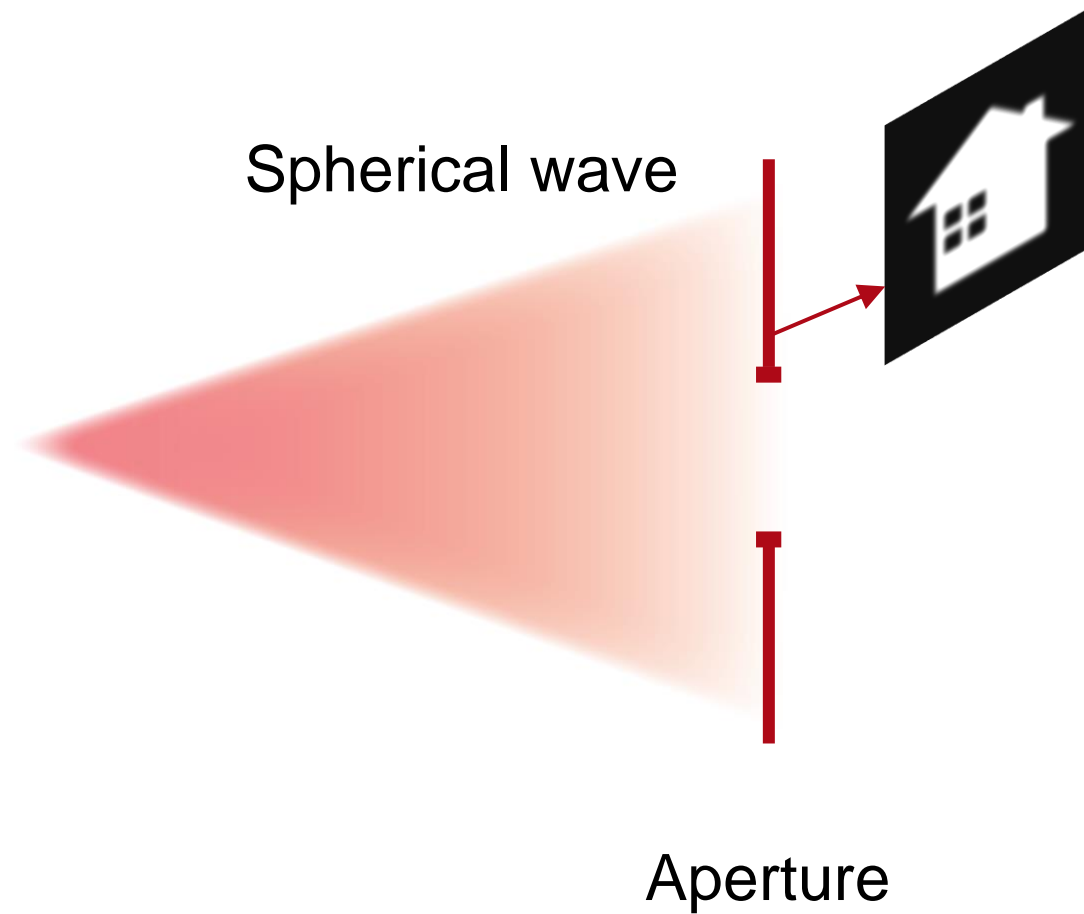
$$V_\ell(\boldsymbol{\rho}, z, \omega) = |V_\ell(\boldsymbol{\rho}, z, \omega)| \exp(i\varphi_\ell(\boldsymbol{\rho}, z, \omega)) \exp(i\psi(\boldsymbol{\rho}, z, \omega))$$

The FFT requires fulfilment of the Nyquist-Shannon sampling theorem  $\Rightarrow$  wrapped phase **must** be well resolved!

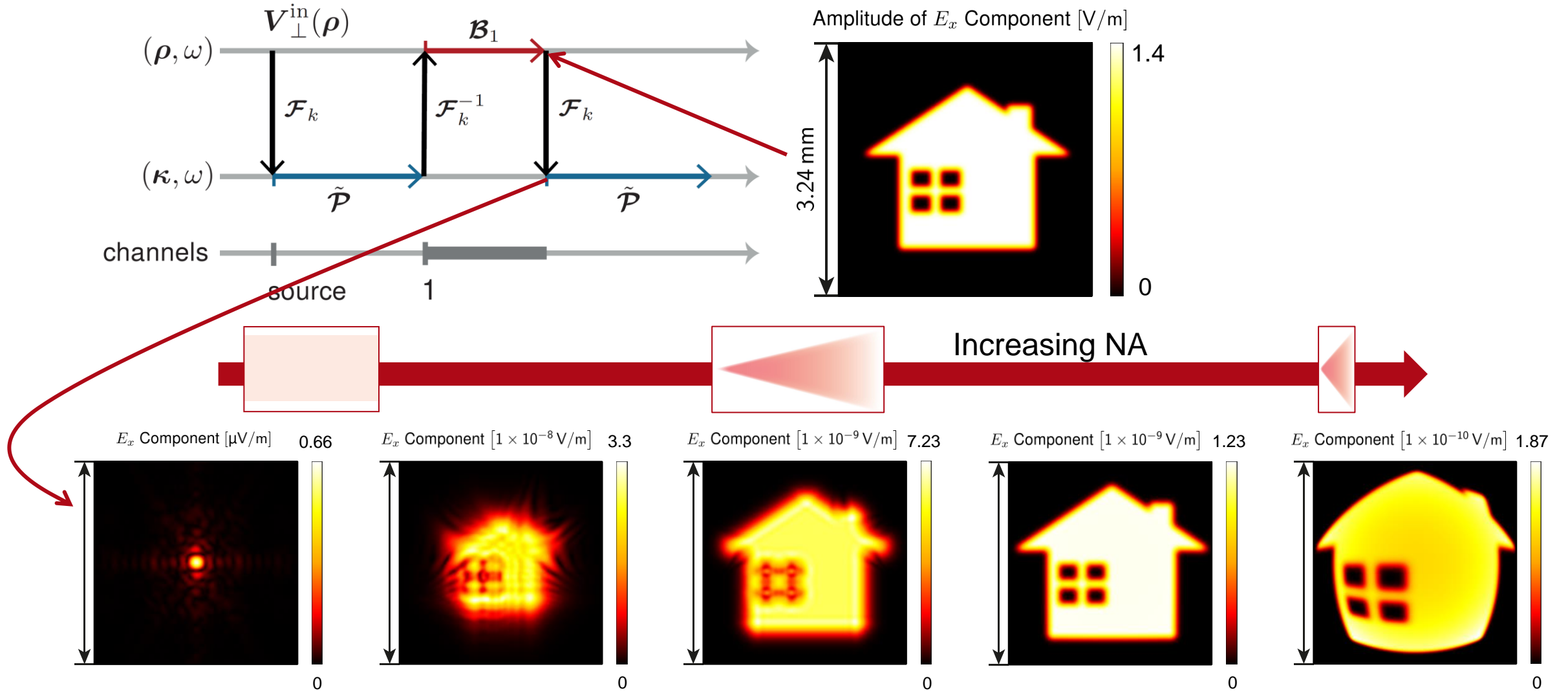
$\Downarrow$   
**Huge sample number  $N$**



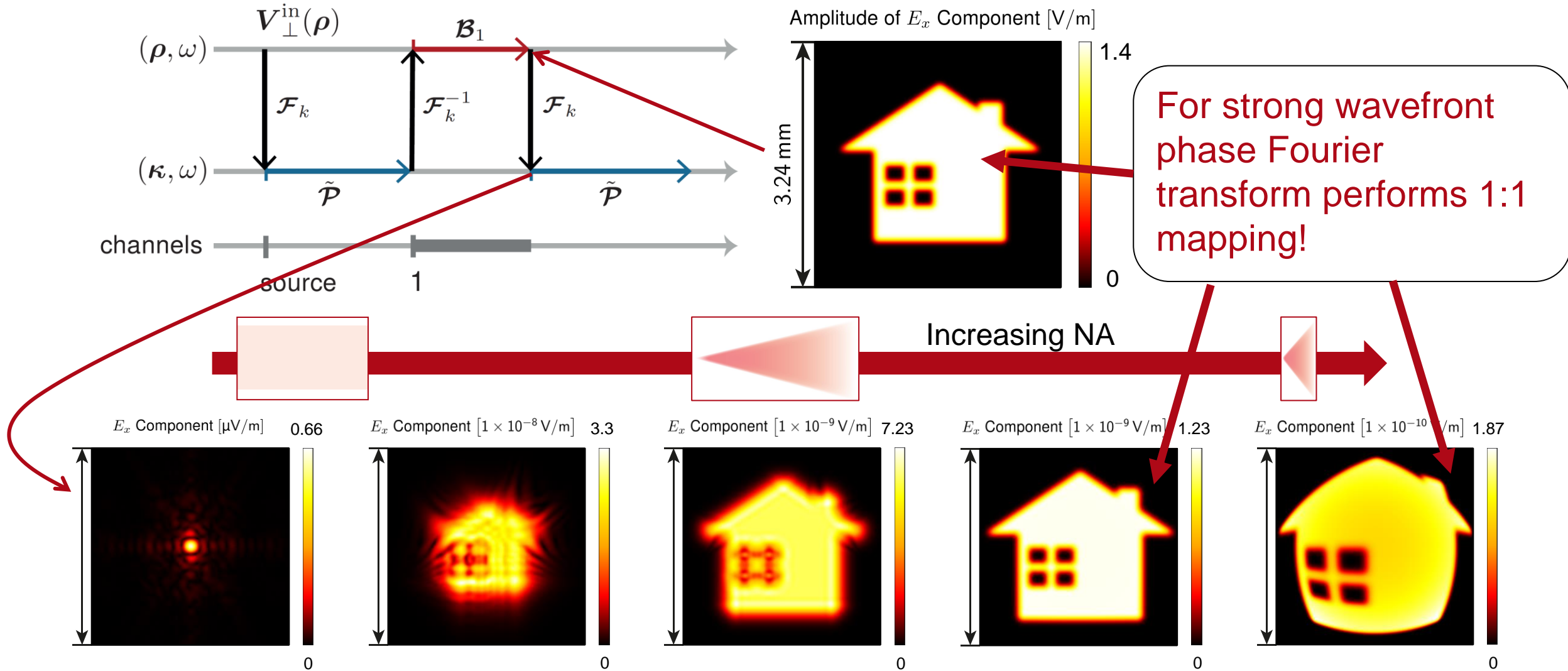
# Modeling the Propagation Through an Aperture



# Results of Fourier Transform

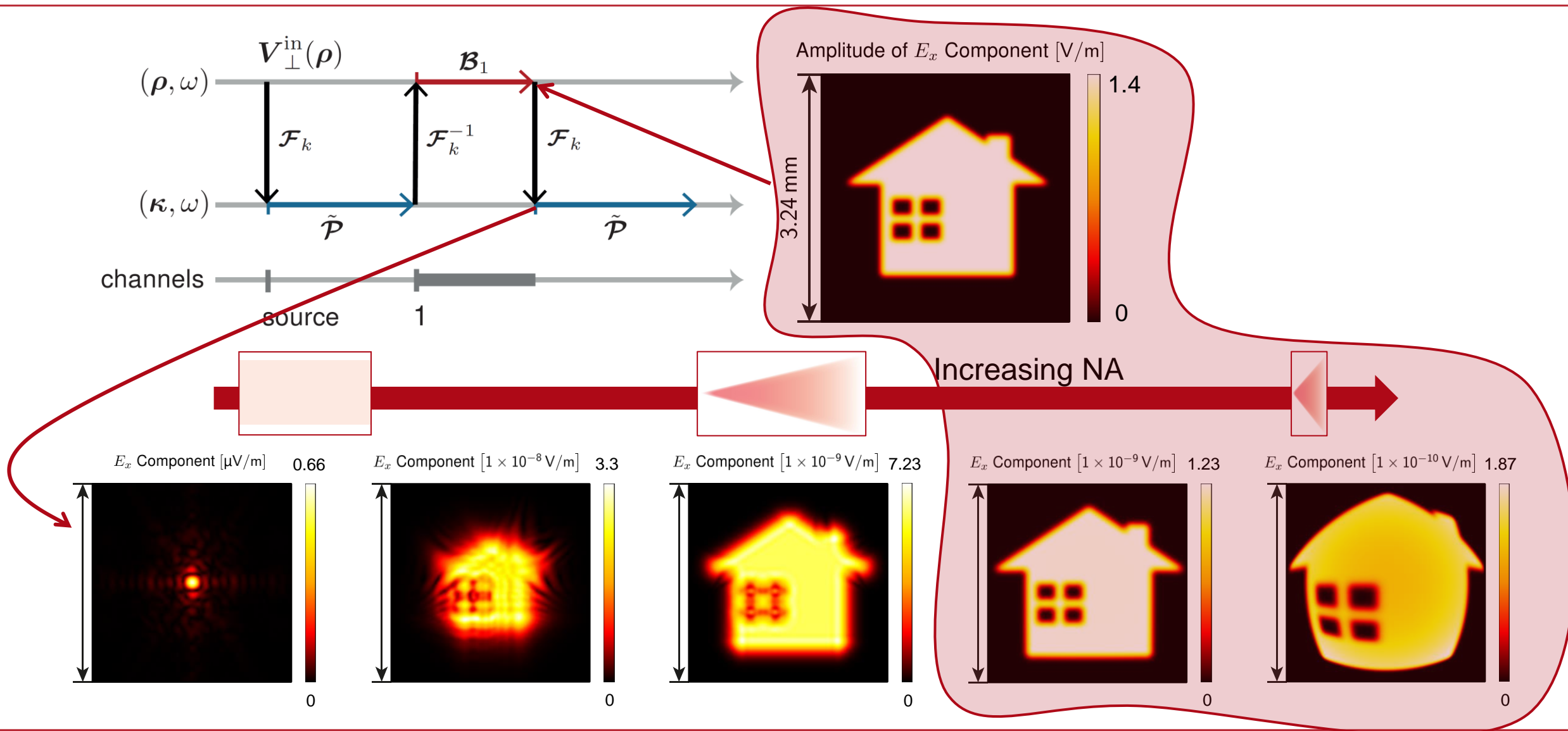


# Results of Fourier Transform



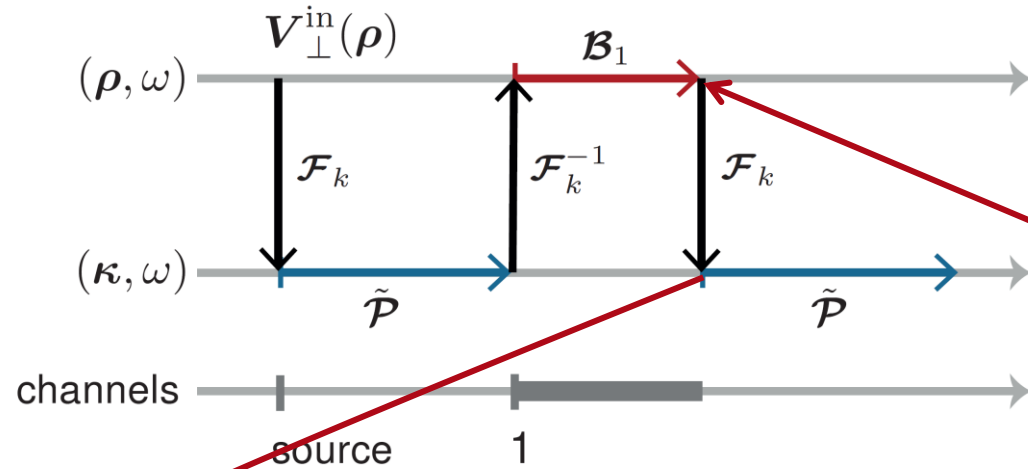


# Results of Fourier Transform





# Results of Fourier Transform



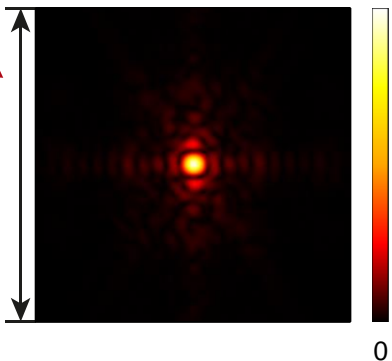
Amplitude of  $E_x$  Component [V/m]



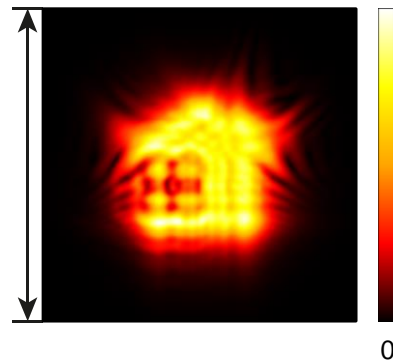
This behaviour can be used to develop an approximate algorithm to compute the Fourier transform that is **extremely accurate** when the field exhibits this behaviour, and **extremely fast**

Increasing NA

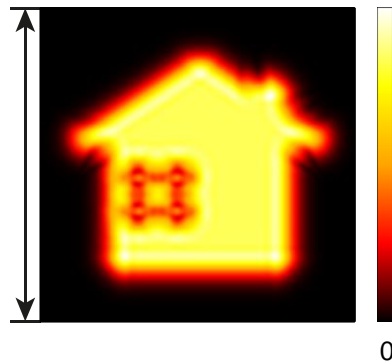
$E_x$  Component [ $\mu\text{V/m}$ ] 0.66



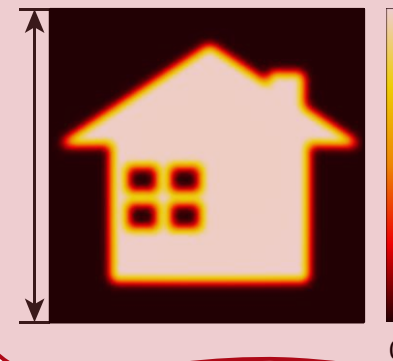
$E_x$  Component [ $1 \times 10^{-8} \text{ V/m}$ ] 3.3



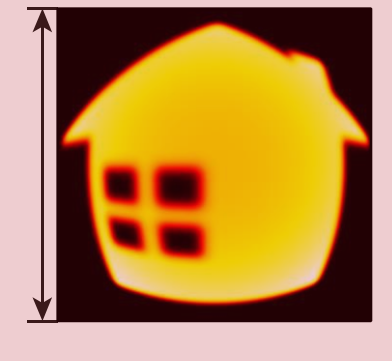
$E_x$  Component [ $1 \times 10^{-9} \text{ V/m}$ ] 7.23



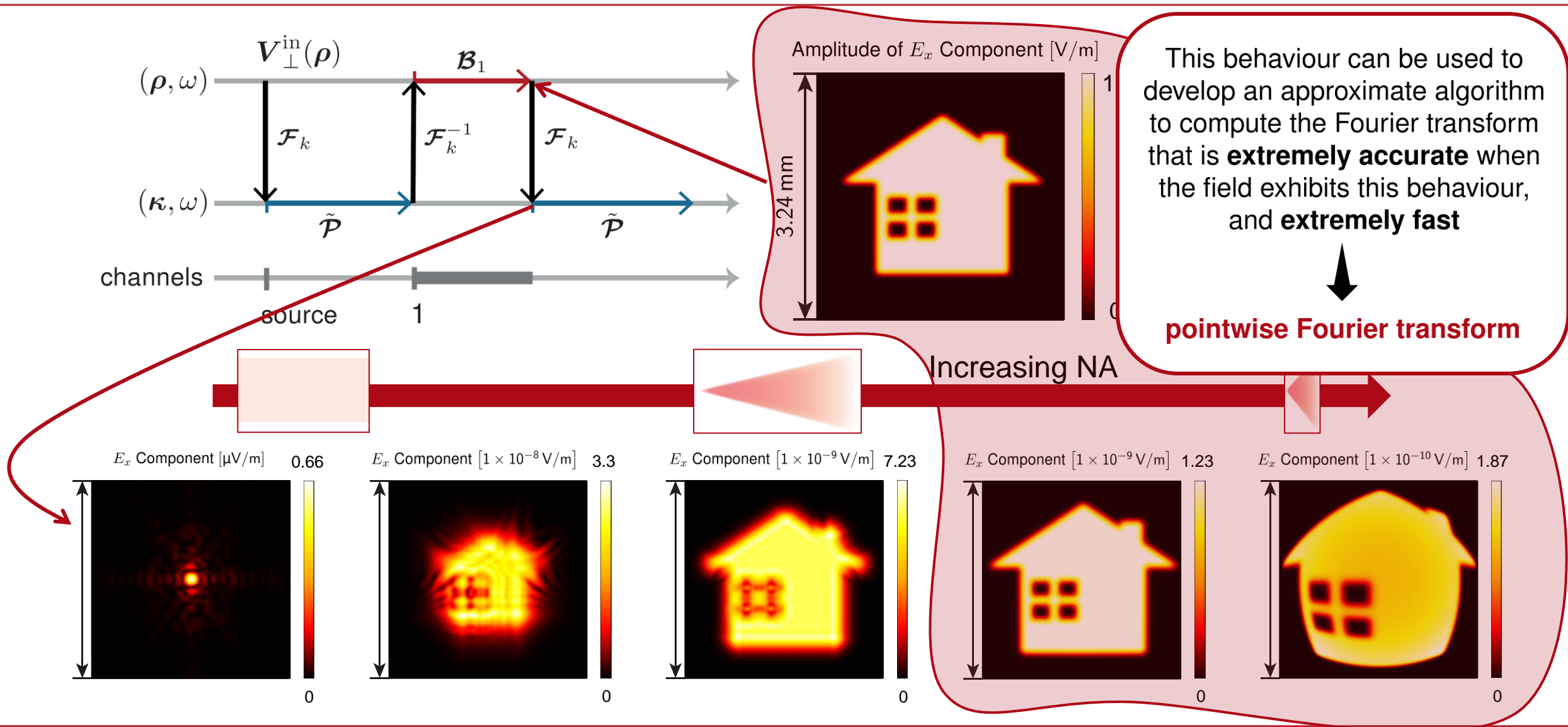
$E_x$  Component [ $1 \times 10^{-9} \text{ V/m}$ ] 1.23



$E_x$  Component [ $1 \times 10^{-10} \text{ V/m}$ ] 1.87

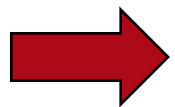


# Results of Fourier Transform

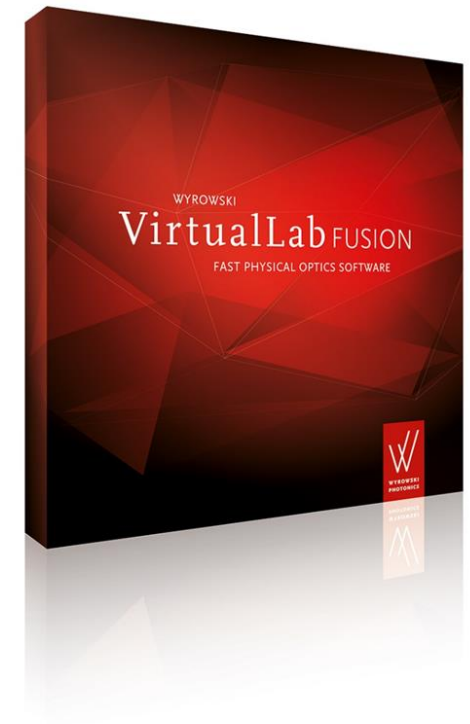


# Types of Fourier Transform Algorithms in VirtualLab Fusion

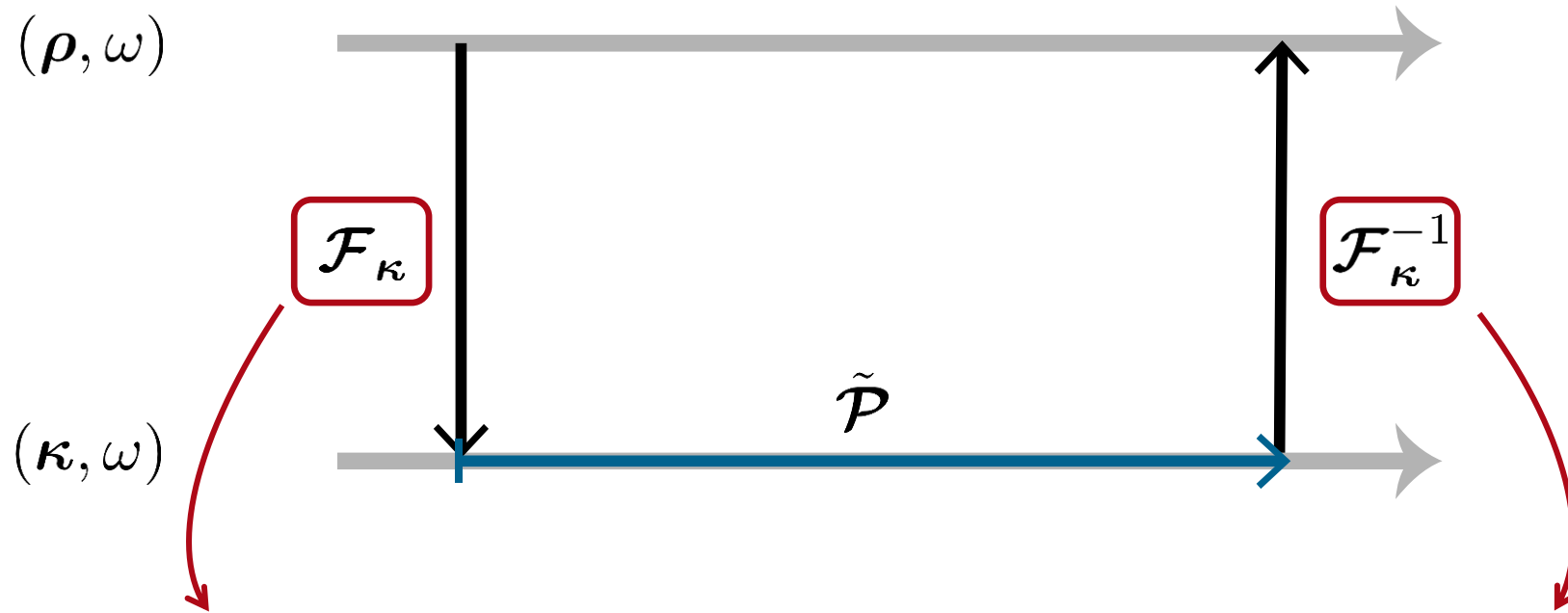
- Fast Fourier Transform (FFT)
  - Fast for weak wavefront phase
- Semianalytical Fourier transform (SFT)
  - Fast for wavefront phase with medium local gradient
- Pointwise Fourier transform (PFT)
  - Accurate for strong wavefront phase



Combination of Fourier transform algorithms essential for fast physical optics!



# Available Fourier Transform Techniques in VirtualLab Fusion



- $\mathcal{F}_\kappa$ : fast Fourier transform (FFT)
- $\mathcal{F}_\kappa^{\text{semi}}$ : semi-analytical Fourier transform (SFT)
- $\mathcal{F}_\kappa^{\text{h}}$ : homeomorphic Fourier transform (HFT)

- $\mathcal{F}_\kappa^{-1}$ : inverse fast Fourier transform (IFFT)
- $\mathcal{F}_\kappa^{-1, \text{semi}}$ : inverse semi-analytical Fourier transform (ISFT)
- $\mathcal{F}_\kappa^{-1, \text{h}}$ : inverse homeomorphic Fourier transform (IHFT)

# References to Our Fourier Transform Publications

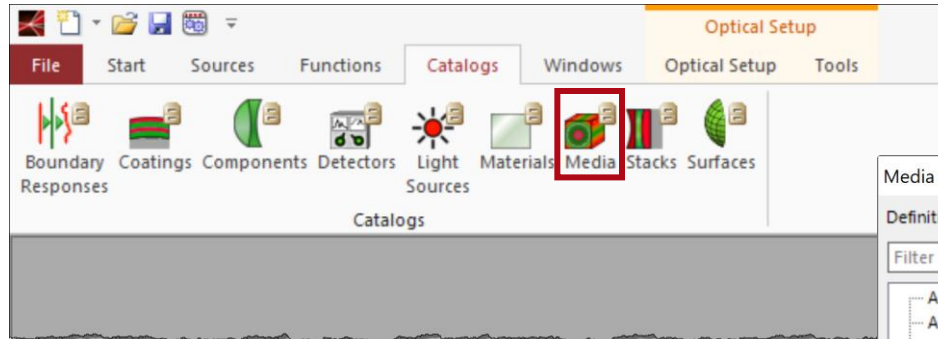
---

- *Theory and algorithm of the homeomorphic Fourier transform for optical simulations*, Z. Wang et al, Optics Express, **28**, 7, 2020
- *Application of the semi-analytical Fourier transform to electromagnetic modeling*, Z. Wang et al, Optics Express, **27**, 11, 2019

Part 4

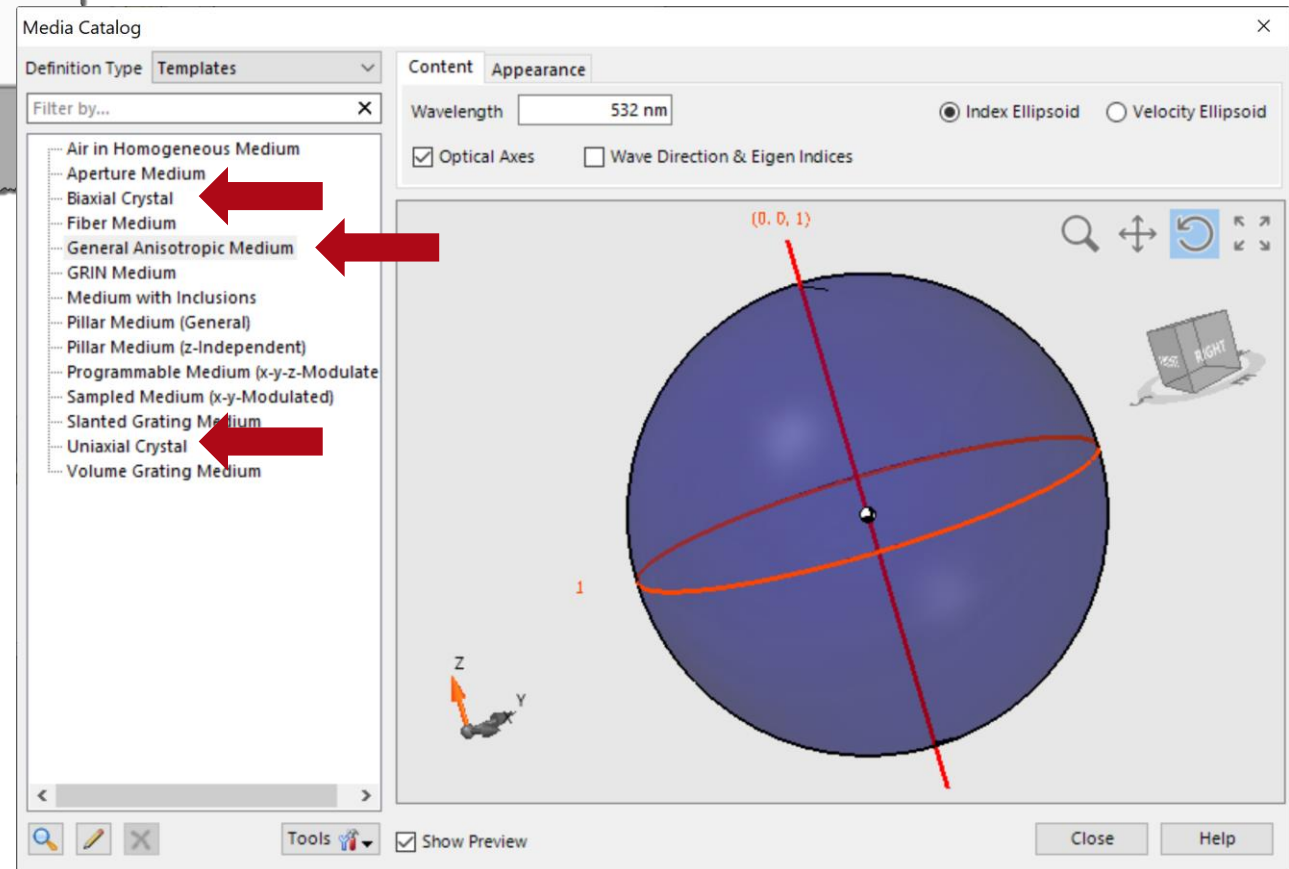
## Optically Anisotropic Media in VirtualLab Fusion

# Anisotropic Media in Catalog

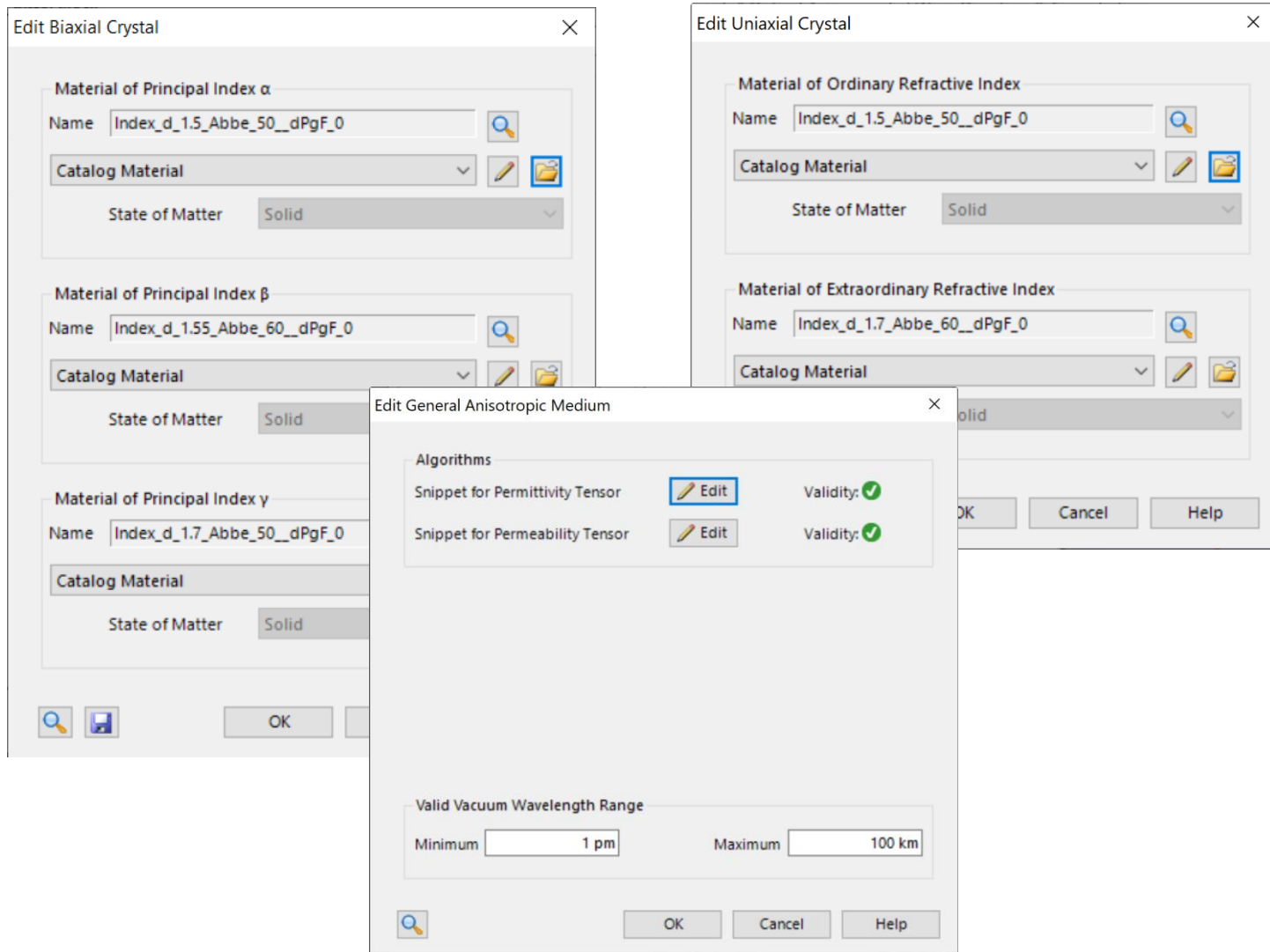


In the new version three different kinds of anisotropic media can be found in the media catalog:

- Uniaxial Crystal
- Biaxial Crystal
- General Anisotropic Media



# Defining the Anisotropic Media



- The Biaxial Crystal is defined by the principal indices of three directions
- The Uniaxial Crystal is defined by the ordinary and extraordinary refractive indices
- General Anisotropic Media can be set up by directly defining the permittivity tensor



# Preview of the Anisotropic Medium

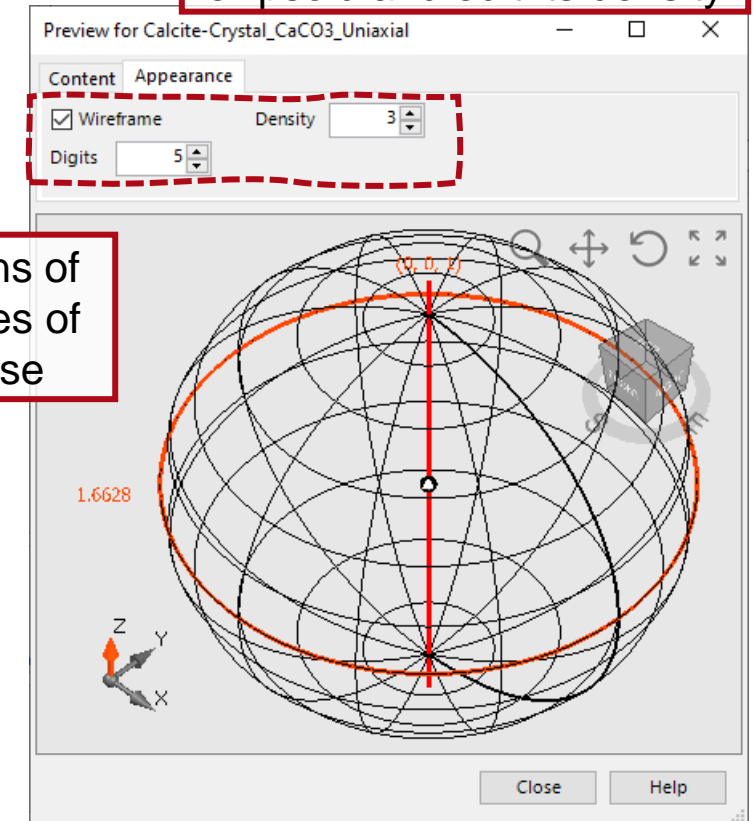
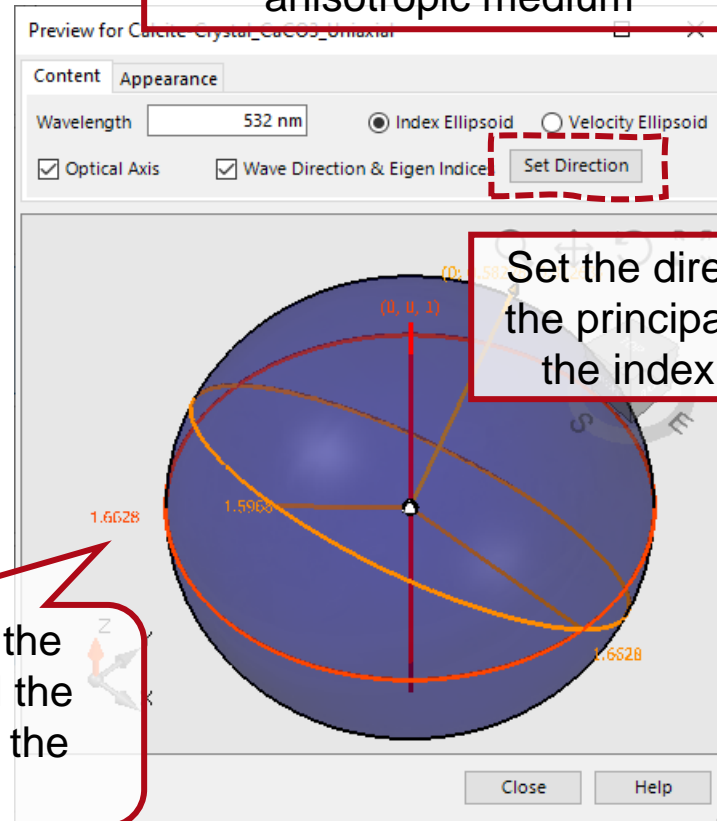
The preview of an anisotropic medium can be displayed through index ellipsoid or velocity ellipsoid, which makes it easy and intuitive to study the properties of the media.

In the Content tab, the user can select between the index/velocity ellipsoid of the anisotropic medium

In the Appearance tab, the user can show the wireframe of the selected ellipsoid and edit its density

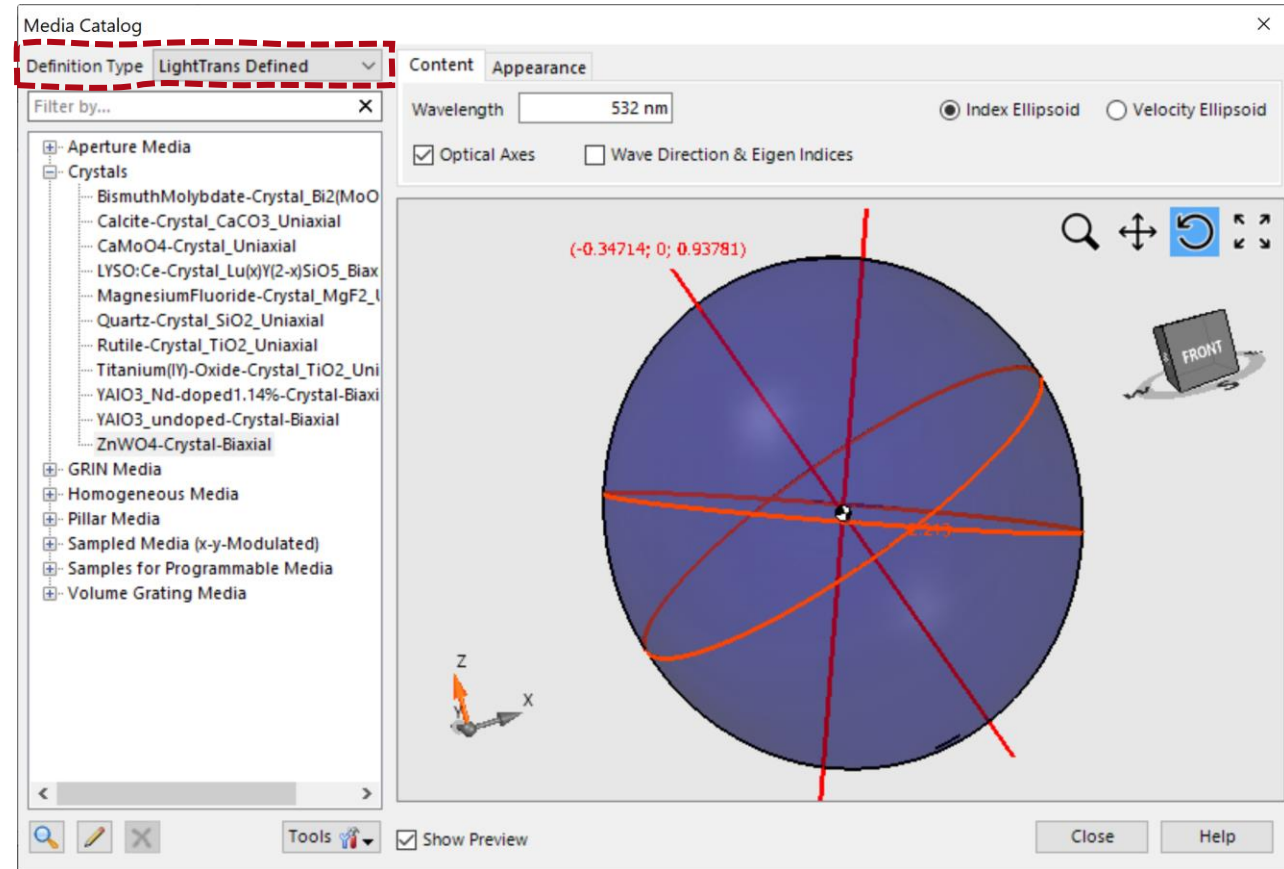
Set the directions of the principal axes of the index ellipse

The half-lengths of the principal axes equal the refractive indices of the normal modes



# Preconfigured Crystals

VirtualLab Fusion comes with a series of pre-configured crystal media which can be accessed from the media catalog. The user also can import & export his own defined media to the catalog.



# Anisotropic Coatings

Anisotropic coatings can be found in the coating catalog and applied to all optical surfaces in VirtualLab Fusion.

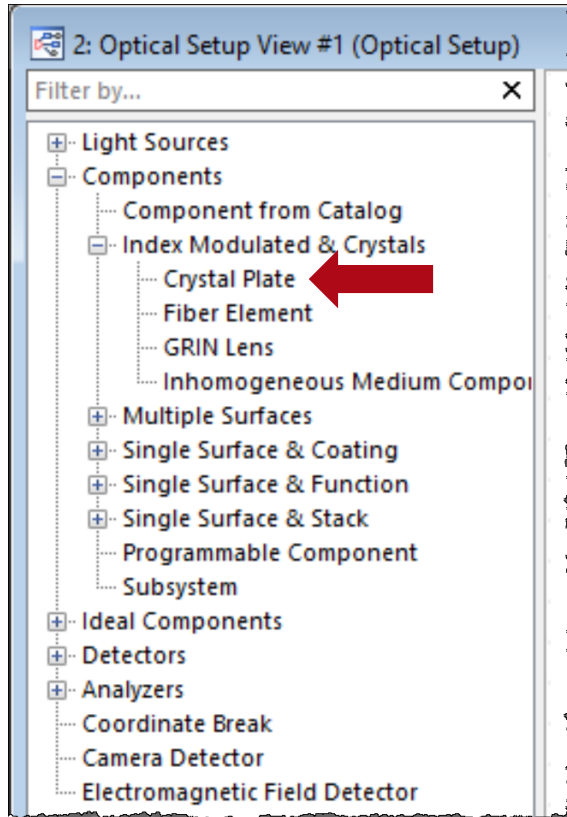
The image shows the 'Coatings Catalog' window with the 'Anisotropic Layer Stack' template selected. A red dashed box highlights the 'Filter by...' dropdown menu. Below it, the 'Define Stack of Anisotropic Layers' dialog is open, showing a diagram of a substrate with coating layers and a table of layer properties.

Index	Thickness	Distance	Medium	Orientation
1	0 mm	0 mm	Biaxial Crystal	$[(\varphi=0^\circ, \theta=0^\circ); (\xi=0^\circ)]$
2	0 mm	0 mm	Air in Homogeneous	N/A

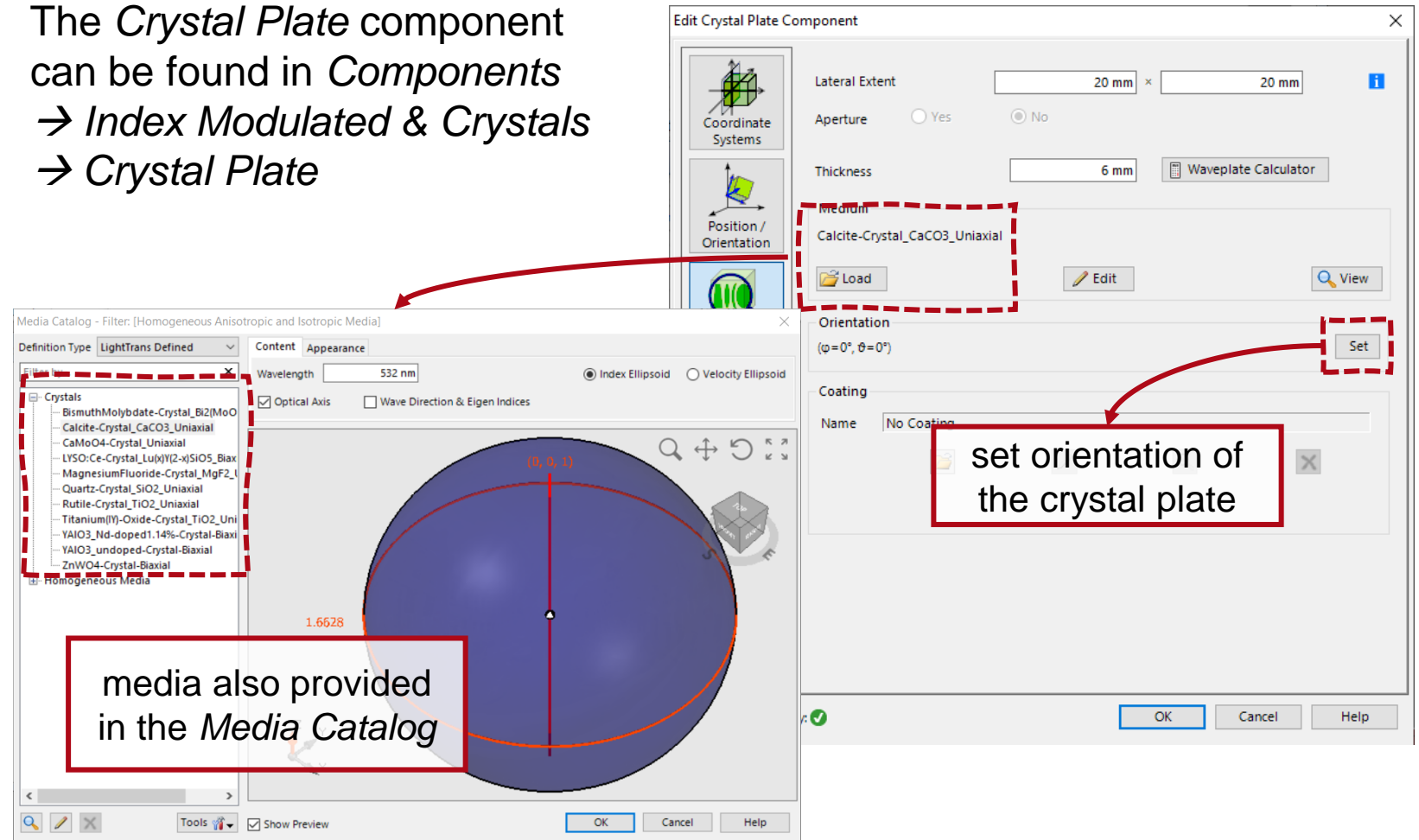
A red box highlights the text: "A coating can alternate layers of isotropic or anisotropic homogeneous media".

The image shows the 'Media Catalog' window with the 'Filter: [Homogeneous Anisotropic and Isotropic Media]' applied. A red dashed box highlights the 'Crystals' list, which includes various anisotropic media like BismuthMolybdate-Crystal, Calcite-Crystal, etc. Below the list, the 'Media Catalog - Filter: [Homogeneous Anisotropic and Isotropic Media]' dialog is open, showing a 3D visualization of a crystal's optical properties. A red box highlights the text: "choose from the predefined anisotropic media, a previously defined media from the catalog or use a template medium and customize the parameters; the preview of the medium is shown on the right".

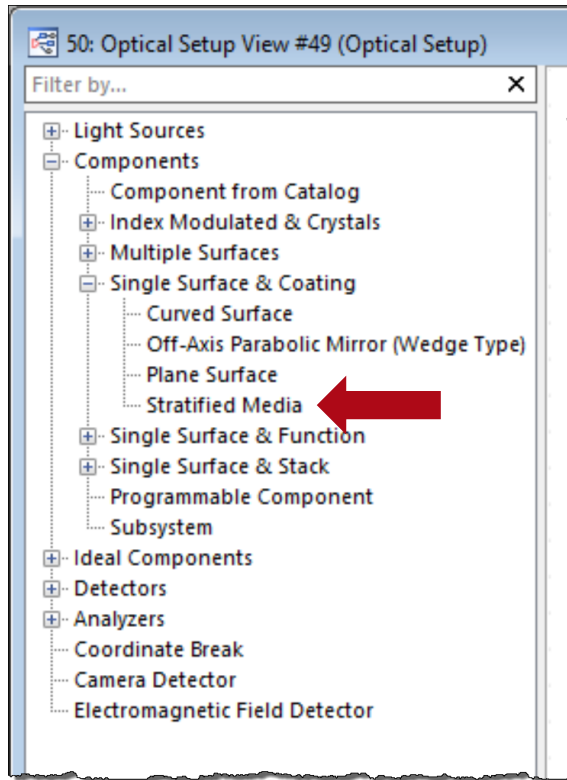
# Anisotropic Crystal Plate



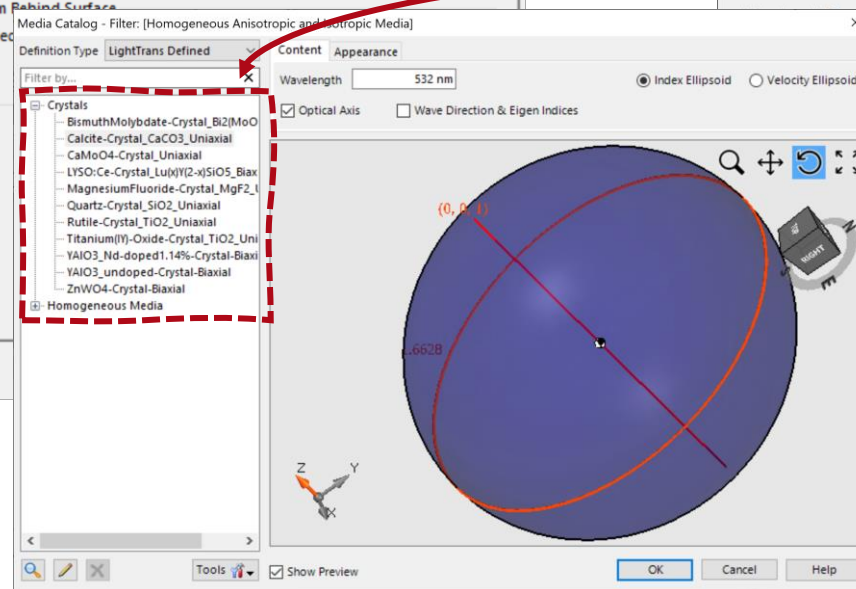
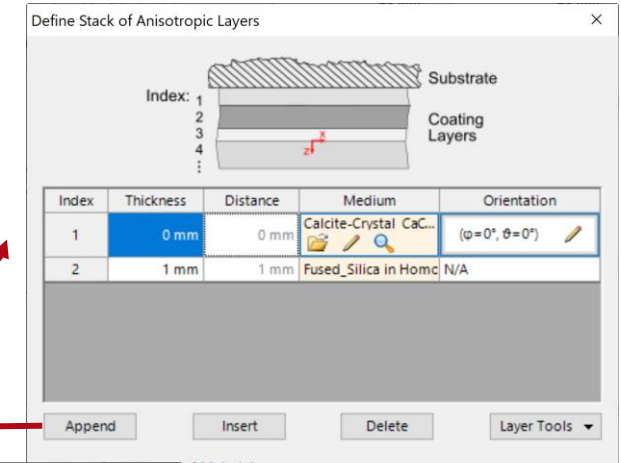
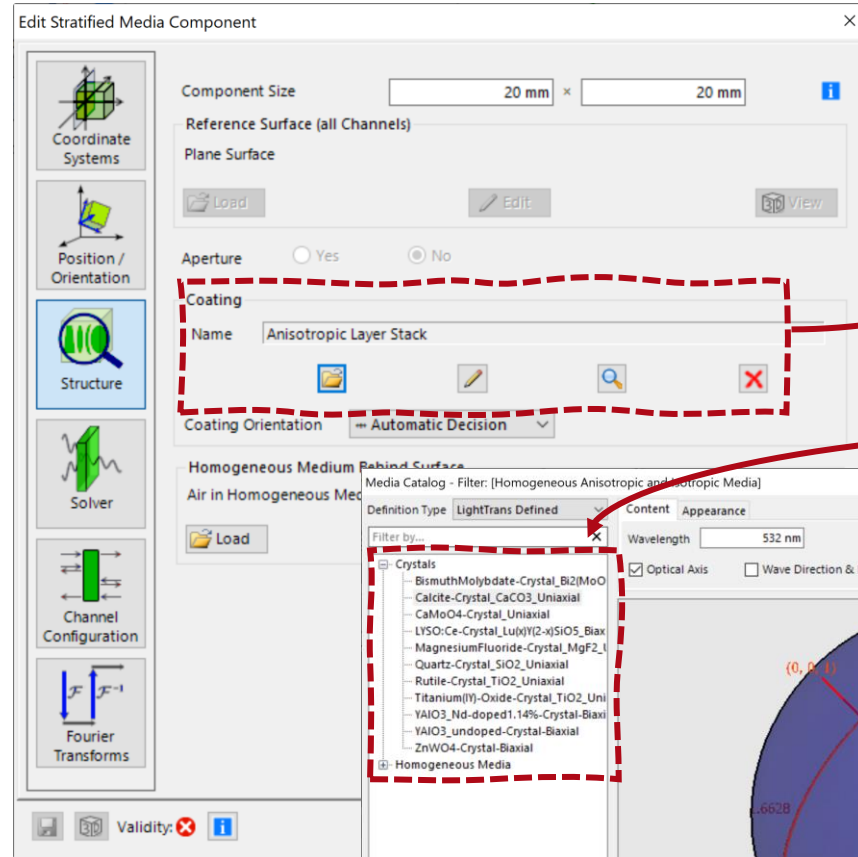
The *Crystal Plate* component can be found in *Components*  
→ *Index Modulated & Crystals*  
→ *Crystal Plate*



# Anisotropic Stratified Media Component



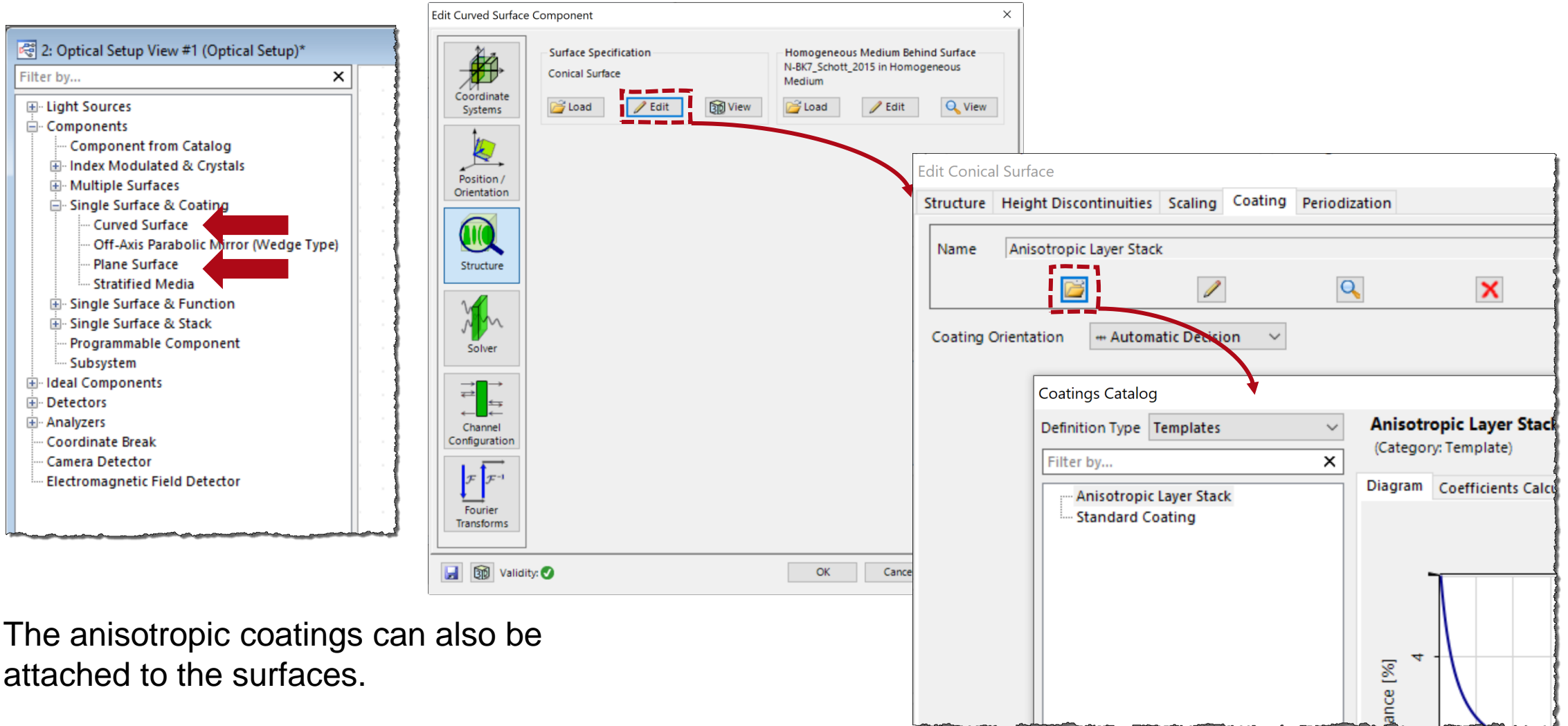
The *Stratified Media* component can be found in *Components* → *Single Surface&Coating* → *Stratified Media*



Anisotropic and isotropic layers can be defined in the same component



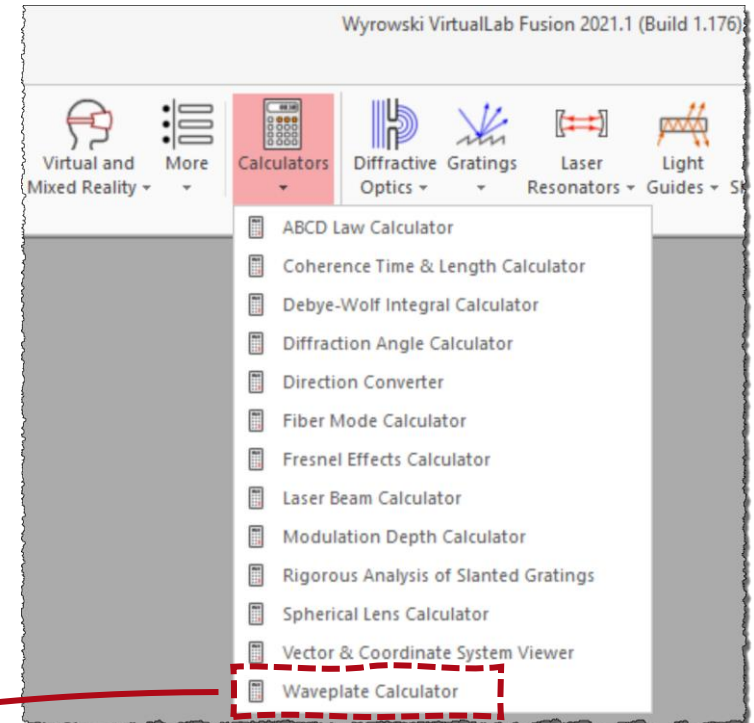
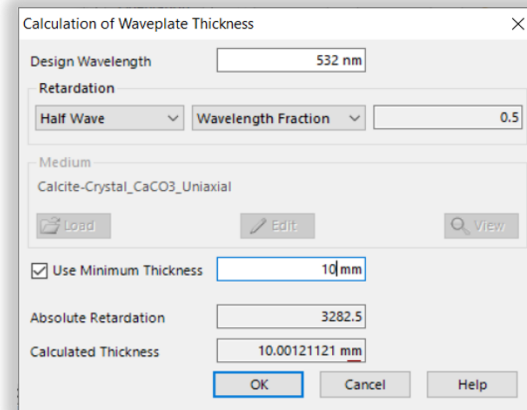
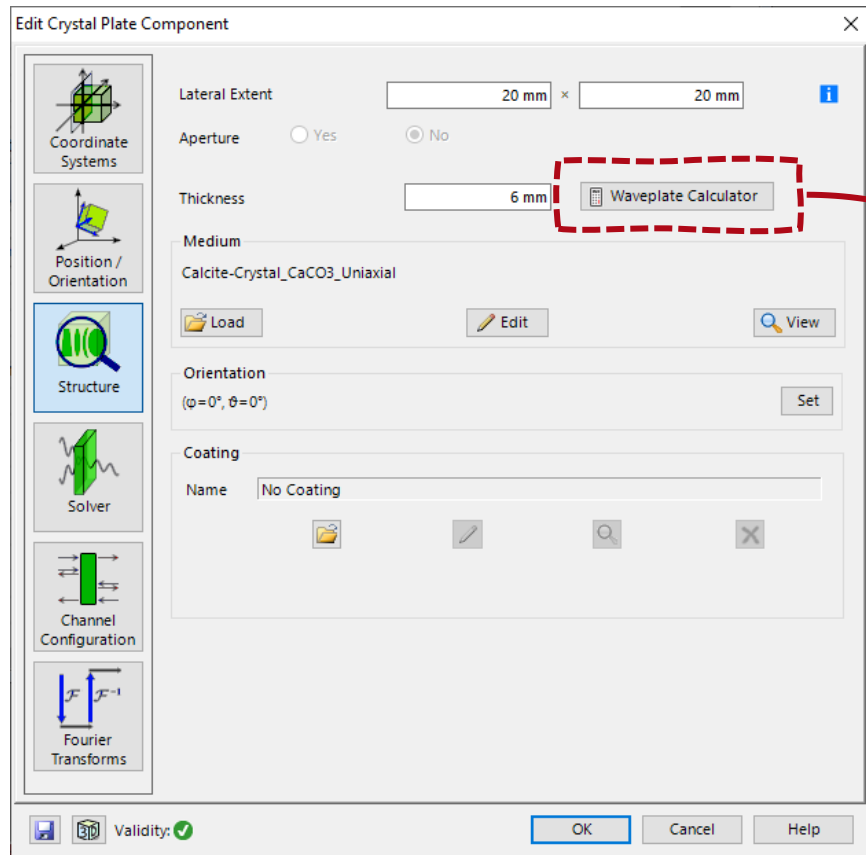
# Anisotropic Surfaces



The anisotropic coatings can also be attached to the surfaces.

# Waveplate Calculator

The *Crystal Plate Component* as well as the *Calculator* Section of the Main Window allows access to the *Waveplate Calculator* which can be used to determine the thickness and retardation of a waveplate with given characteristics.



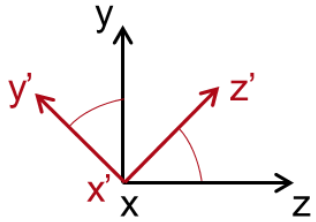
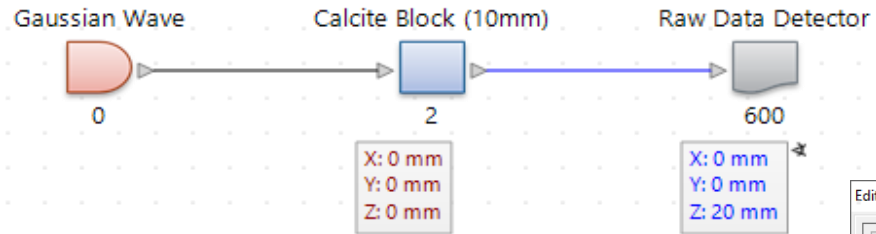
Example 01

## **Birefringence Effect of Anisotropic Calcite Crystal**

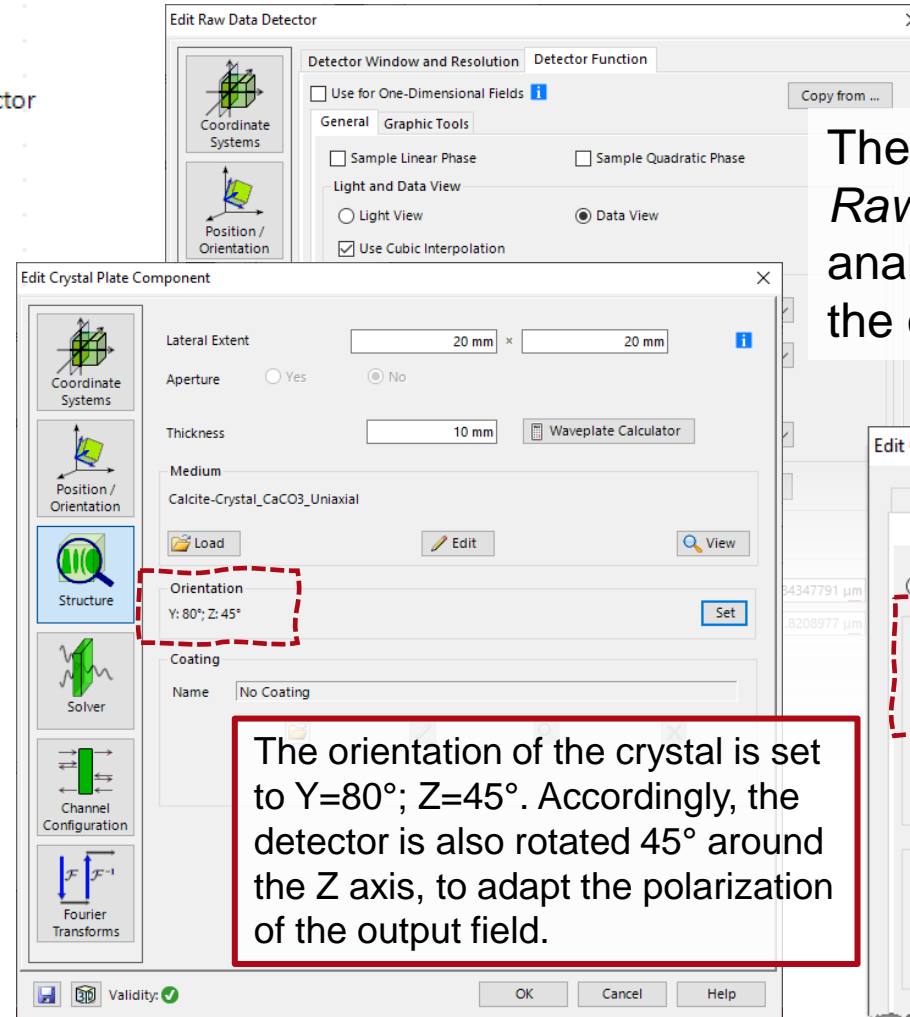
 [see the full Application Use Case](#)



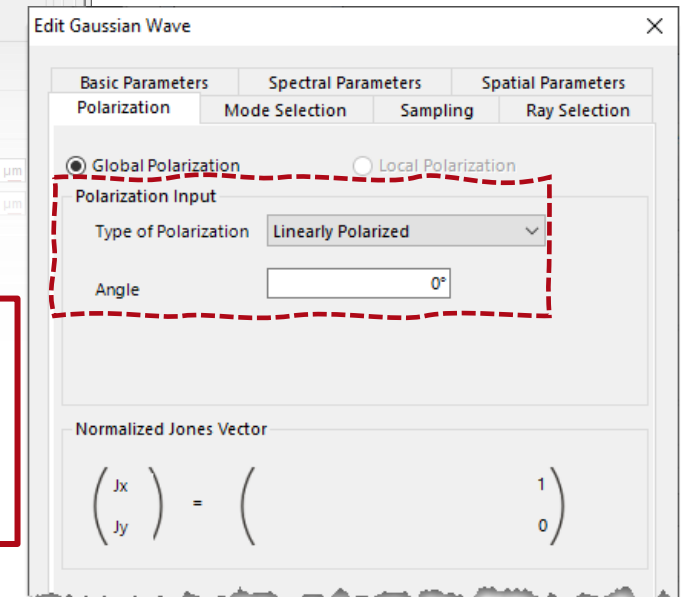
# System Building Blocks



The orientation of the optic axis (marked in red) of the crystal needs to be adjusted in order for the birefringence to be observed.

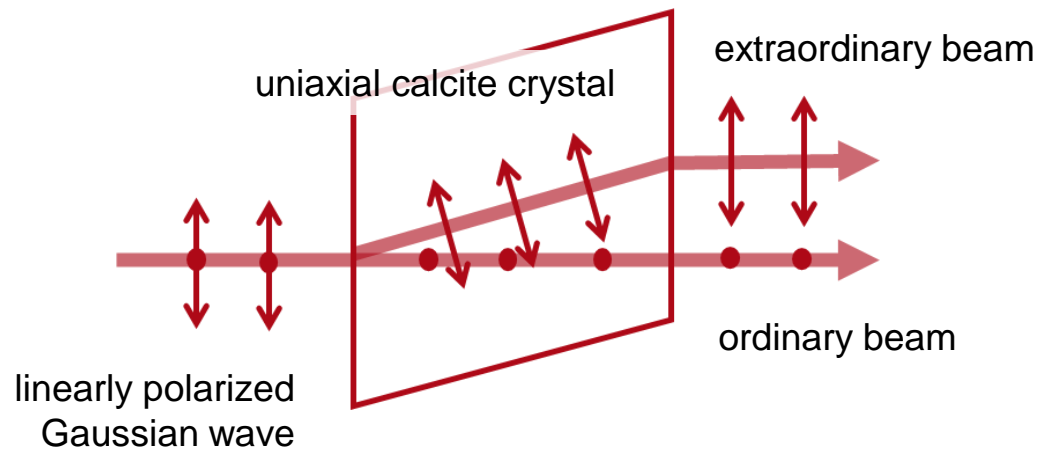


The source is linearly polarized. A *Raw Data Detector* is used to analyze the polarization state of the output field.

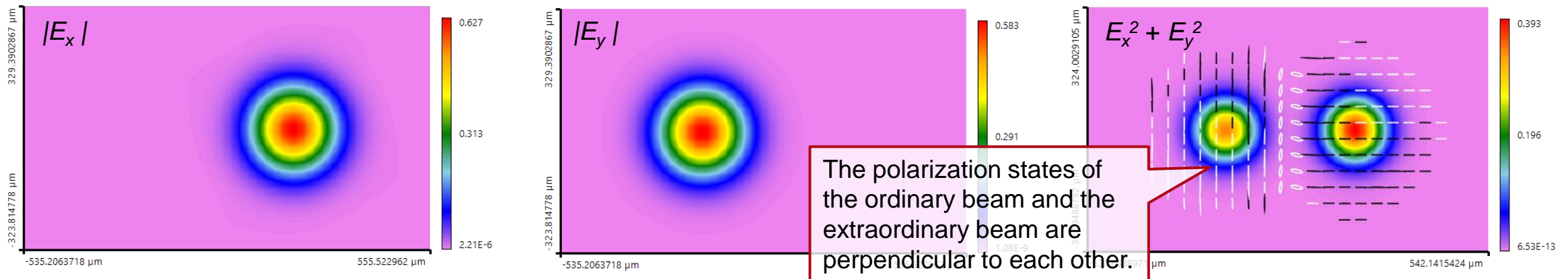


The orientation of the crystal is set to Y=80°; Z=45°. Accordingly, the detector is also rotated 45° around the Z axis, to adapt the polarization of the output field.

# Birefringence Effect in Uniaxial Crystals

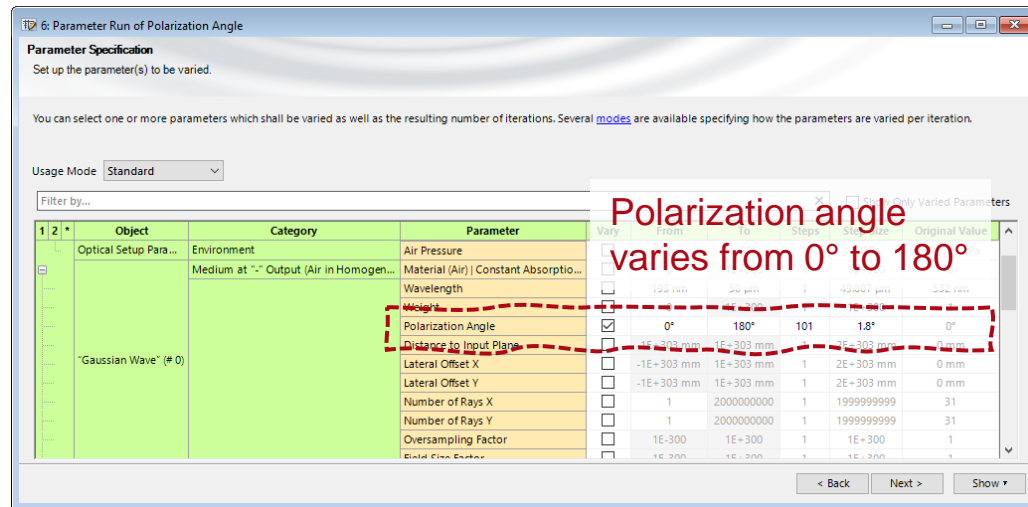


When a beam which propagates along the optic axis of the crystal (and whose field vector therefore lies in the perpendicular plane to the optic axis) impinges on the crystal, it will not “see” the birefringence, and will pass through the crystal at a single velocity. However, when the beam propagates at an angle with respect to the optic axis, it will be refracted into two different modes (ordinary and extraordinary) as it enters the crystal. The two modes propagate with different velocities inside the crystal and their polarization is perpendicular to each other. This is the phenomenon known as double refraction or birefringence.

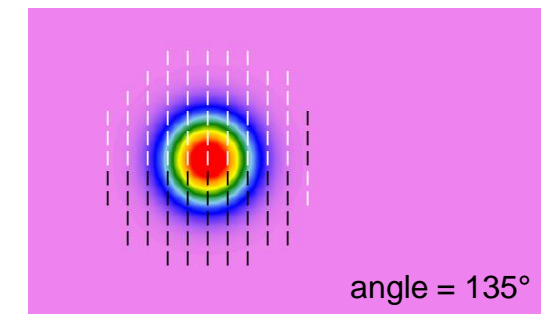
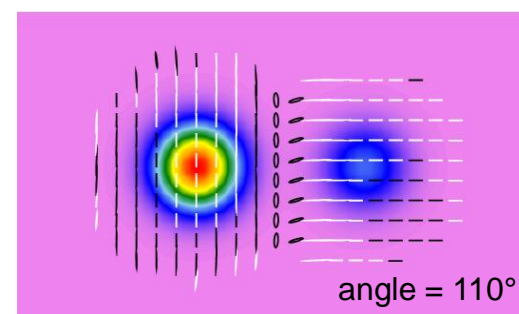
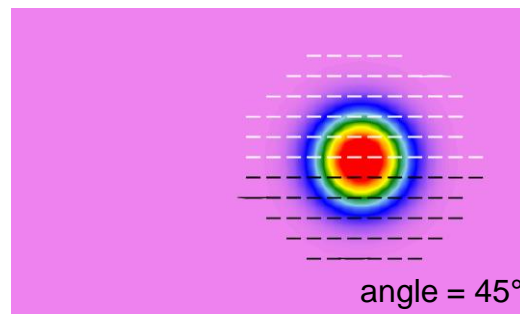
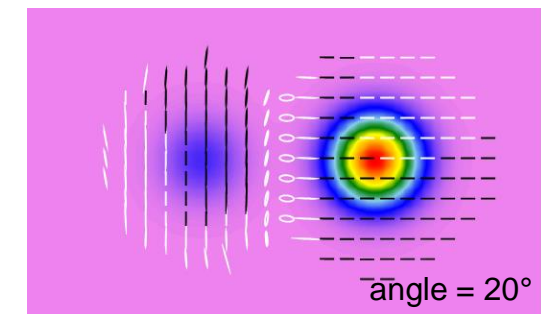
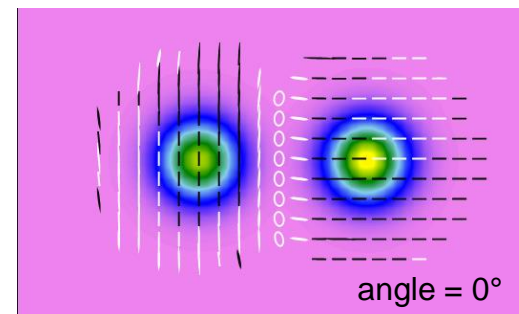


Field tracing result on the detector plane; please note that, the detector window is rotated to adapt the polarization direction.

# Birefringence for Different Initial Polarization States



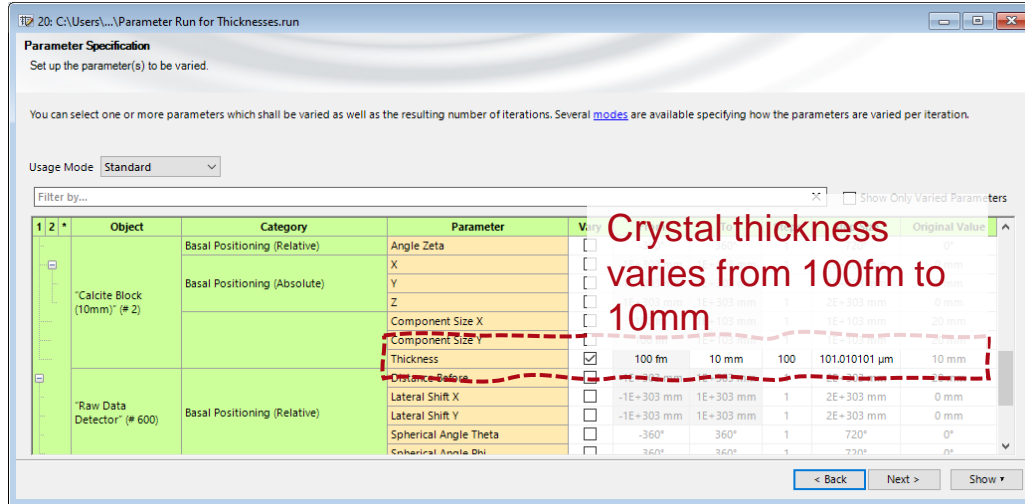
With the orientation of the crystal fixed, the polarization angle of the incident Gaussian wave is scanned with a Parameter Run. As the field tracing results show, the incident beam is distributed into two normal polarization states inside the crystal. When the incident polarization is perpendicular to the optic axis (here, *Polarization Angle* 135°) only the ordinary beam will propagate inside the crystal. When the incident polarization lies along the projection of the optic axis on the entrance plane of the crystal, however, only the extraordinary beam will be observed (here, *Polarization Angle* 45°).



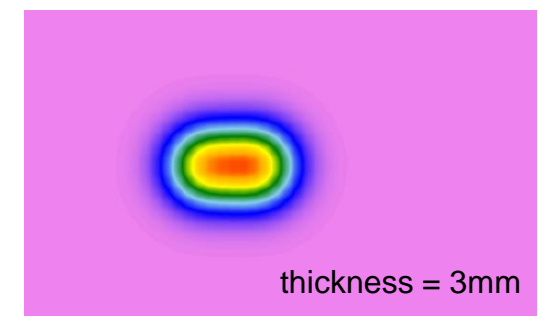
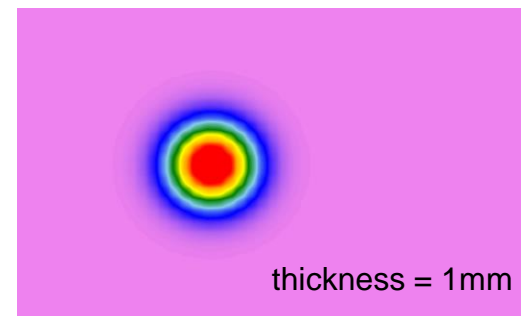
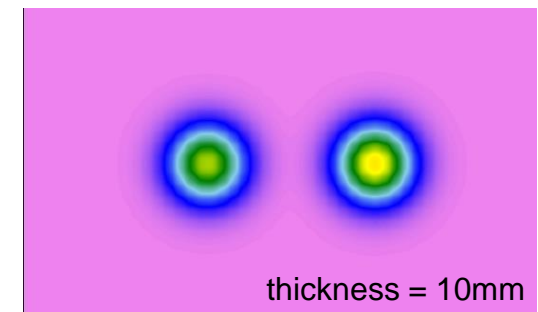
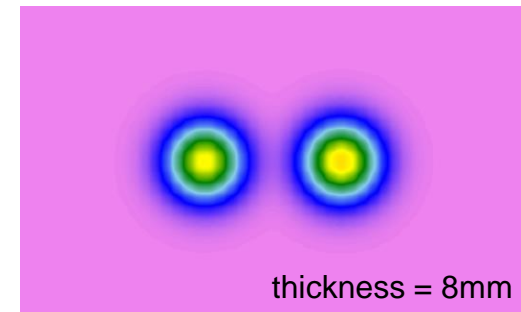
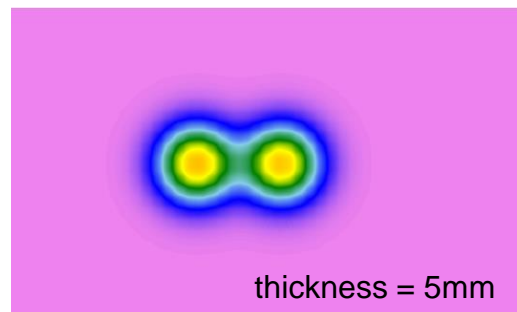
Field tracing results from parameter run, the animation of the varying results is available in the sample file. Please note that the detector is rotated 45° to adjust the polarization direction.

# Birefringence for Varying Crystal Thickness

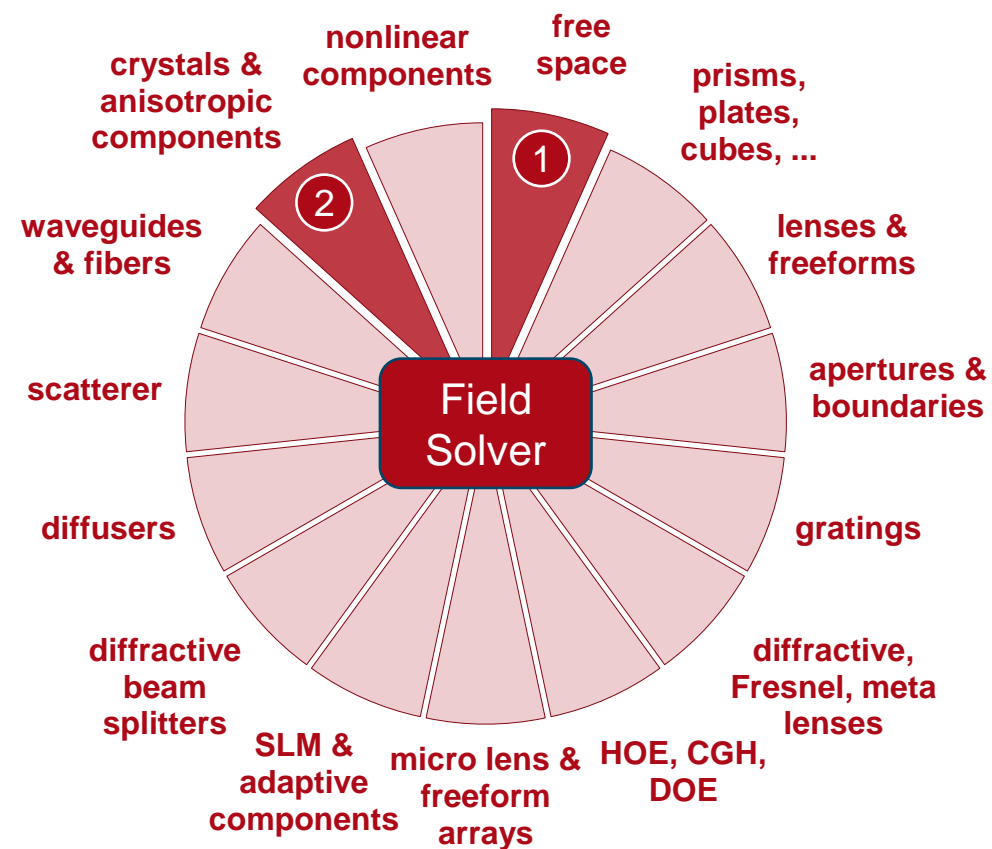
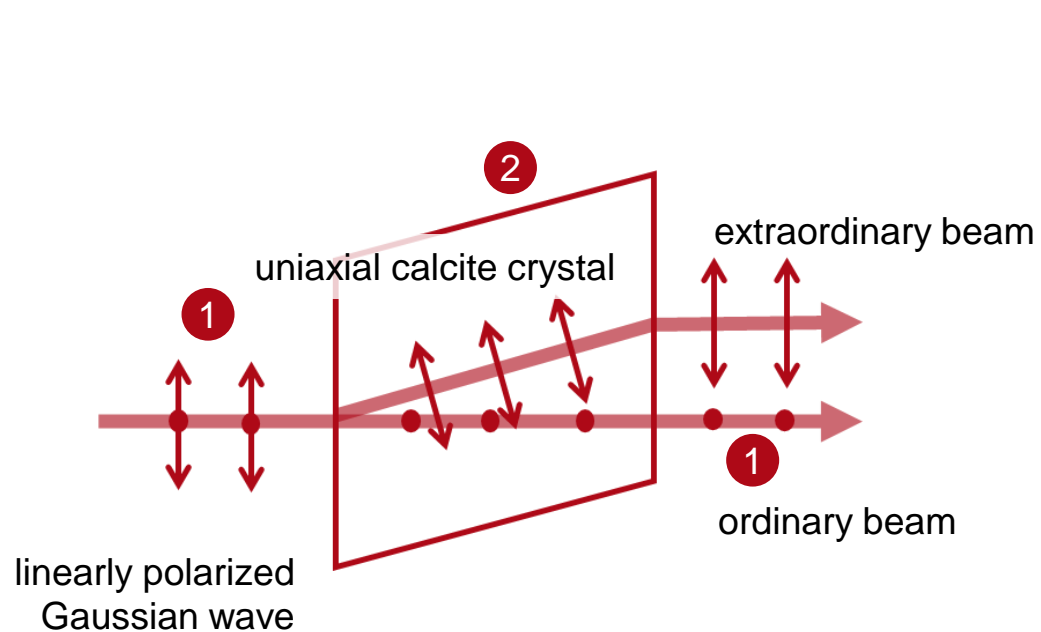
By varying the thickness of the crystal, the shift of the extraordinary beams is observable. As the field tracing results show, the thicker the calcite crystal, the larger the lateral separation between the two beams!



Field tracing results from parameter run, the animation of the varying results is available in the sample file. To be noticed, the detector window is rotated to adapt the polarization direction.



# VirtualLab Fusion Technologies



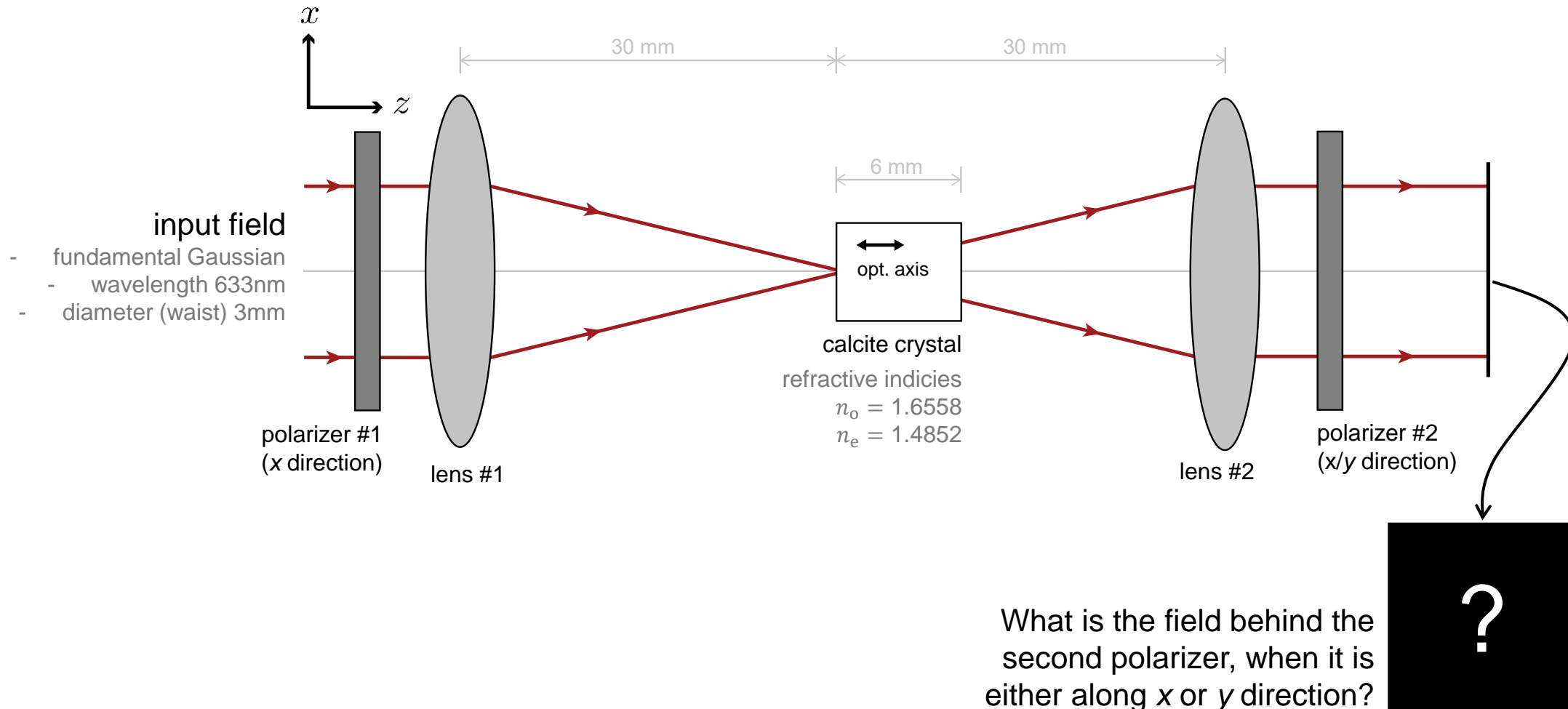
# idealized component

Example 02

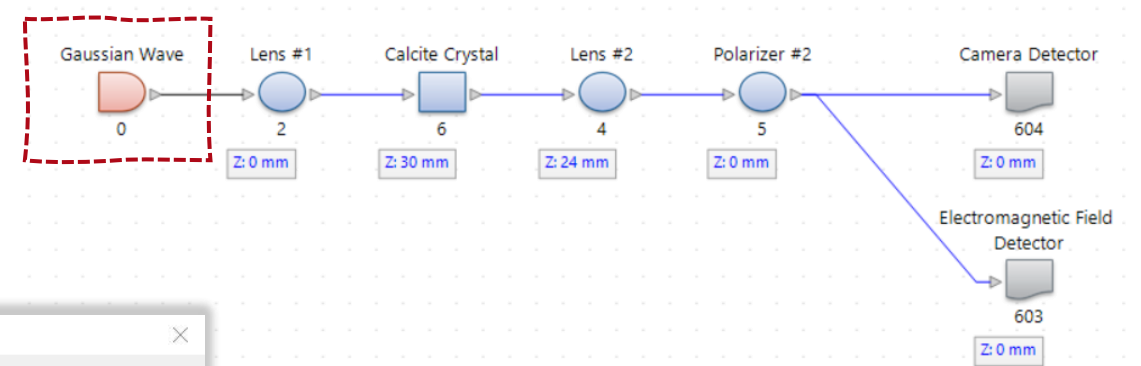
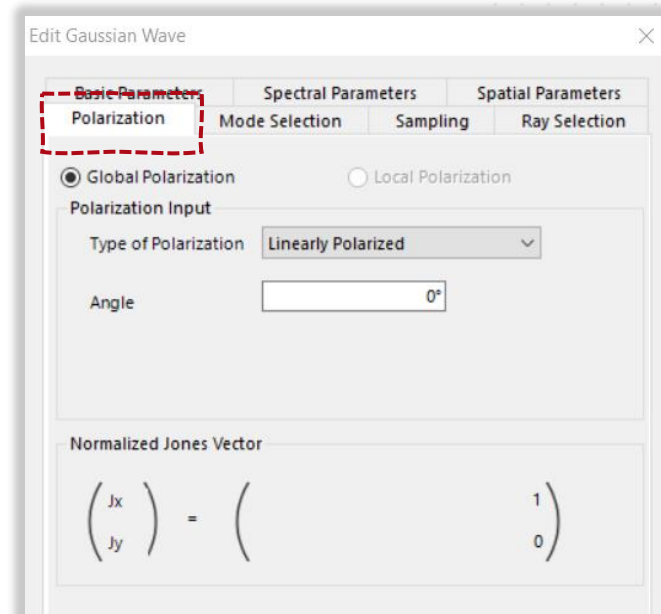
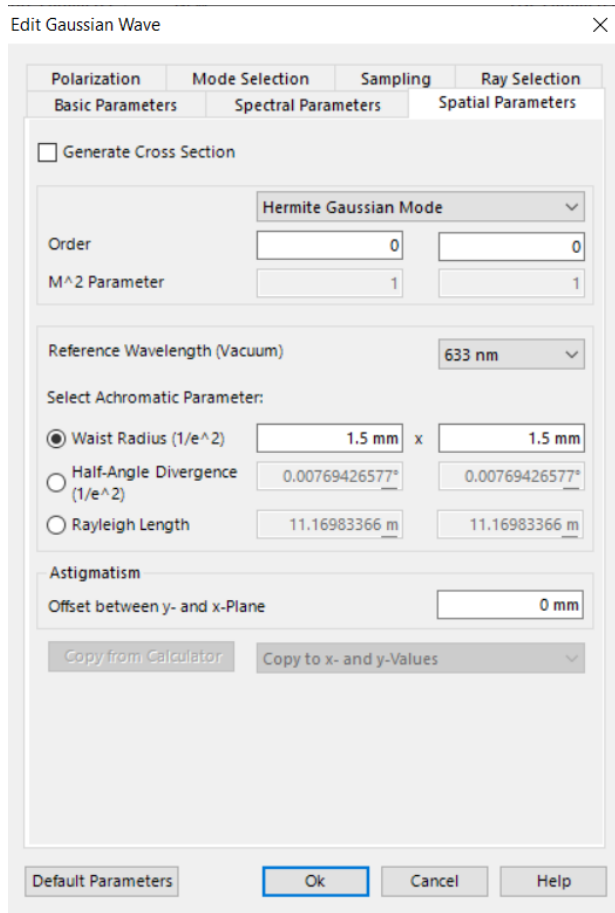
## Polarization Conversion in Uniaxial Crystals

 [see the full Application Use Case](#)

# Modeling Task



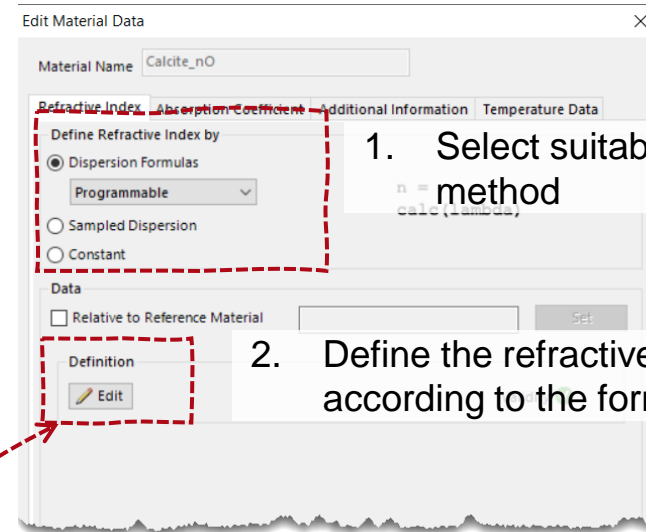
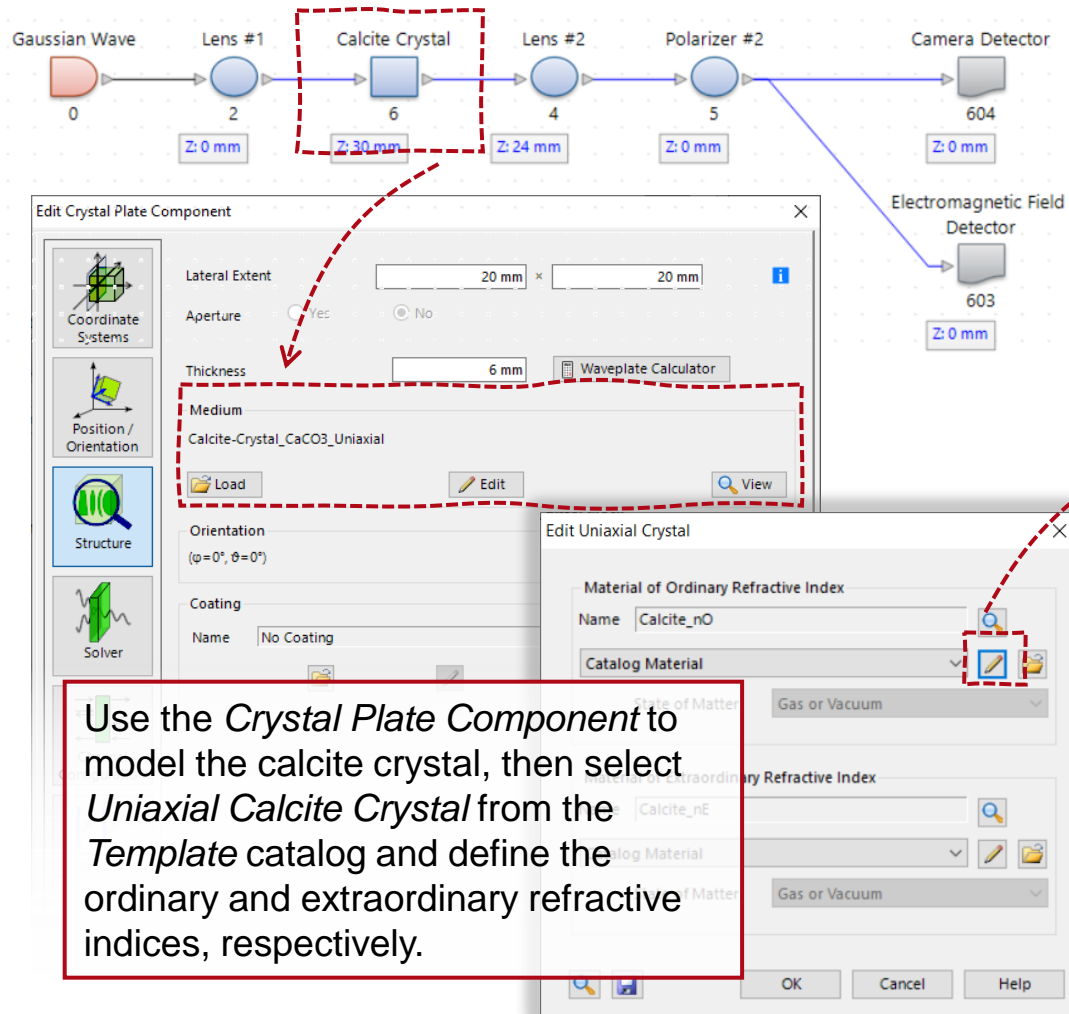
# System Building Blocks – Source



The 1<sup>st</sup> polarizer changes the Gaussian wave into x polarized. We assume this as the starting point for our system, so the corresponding polarization state (linearly polarized along x) is directly defined in the source.



# System Building Blocks – Uniaxial Calcite Crystal



Tips: after configuring the material, use the Save tab to save the new material to the *User Defined* material catalog and load it easily for the next simulation.

## Uniaxial Calcite Crystal

- Thickness: 6mm
- Ordinary refractive index

$$n_o = \left( 2.69705 + \frac{0.0192064}{\lambda^2 - 0.0182} - 0.0151624\lambda^2 \right)^{1/2}$$

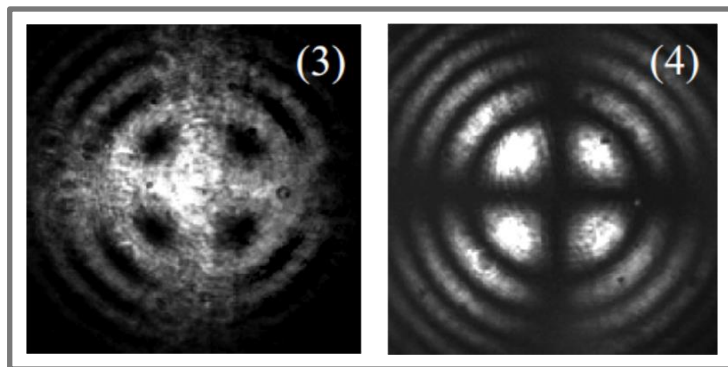
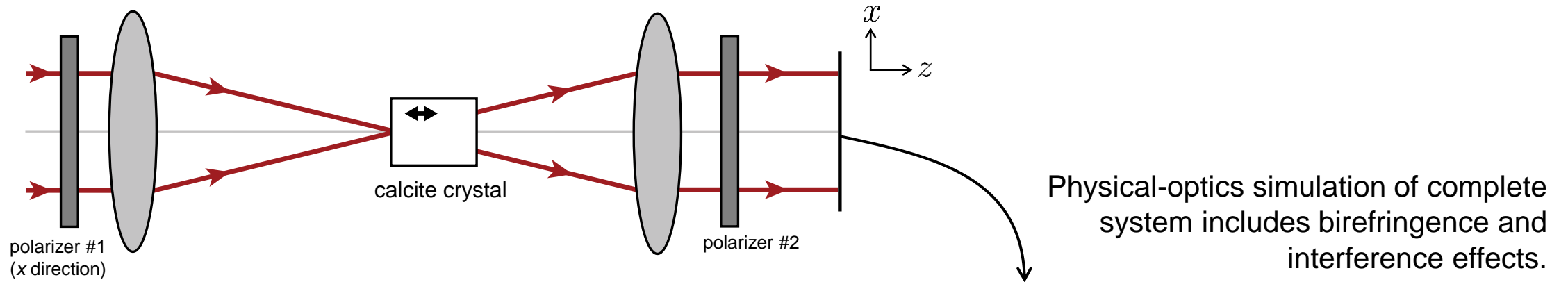
- Extraordinary refractive index

$$n_e = \left( 2.18438 + \frac{0.0087309}{\lambda^2 - 0.01018} - 0.0024411\lambda^2 \right)^{1/2}$$

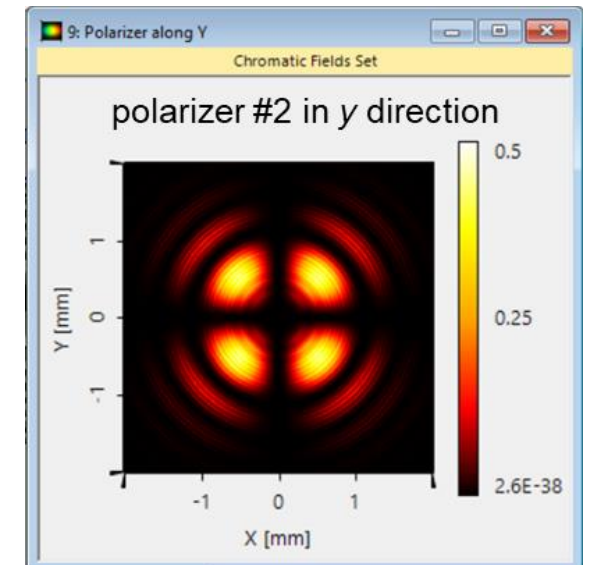
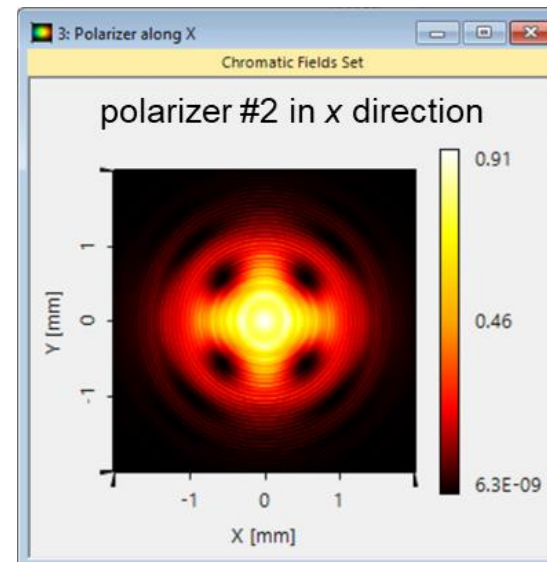
with  $\lambda$  in micrometers.

Parameters follow from Y. Izdebskaya *et al.*, Opt. Express **17**, 18196-18208 (2009)

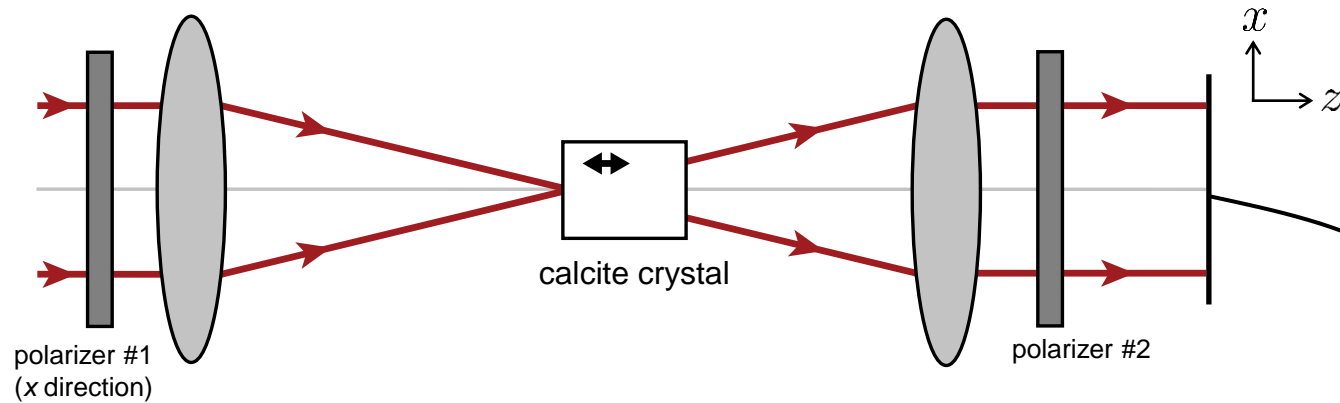
# Results



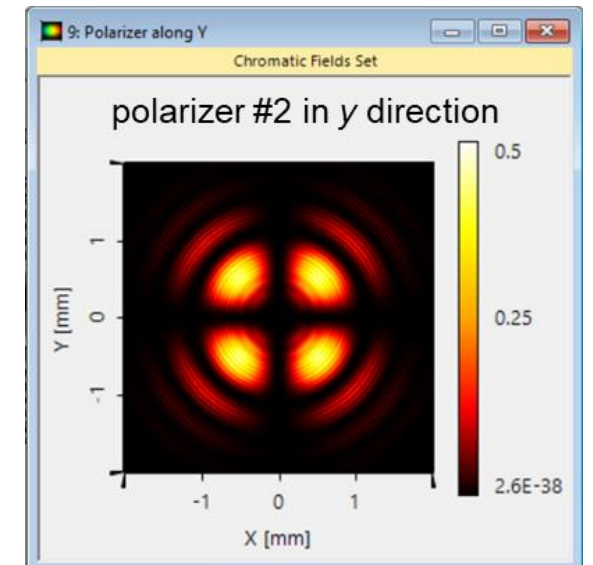
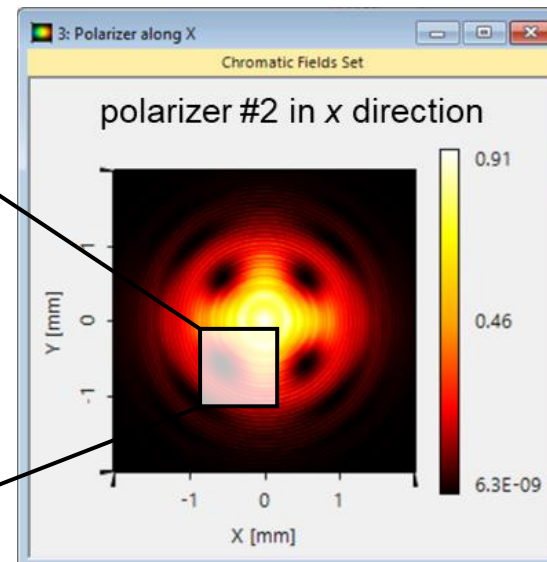
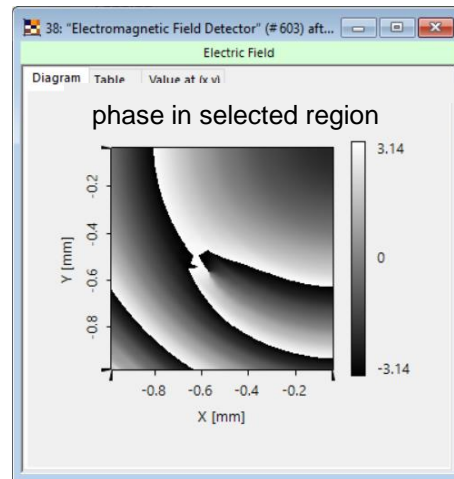
Experimental measurements from Y. Izdebskaya *et al.*, Opt. Express **17**, 18196-18208 (2009)



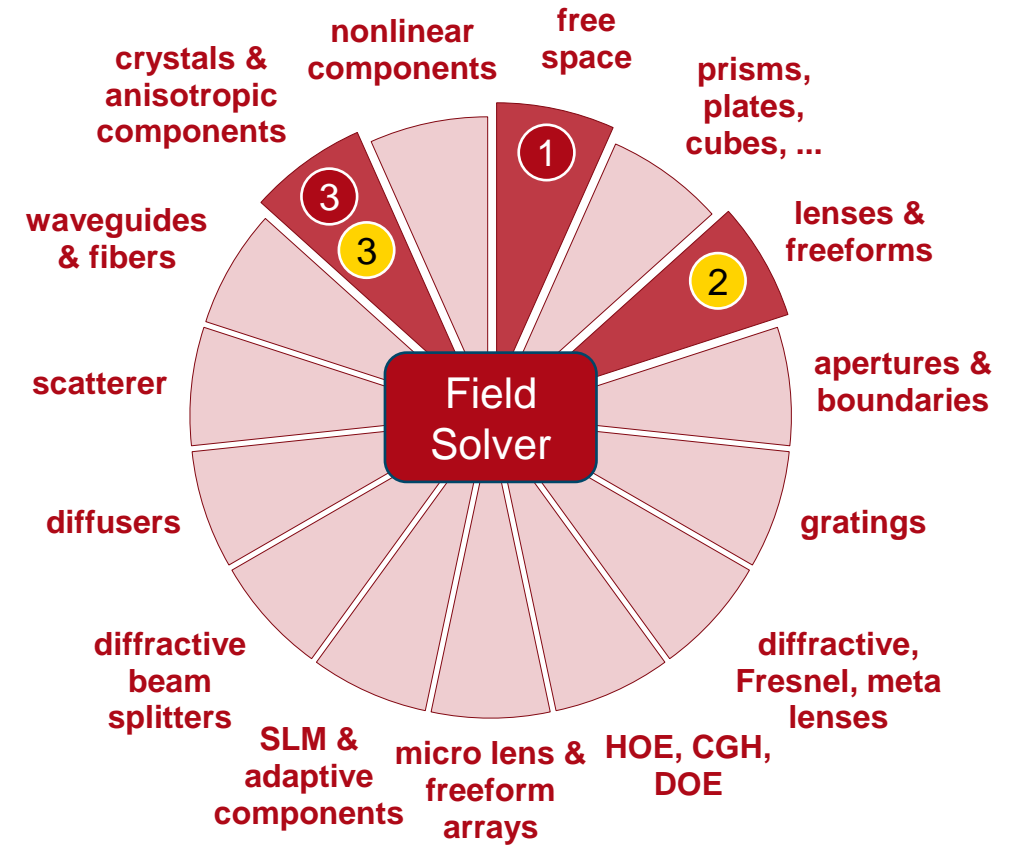
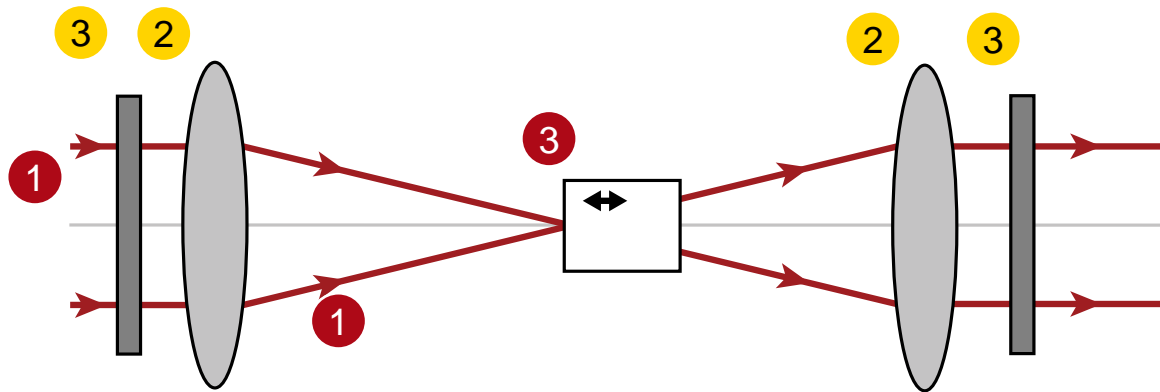
# Results



Visualization of phase distribution reveals a phase dislocation/vortex phase.



# VirtualLab Fusion Technologies



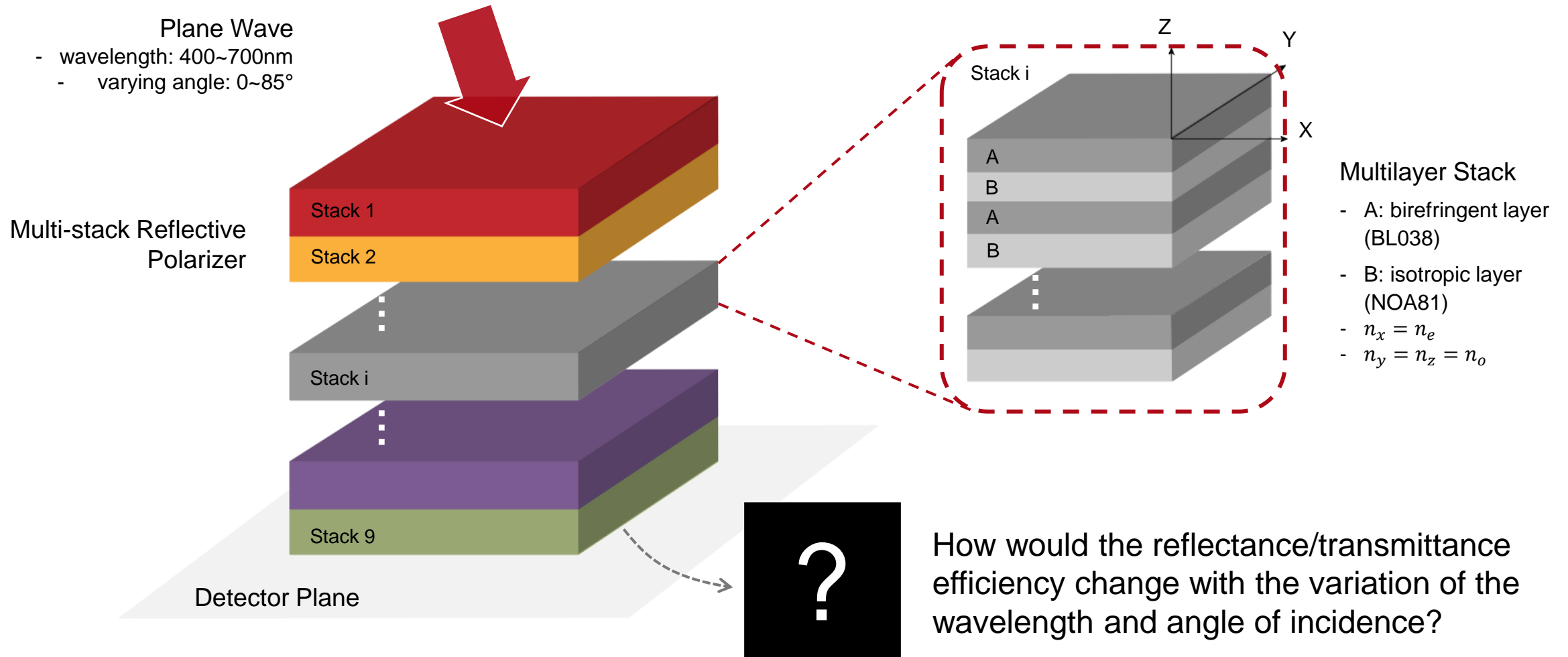
# idealized component

Example 03

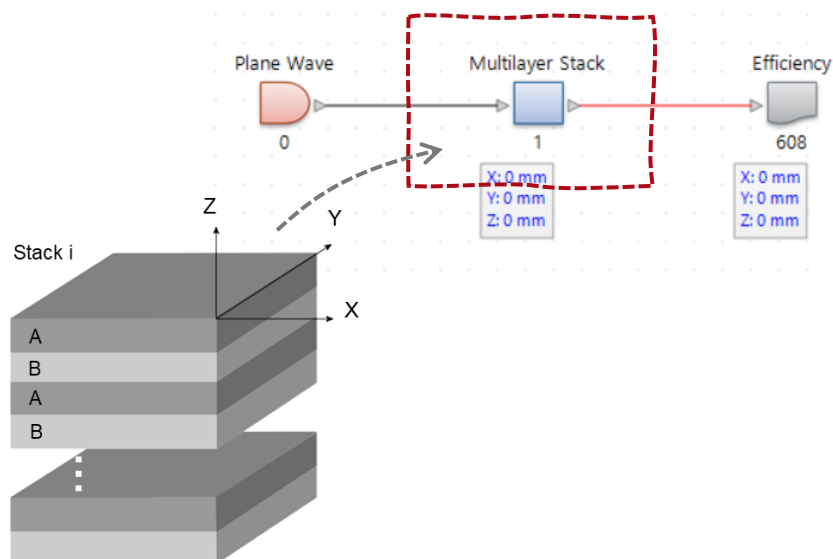
## **Simulation of Multilayer Birefringent Reflective Polarizer with VirtualLab Fusion**

 [see the full Application Use Case](#)

# Task Description



# Modeling of the Multilayer Stack



A Stratified Media Component is used to model the multilayer stack.

Select *Anisotropic Layer Stack* from the *Template* catalog and use the tool tabs to edit the layers.

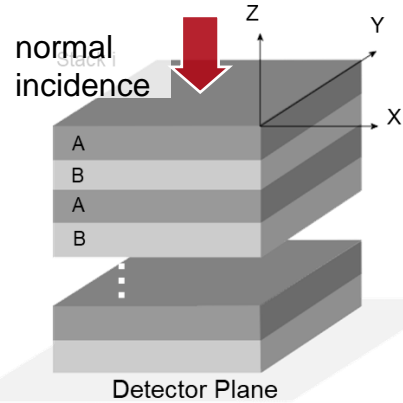
Index	Thickness	Distance	Medium	Orientation
1	75.55 nm	75.55 nm	BL038_Uniaxial_Cryst	( $\phi=0^\circ$ , $\theta=90^\circ$ )
2	87.58 nm	163.13 nm	NOA81 in Homogene	N/A
3	75.55 nm	238.68 nm	BL038_Uniaxial_Cryst	( $\phi=0^\circ$ , $\theta=90^\circ$ )
4	87.58 nm	326.26 nm	NOA81 in Homogene	N/A
5	75.55 nm	401.81 nm	BL038_Uniaxial_Cryst	( $\phi=0^\circ$ , $\theta=90^\circ$ )
6	87.58 nm	489.39 nm	NOA81 in Homogene	N/A
7	75.55 nm	564.94 nm	BL038_Uniaxial_Cryst	( $\phi=0^\circ$ , $\theta=90^\circ$ )
8	87.58 nm	652.52 nm	NOA81 in Homogene	N/A

Wavelength Range of Materials

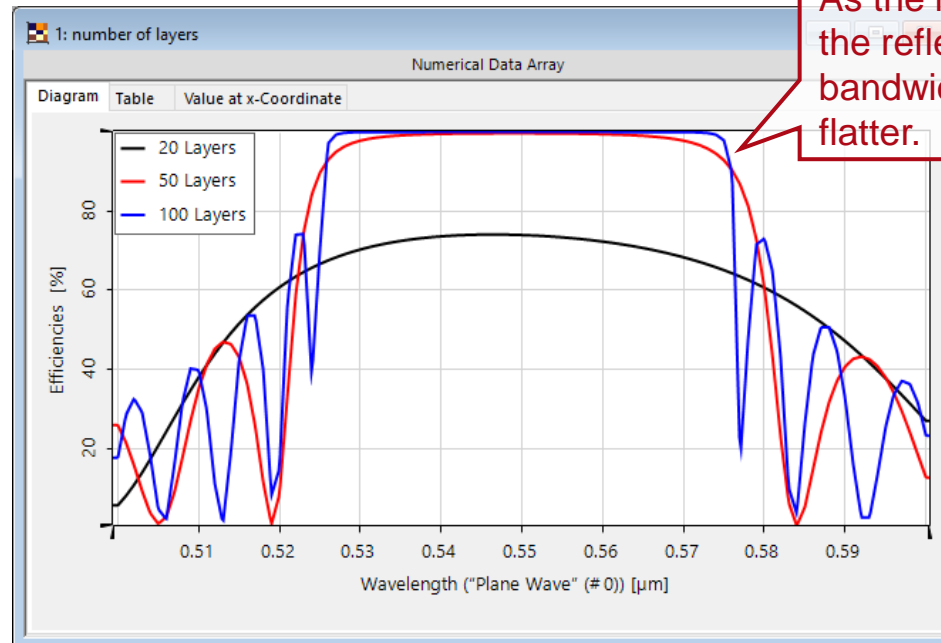
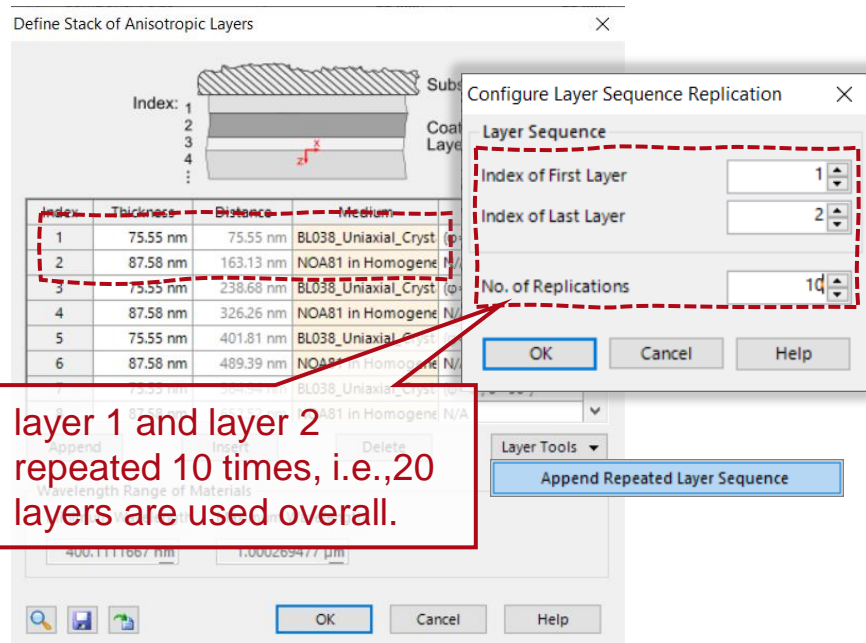
Minimum Wavelength: 400.1111667 nm  
Maximum Wavelength: 1.000269477  $\mu\text{m}$



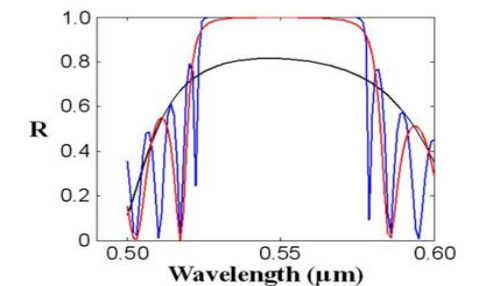
# Number of Periodic Layers to Establish Bragg Condition



- When the unpolarized plane wave hits the reflective polarizer, one direction of linear polarized light will pass through while the other component will be reflected back and depolarized, then it will be reflected again for another cycle. After several cycles, more and more light will be able to pass through the polarizer and therefore the energy efficiency is enhanced.
- In order to achieve the highest possible efficiency, the aim is to fulfill the Bragg reflection condition. Therefore, a minimum number of periodic layers is required. We used a *Parameter Run* to scan the wavelength range and calculate the efficiency with 20 layers, 50 layers, and 100 layers respectively.



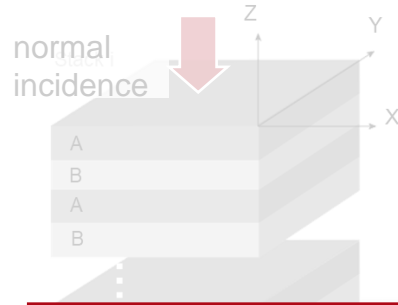
As the number of layers increases, the reflectance within the desired bandwidth becomes higher and flatter.



simulation result compare with Li et. al. J. Display Technol. 5, 335-340 (2009)



# Number of Periodic Layers to Establish Bragg Condition

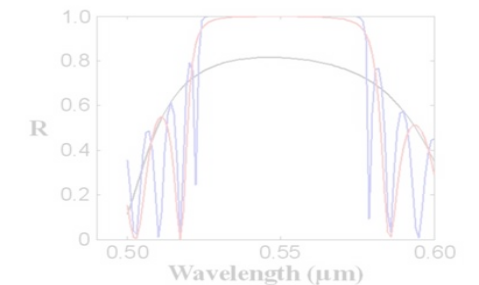
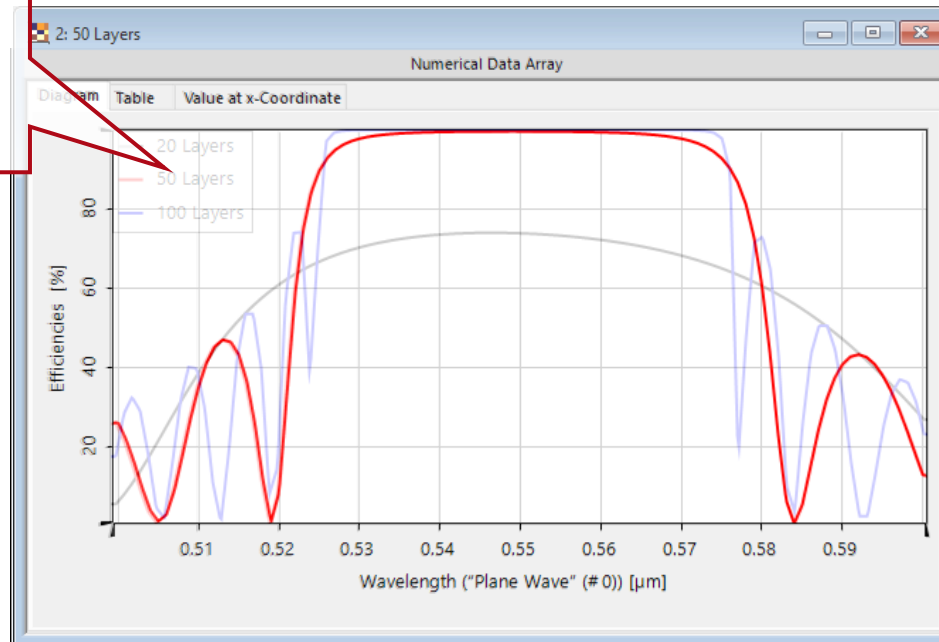


- When the unpolarized plane wave hits the reflective polarizer, one direction of linear polarized light will pass through while the other component will be reflected back and depolarized, then it will be reflected again for another cycle. After several cycles, more and more light will be able to pass through the polarizer and therefore the energy efficiency is enhanced.
- In order to achieve the highest efficiency, the Bragg reflection condition is aimed to establish here. Therefore, a minimum number of periodic layers is required. We used *Parameter Run* to scan within the wavelength range and calculate the efficiency with 20 layers, 50 layers, and 100 layers respectively.

Considering the material cost and fabrication complexity will also increase with more layers, a minimum of 50 layers can be used to achieve acceptable reflectivity and bandwidth.  
- Li2009

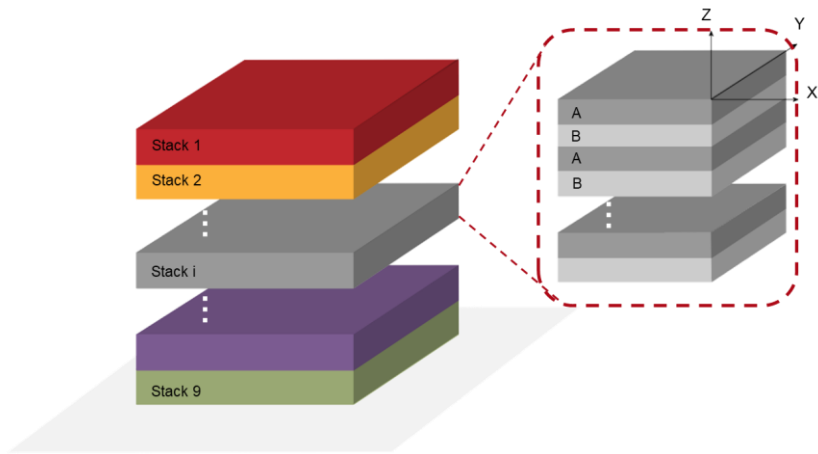
Index	Thickness	Distance	Medium
1	75.55 nm	75.55 nm	BL038_Uniaxial_Cryst
2	87.58 nm	163.13 nm	NOA81 in Homogene N
3	75.55 nm	236.68 nm	BL038_Uniaxial_Cryst
4	87.58 nm	326.26 nm	NOA81 in Homogene N
5	75.55 nm	401.81 nm	BL038_Uniaxial_Cryst
6	87.58 nm	489.39 nm	NOA81 in Homogene N

layer 1 and layer 2 repeated 10 times, i.e., 20 layers are constructed

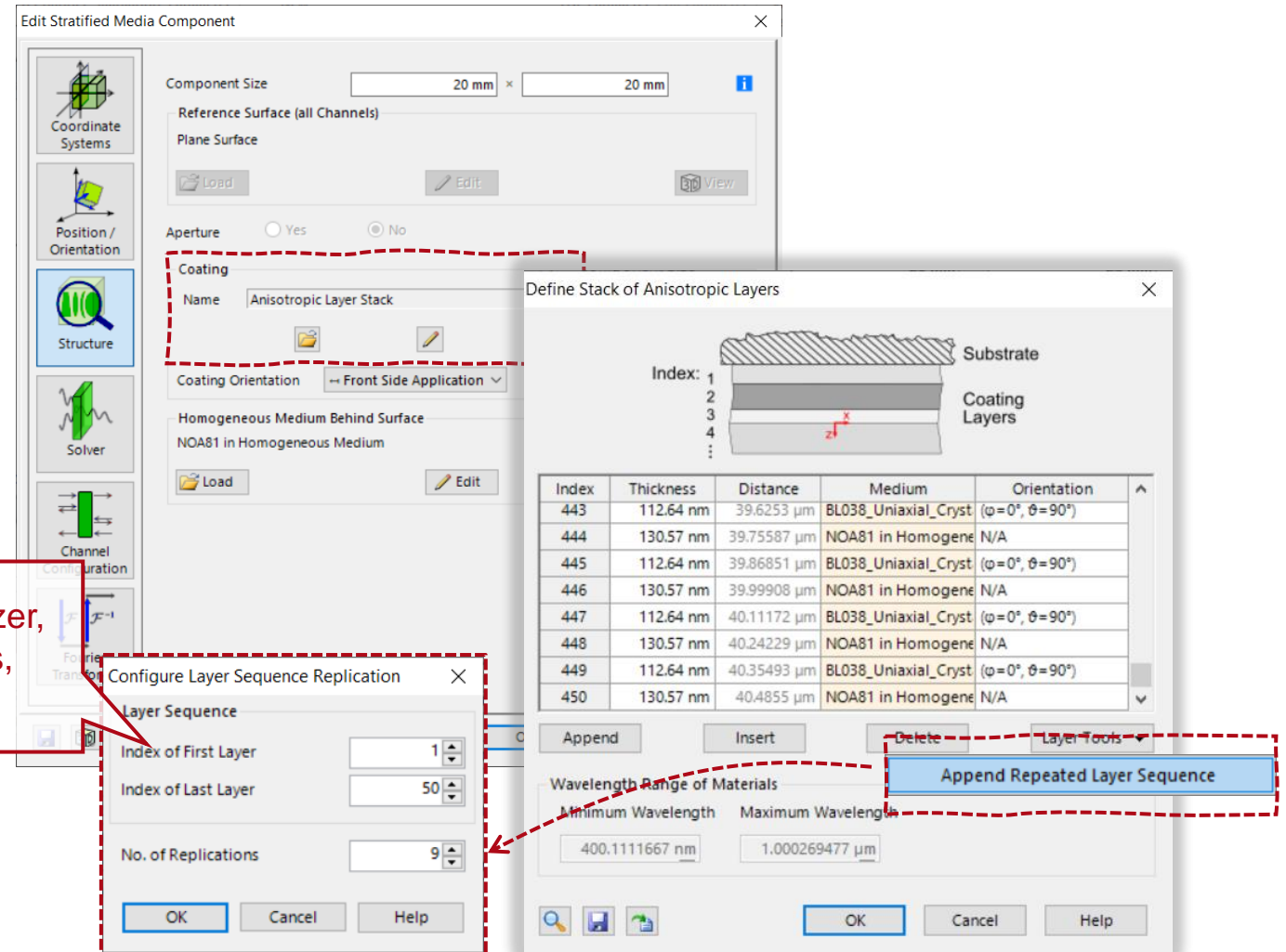


simulation result compare with Li et. al. J. Display Technol. 5, 335-340 (2009)

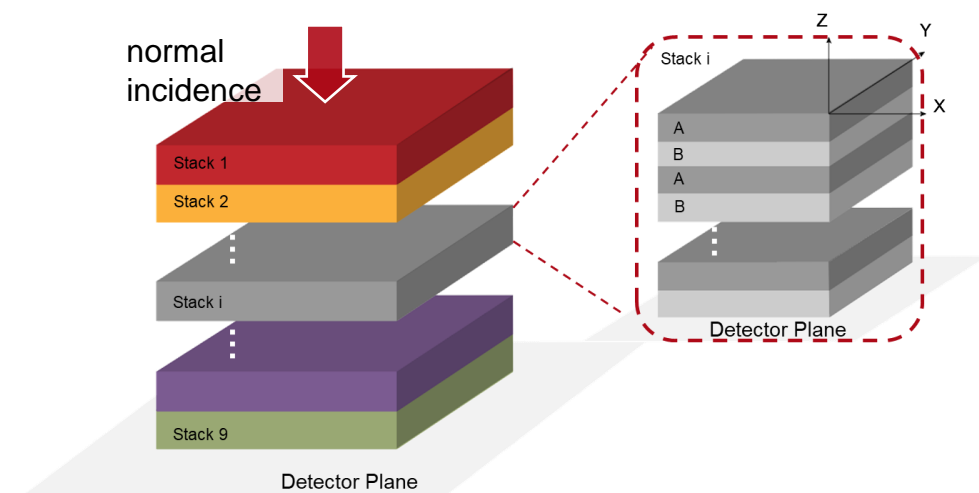
# Modeling of Multi-Stack Reflective Polarizer



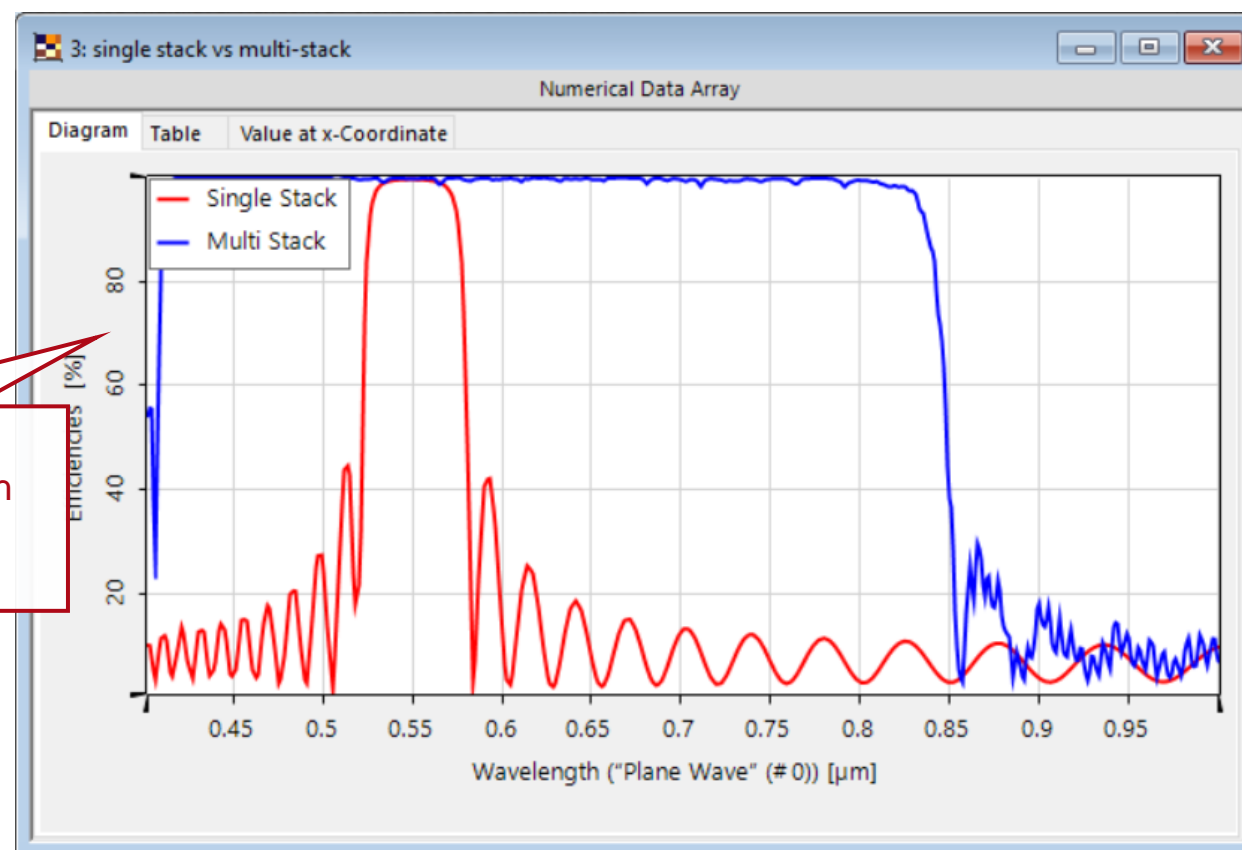
Nine stacks in the reflective polarizer, each stack with 50 alternate layers, hence 450 layers in total.



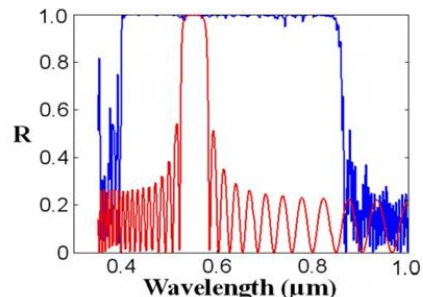
# Expanded Bandwidth by the Multi-Stack Method



The reflection efficiencies of single-stack and multi-stack structures were calculated under wavelength scanning. The simulation shows that, compared with the single stack, an expanded bandwidth is achieved through the multi-stack method.

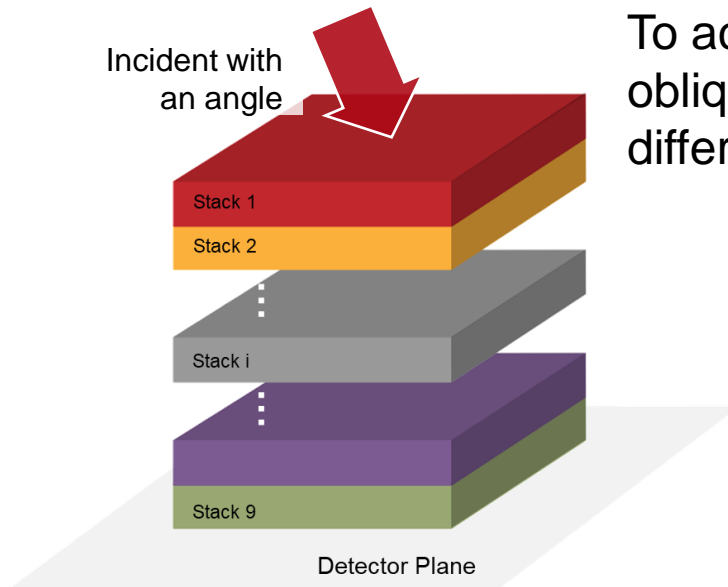


Multi-stack structure achieves reflectance  $\sim 100\%$  for a much broader bandwidth when compared to a single stack.

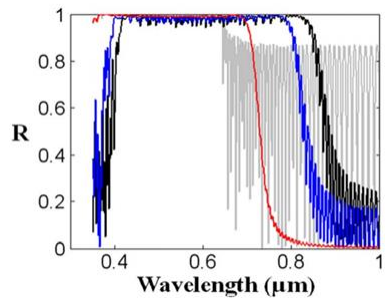


simulation result compare with Li et. al. J. Display Technol. 5, 335-340 (2009)

# Investigation of Reflectance Efficiency with Different Incident Angle

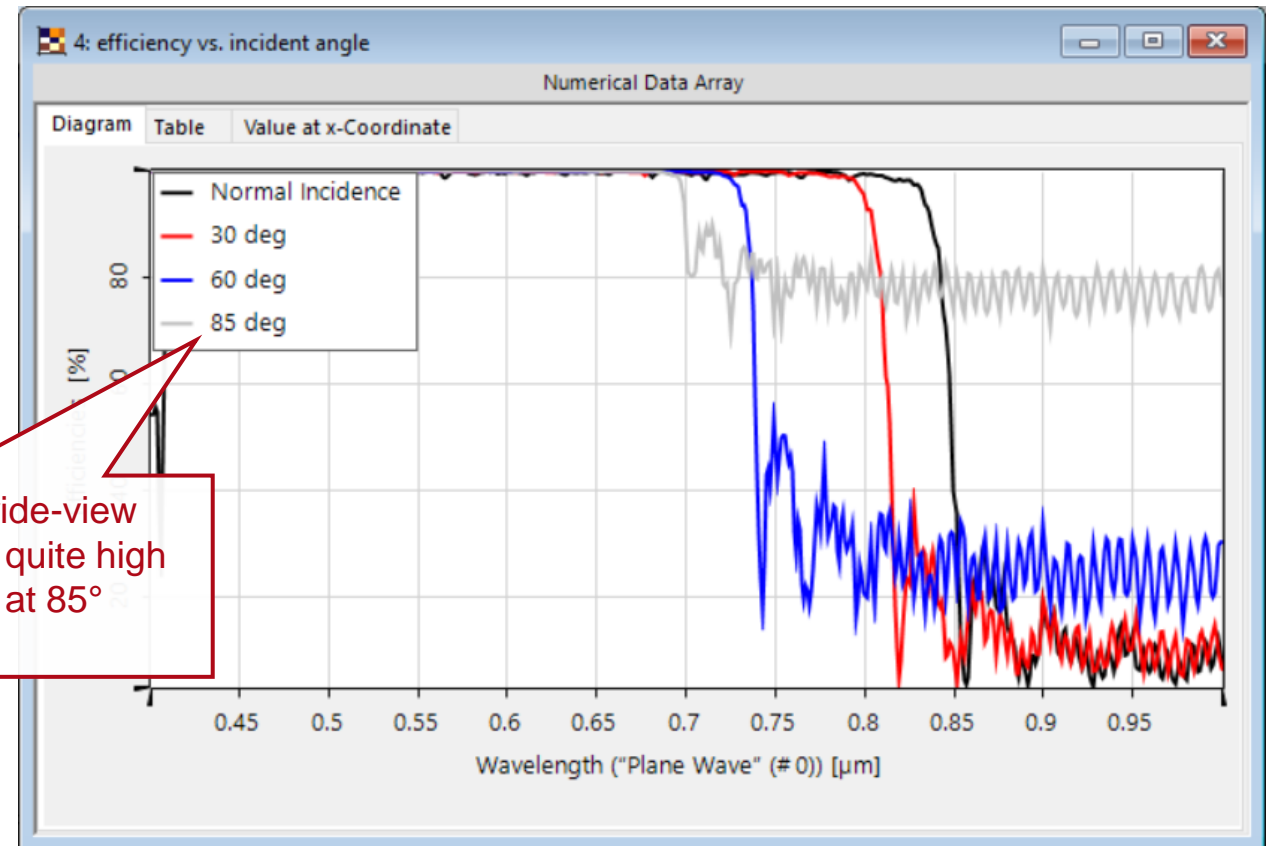


To achieve a wide-view LCD, the reflective polarizer should also be designed for oblique incidence. Therefore, the performance of the reflective polarizer at different incident angles is further investigated.



simulation result compare with Li et. al. J. Display Technol. 5, 335-340 (2009)

For the application of a wide-view LCD reflectance remains quite high in the visible region even at 85° incident angle.

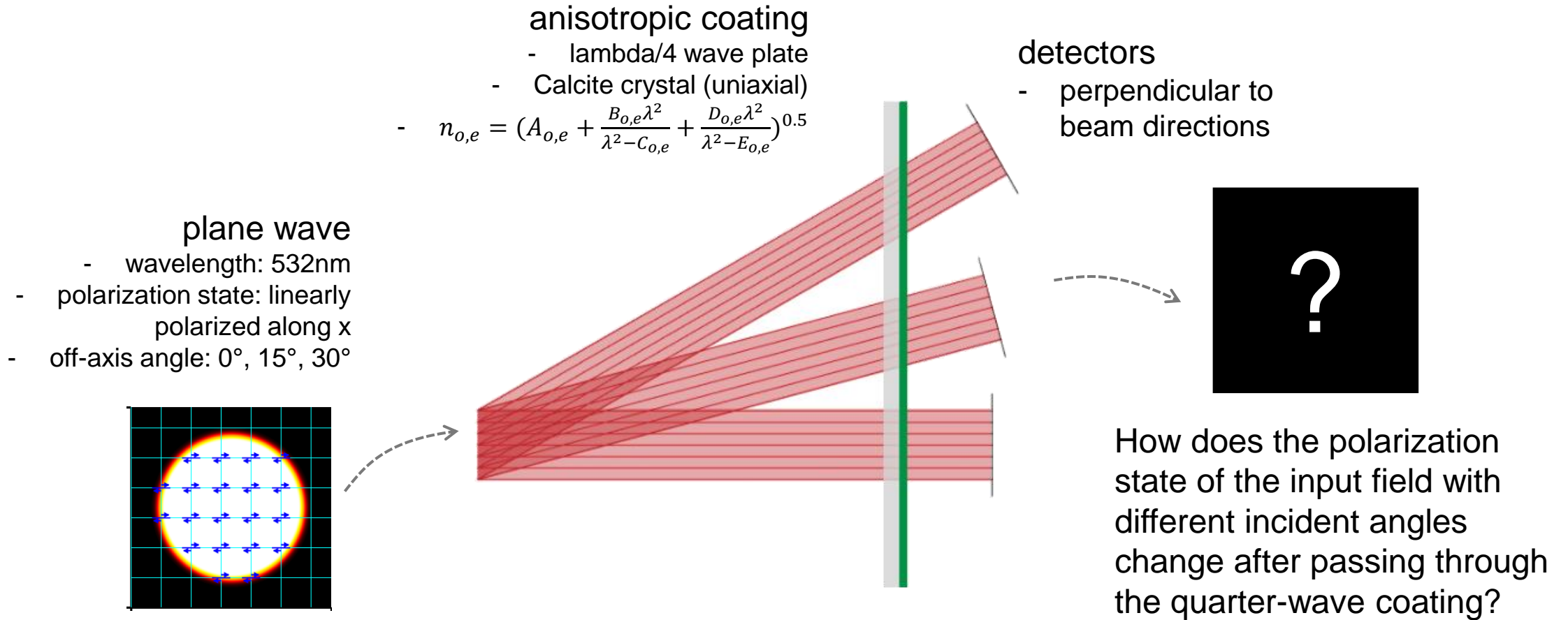


Example 04

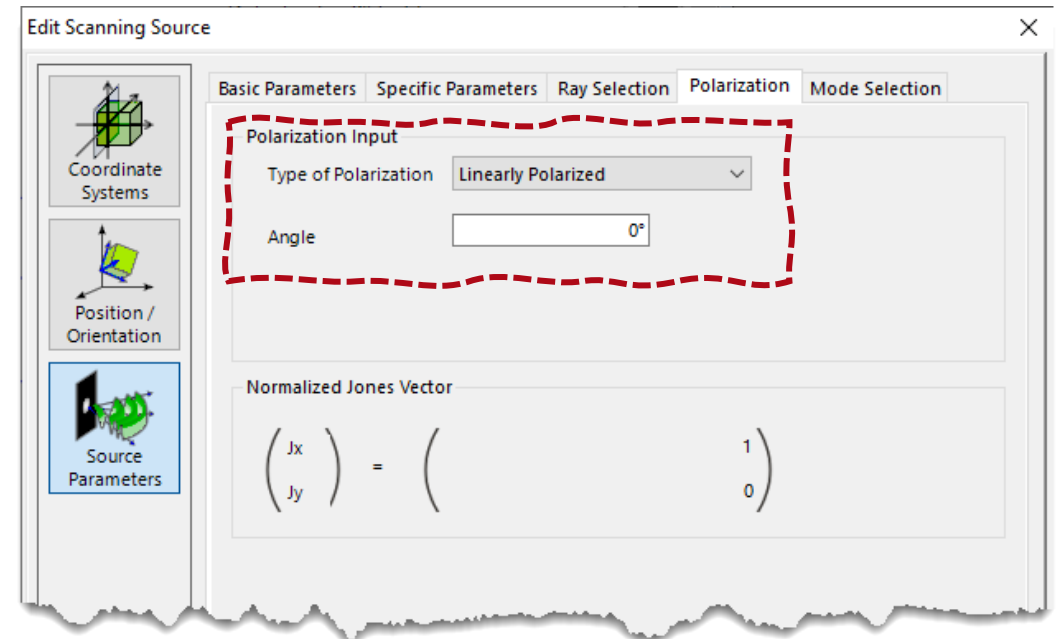
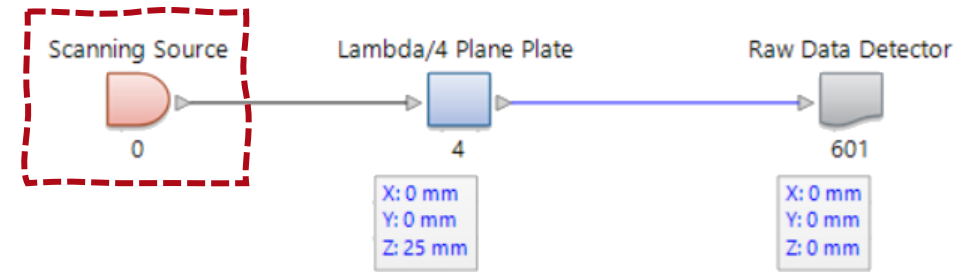
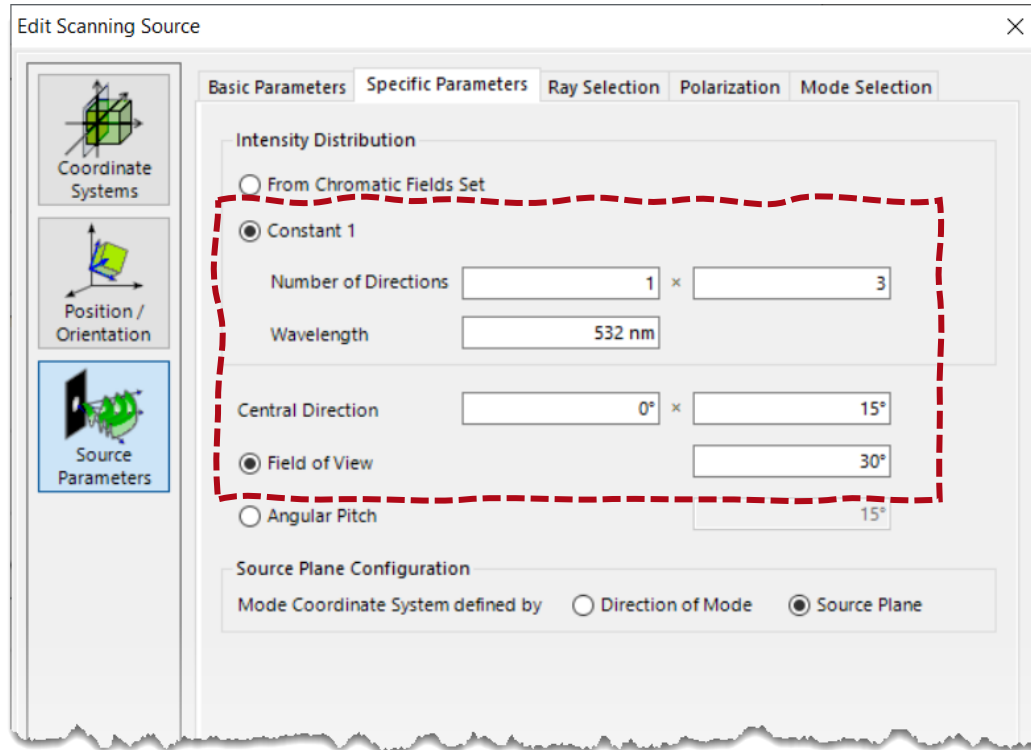
## **Simulation and Analysis of Anisotropic Coating on Plane and Curved Surface**

 [see the full Application Use Case](#)

# Quarter-Wave Plate Coating on Plane Surface



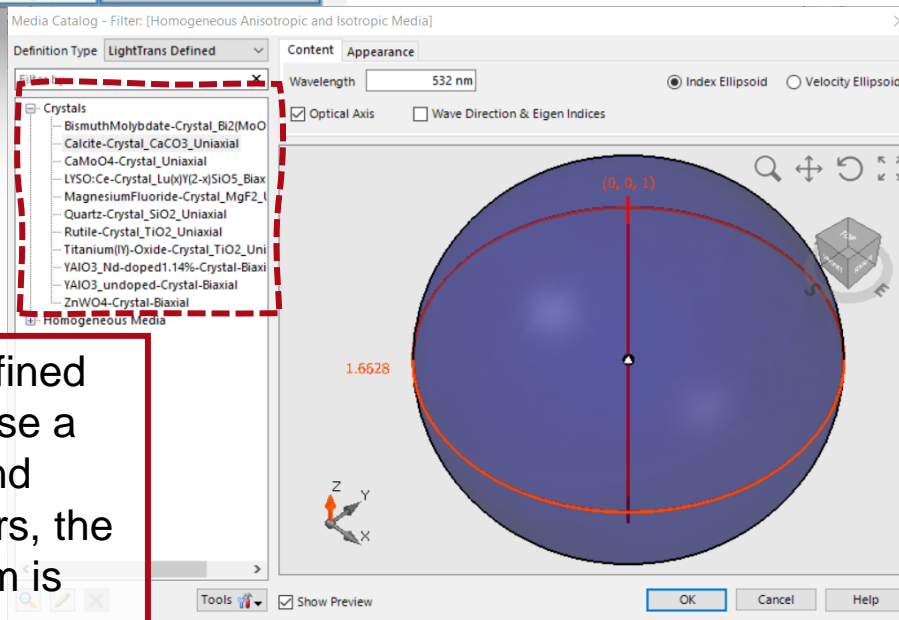
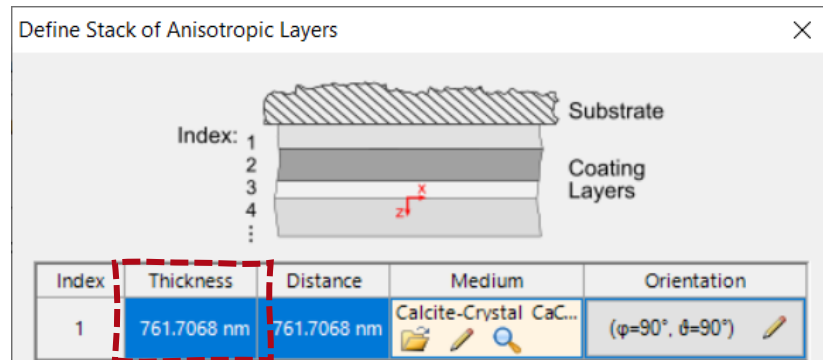
# System Building Blocks – Source



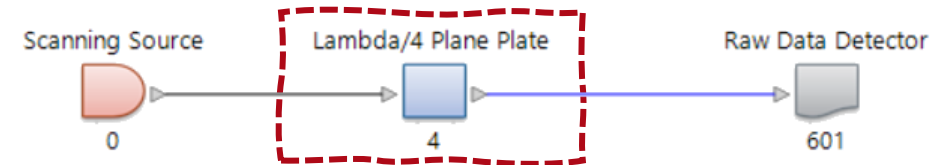
A *Scanning Source* is used to model the input plane waves. It is a convenient tool for the specification of several directions simultaneously and for polarization management.



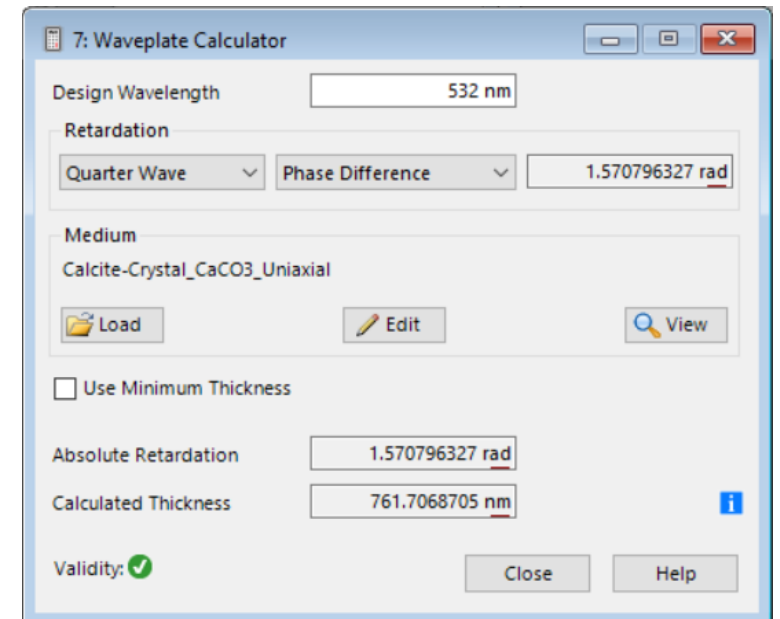
# System Building Blocks – Coating on Surfaces



choose from the predefined anisotropic media or use a template medium and customize the parameters, the preview of the medium is shown on the right

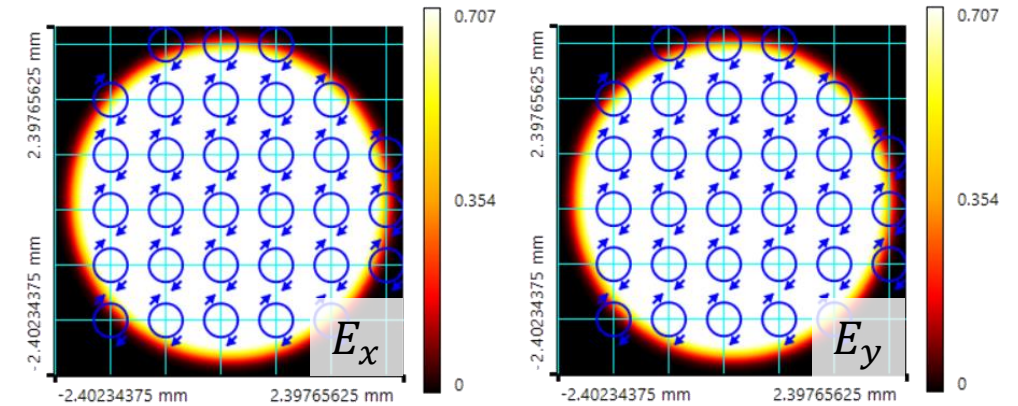
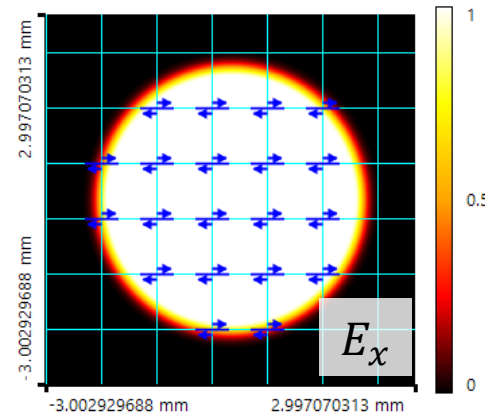
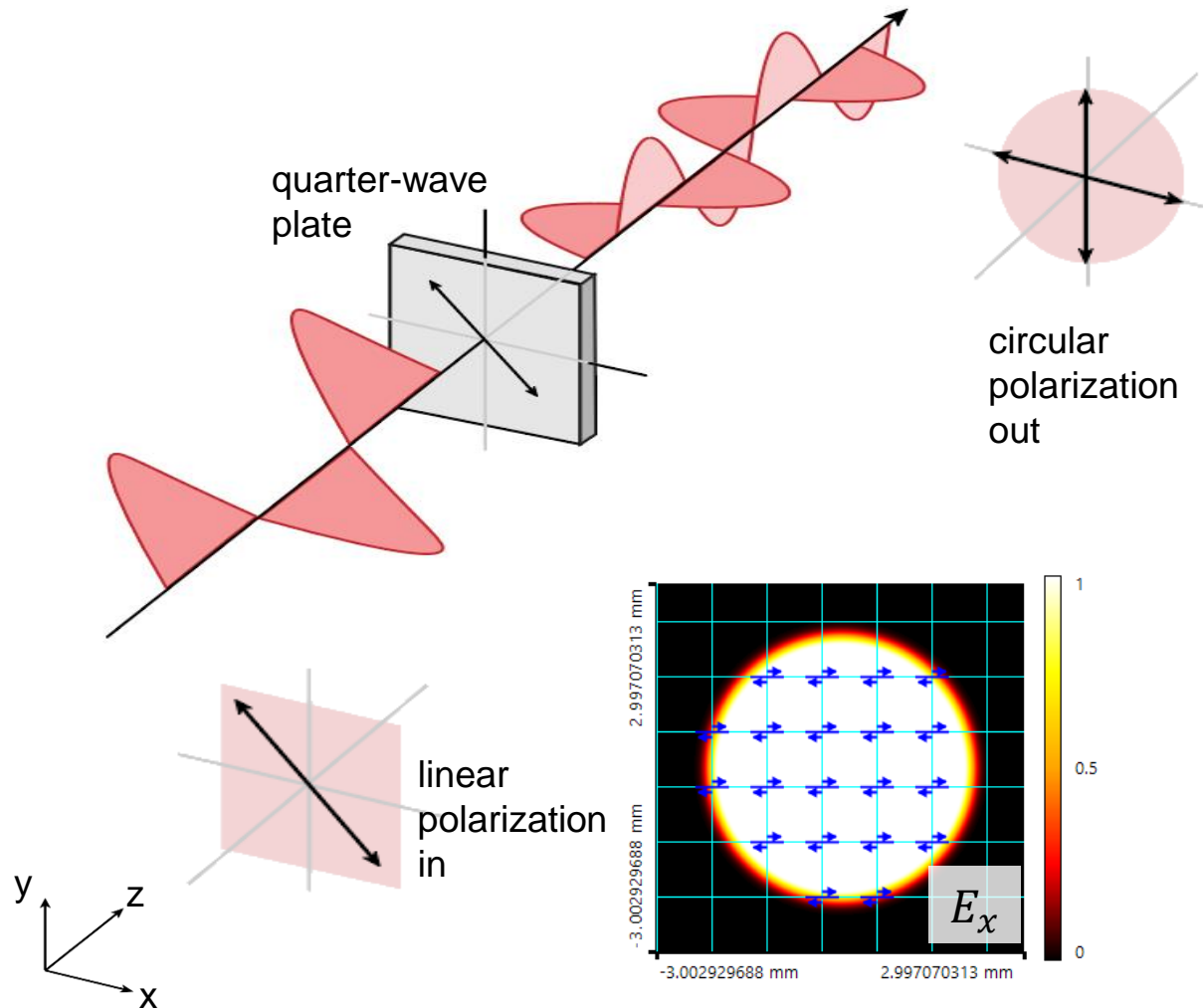


With the help of the *Waveplate Calculator*, the thickness of the coating layers can be calculated to achieve the desired retardation between the field components.



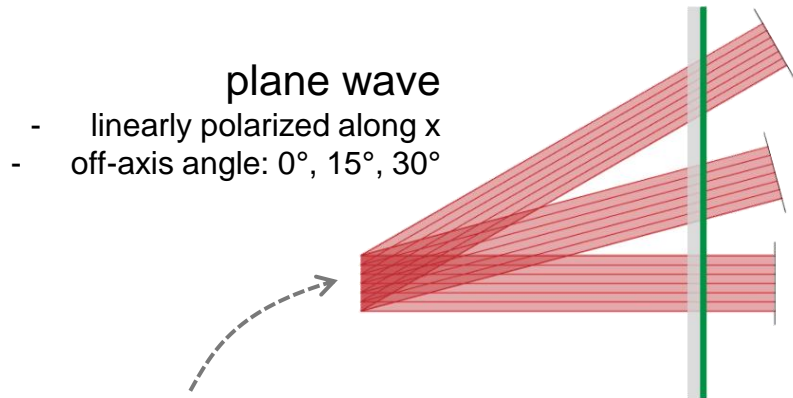


# Polarization Conversion at a Quarter-Wave Plate

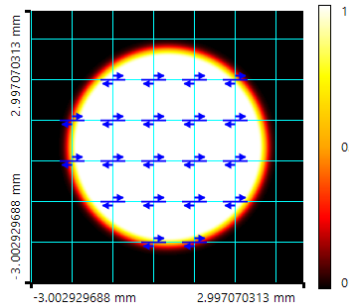


In the idealized situation, when linearly polarized light impinges on a quarter-wave plate at  $45^\circ$  to the optic axis, the transmitted light is divided into two equal electric field components. One of these is retarded by a quarter wavelength and the overlap of both beams at the exit plane of the plate generates circularly polarized light. And vice versa: if the incident light is circularly polarized, it will be transformed into linearly polarized light.

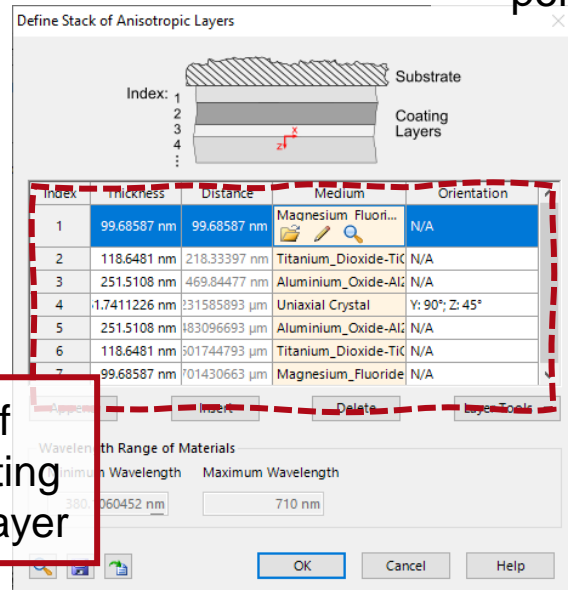
# Influence of Fresnel Effect Deviation



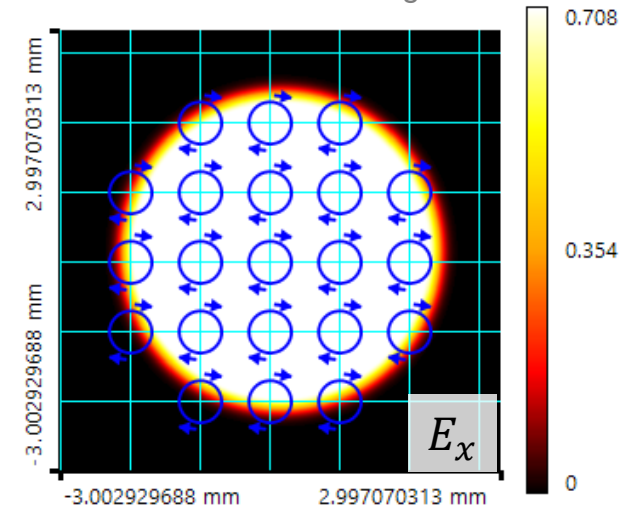
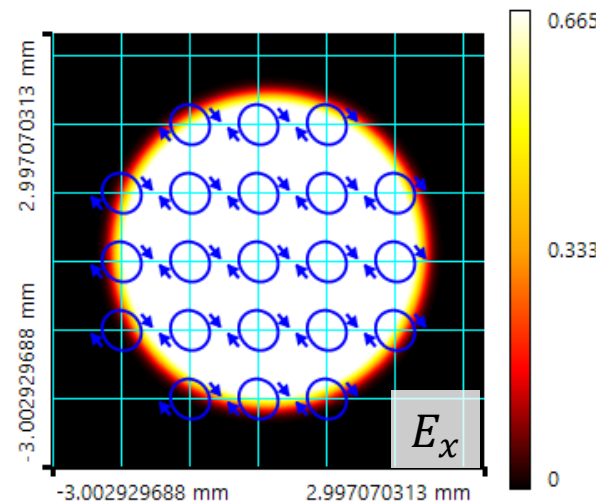
- However, when a real quarter-wave coating is configured, the two divided electric field components will face different refraction indices inside the crystal.
- Hence, the Fresnel effect when leaving the crystal will differ for the two electromagnetic field components as well, and the polarization state of the transmitted light will form an ellipse instead of a perfect circle.
- In order to eliminate this influence, an additional anti-reflection coating is applied together with the crystal coating. Then the perfect circularly polarized light is observed.



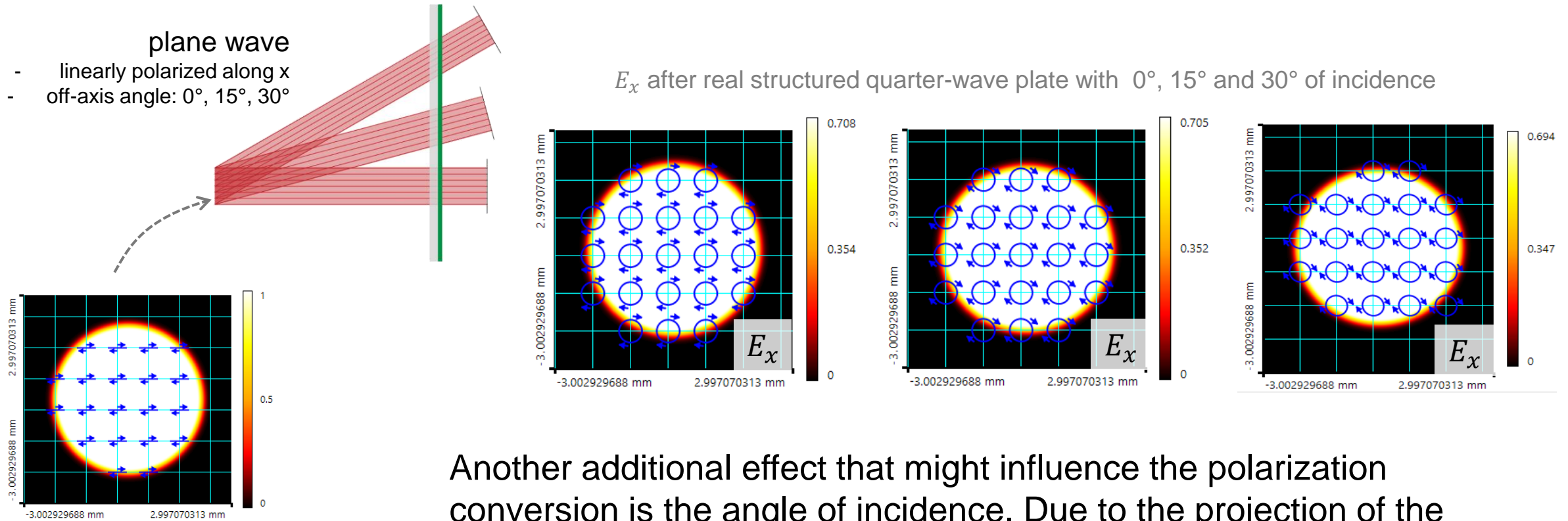
combination of  
isotropic AR coating  
and anisotropic layer



$E_x$  after real structured quarter-wave plate with & without AR coating

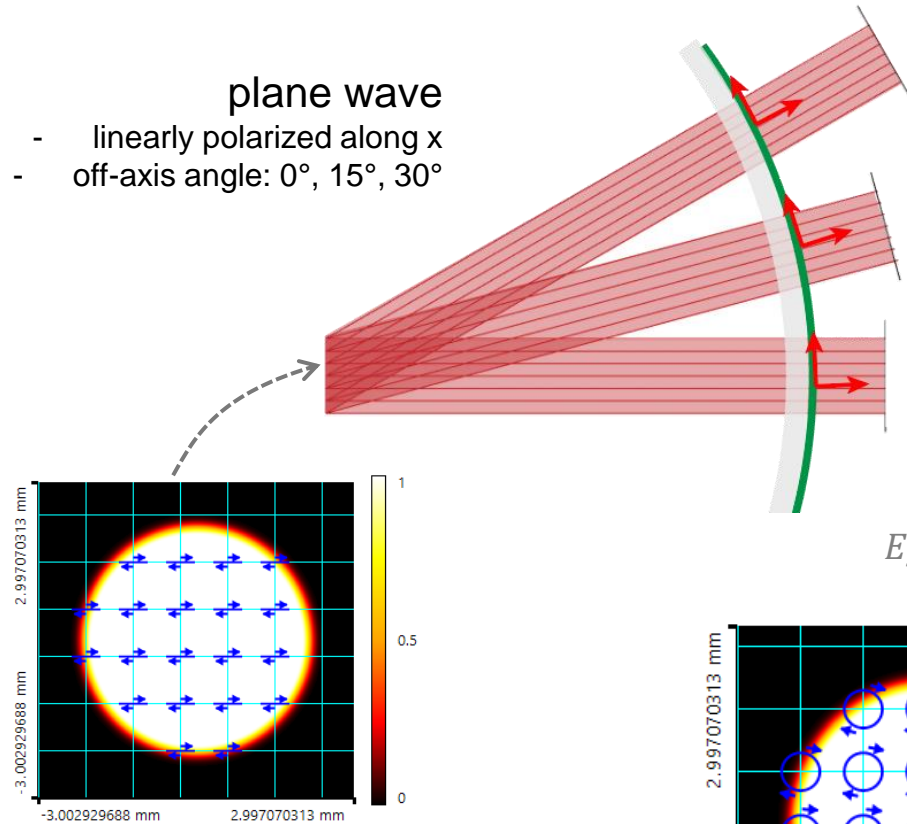


# Quarter-Wave Plate Coating on Plane Surface



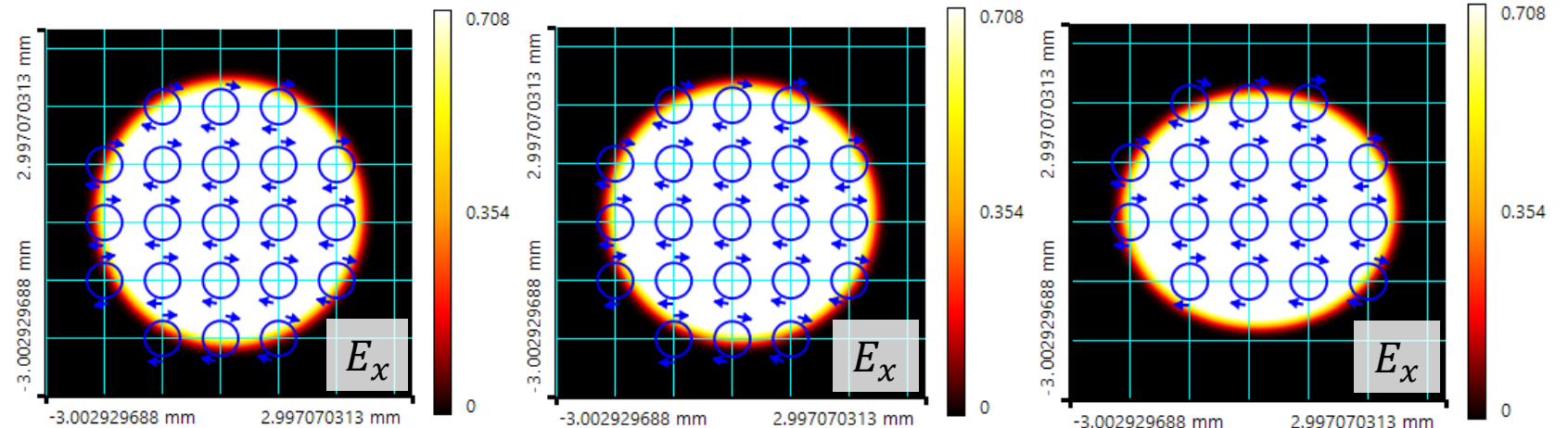
Another additional effect that might influence the polarization conversion is the angle of incidence. Due to the projection of the components of the field on the plane of the plate, the resulting polarization state will become more elliptical with increasing angle.

# Quarter-Wave Plate Coating on Curved Surface



If a quarter-wavelength coating is applied to a curved surface instead, which curvature allows the light to propagate along the normal vector of the surface, the effect of different projections of the field components can be avoided. This results in perfect circular polarization for all angles of incidence.

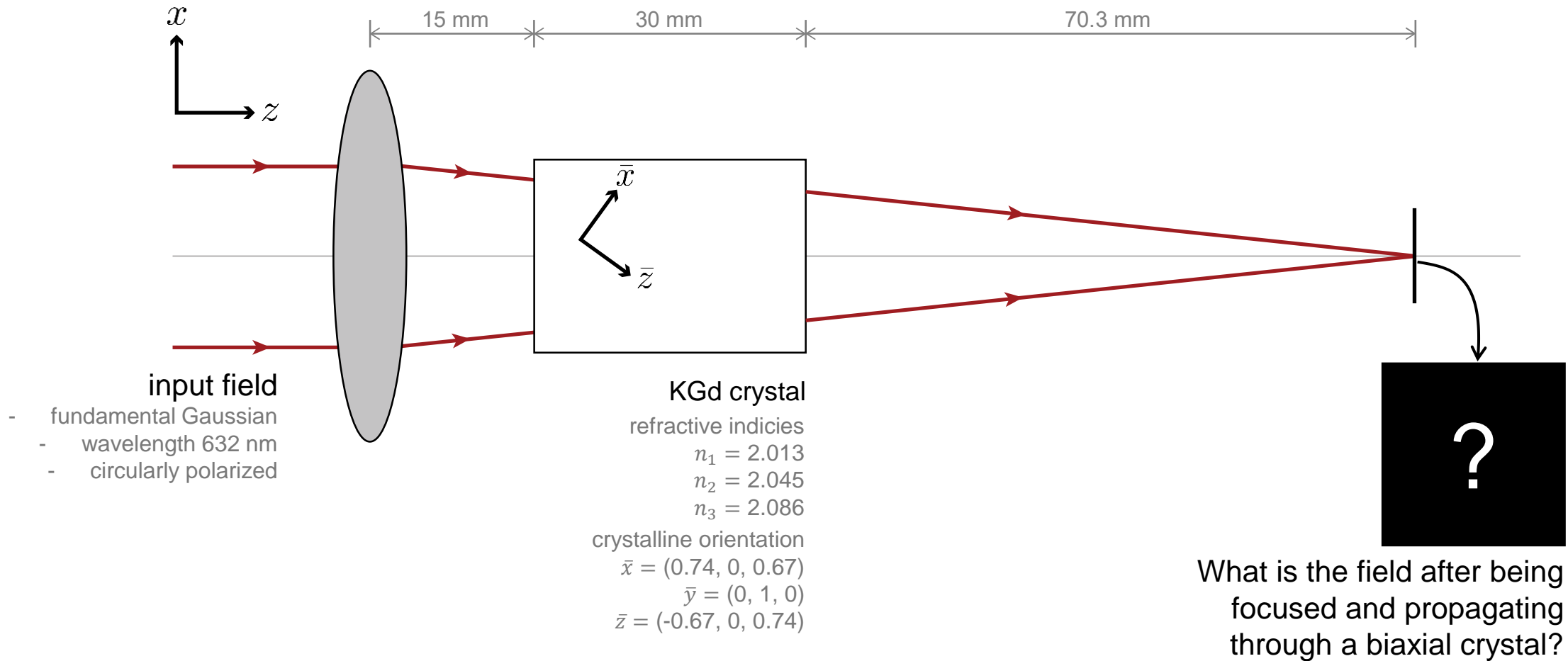
$E_x$  after real quarter-wave coating on curved surface with 0°, 15° and 30° of incidence



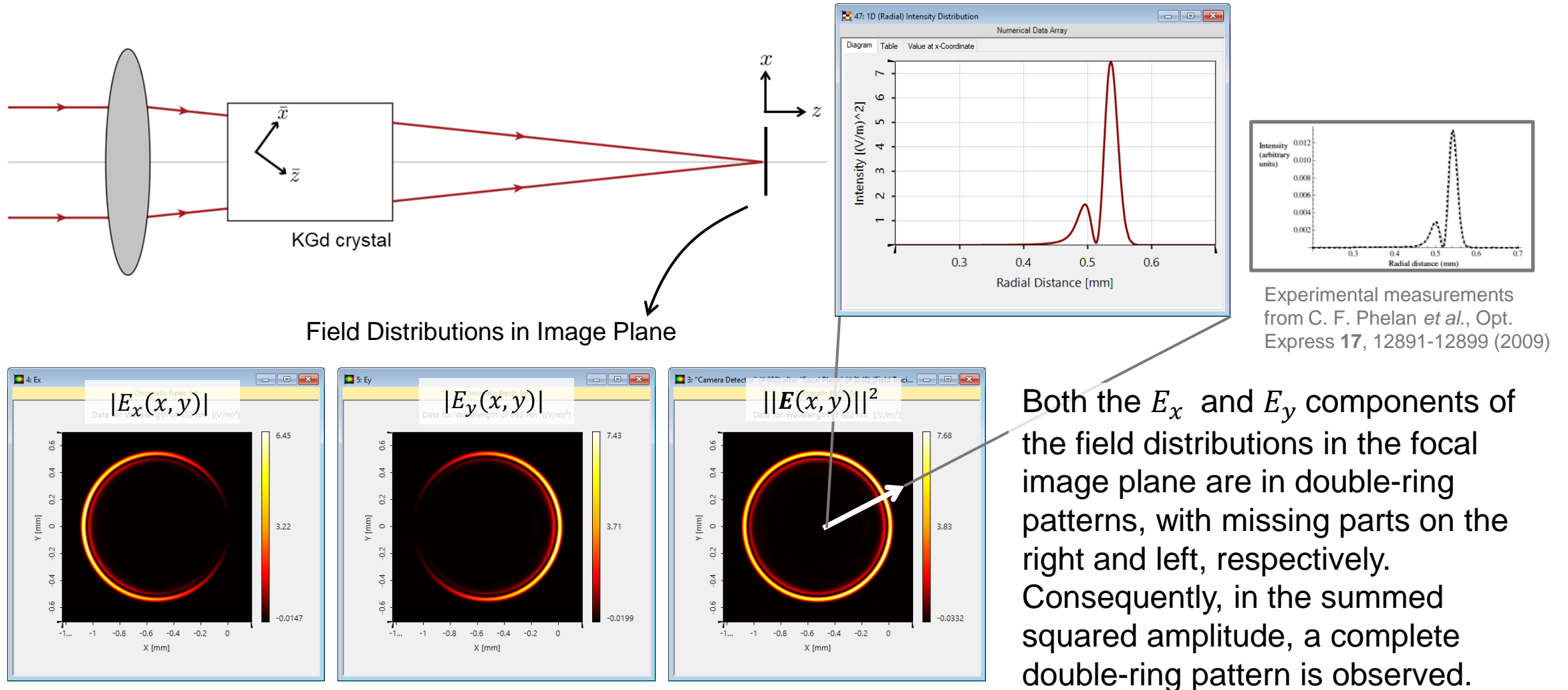
Example 05

## Conical Refraction in Biaxial Crystals

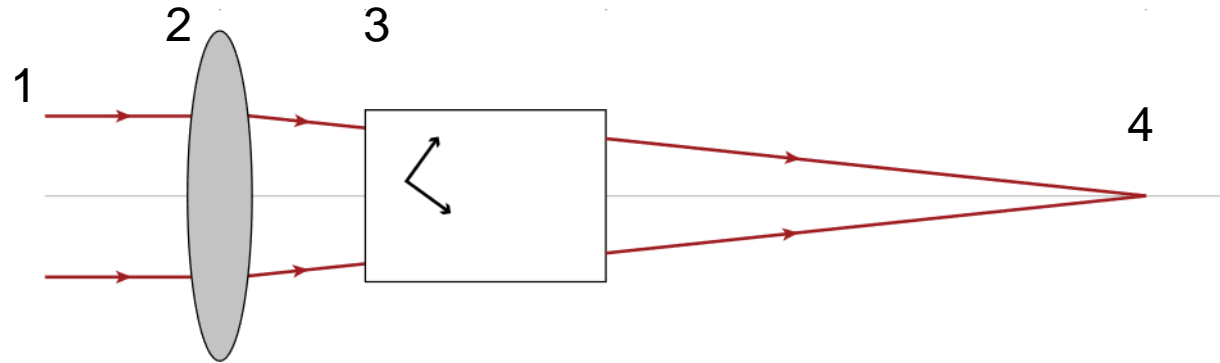
# Modeling Task



# Simulation Results



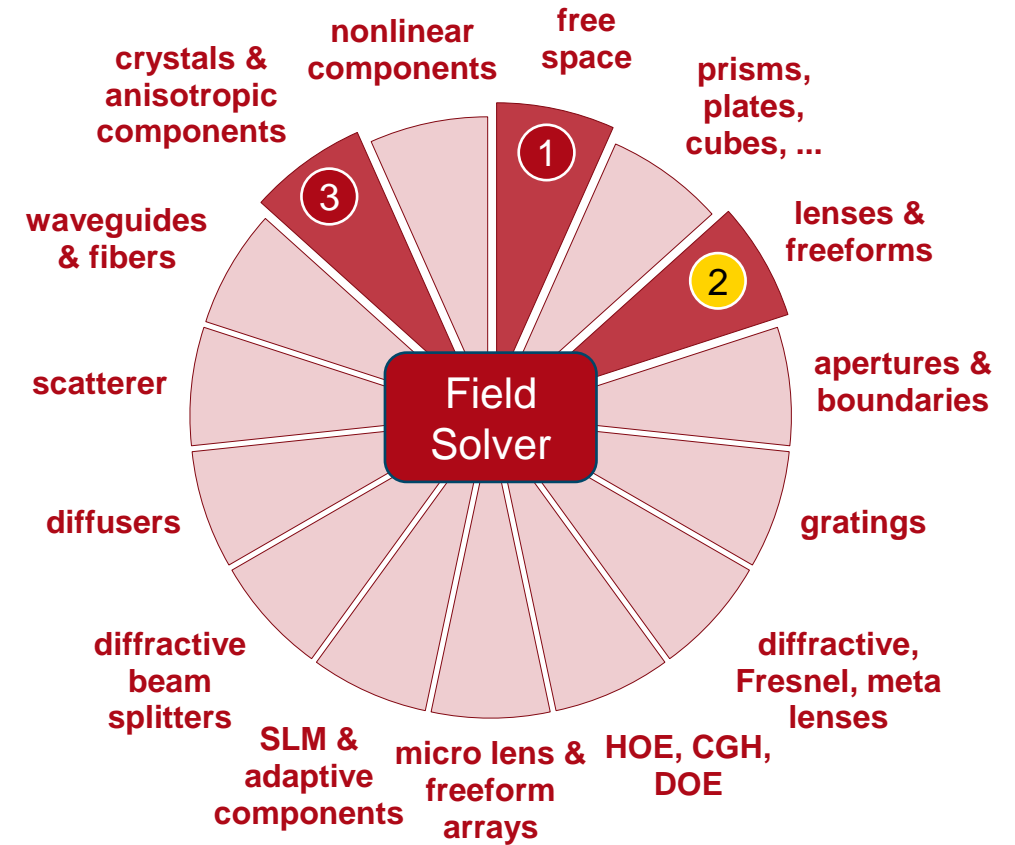
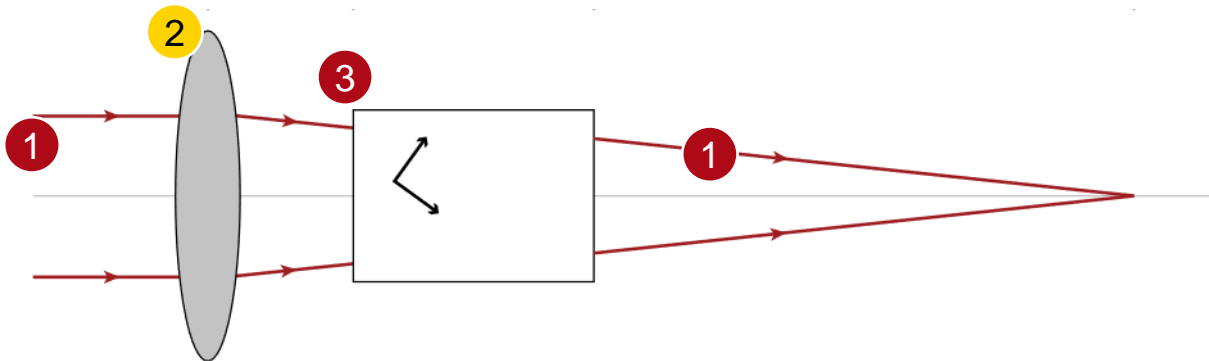
# Summary – Components...



... of Optical System	... in VirtualLab Fusion	Source Model/Component Solver
1. Source	Gaussian Source	
2. Lens	Ideal Lens	
3. KGd Crystal	Crystal Plate	Layer Matrix [S-Matrix]
4. Detector	Camera Detector	-



# VirtualLab Fusion Technologies



# idealized component